

UNIVERSITY OF OSLO
Department of Physics

**Combined heat
transfer in a
system for solar
heating and
radiative cooling**

Øystein Soteland

October 15, 2009



Abstract

The goal of this work is to study a system, which covers both the demands for heating and cooling of a building. The system is designed to be one large central installation for storage and distribution. Such systems obviously reveal a large cost-competitiveness. The design foresees solar collectors for heating and radiative cooling panels, which could be combined with an external electric fan, for cooling the water in the storage. In the present system design, the heat storage tank is divided in several sections in order to allow domestic hot water heating and cooling (summer) or DHW- and space heating (winter). It was investigated how well the heating- and cooling gains could be separated for the demand during typical days during summer. The stratification has been studied in particular in this thesis, and especially with respect to energy considerations when using the system for cooling. The results of the experiments indicate that there are potential benefits of using this type of solar system for cooling. The gain in cooling energy has been found to be in the range of 5.4 kWh to 6.2 kWh and the stratification of the tanks were found to be adequate.

Preface

The process of writing this master's thesis has been a great learning experience. I have come to realize that research is not just doing an experiment. Research is about making a experimental setup, learning theory, reading research papers, conducting experiments and analyzing results.

I have also learned that writing a master's thesis is just as much about learning how to write a master's thesis as it is actually writing it. During the process there have also been several obstacles. Figuring out how to deal with these obstacles along the way has also been an experience that is important to remember.

During the time of my thesis I have had much help and support. My supervisors, John B. Rekstad and Michaela G. Meir, have helped me with experiments, problem solving and the writing process. Their guidance has been very much appreciated.

Co-students that I have been sharing office with has also been helpful. In addition to a friendly and good environment, I have used Espen, Henning, Catarina and Svetlana to challenge my ideas and experiments. They have surely made my time of writing a better experience. Furthermore, I would like to thank friends and colleagues for their help during this thesis. I would also like to thank my family for being understanding of long absences from my hometown.

The person who might have been most affected by my writing is my girlfriend. Therefore I thank my Elizabeth for her love, support and patience, during my work. Thank you for being there with me and for me.

Oslo, October 2009

Øystein Soteland

Contents

Abstract	iii
Preface	v
1 Introduction	1
2 Background	5
2.1 Energy potential of the Sun	5
2.2 Heat from solar radiation	6
2.3 Collector based cooling	7
2.4 Heat storage	8
3 Theoretical background	9
3.1 Blackbody radiation	9
3.2 Night sky radiation	11
3.3 Convection	12
3.4 Heat	13
3.4.1 Heat conduction	13
3.4.2 Heat capacity	14
3.4.3 Thermal expansion	15
4 Experimental setup and methods	17
4.1 Overview	17
4.2 The tank system	18
4.2.1 Internal DHW tank	19
4.2.2 Solar tank	22
4.2.3 Floor tank	23
4.2.4 Pumps	24
4.3 Solar loop	25
4.3.1 External auxiliary cooler	25

4.3.2	Auxiliary heater	26
4.4	Normal operating state for heating	26
4.4.1	Operating state for cooling	27
4.5	Temperature monitoring	28
4.6	Temperature sensors	28
4.7	List of equipment	31
4.8	Hardware and logging software	32
4.8.1	LabVIEW	32
4.9	Methods	35
4.9.1	Weighting of sensors	35
4.9.2	Calculation of heat loss and gain	35
4.9.3	Heat loss	37
4.9.4	Simulation of heat transfer	37
4.10	Uncertainties	39
4.10.1	Temperature sensors	40
4.10.2	Volume of tanks	40
4.10.3	Conductive heat loss	42
5	Experiments	43
5.1	Execution of the experiments	43
5.2	Experiment list	44
5.3	General description of plots	44
5.3.1	Temperature plots	44
5.3.2	Stratification plots	46
5.3.3	Temperature change plots	46
5.4	Resulting plots	46
6	Results	59
6.1	General temperature plot	59
6.1.1	DHW tank	59
6.1.2	Solar tank	61
6.1.3	Deviating sensors	62
6.2	Heat layers - stratification	62
6.3	Simulated theoretical and measured heat transfer	64
6.4	Calculated energy gain and loss	65
6.4.1	Efficiency of tank system	67
6.4.2	Heat loss	68

7 Discussion	73
7.1 Practical problems	73
7.1.1 Cracked cooler	73
7.1.2 Sensors not submerged in water	74
7.2 Stratification	75
7.2.1 DHW tank	75
7.2.2 Solar tank	76
7.2.3 Floor tank	77
7.3 Energy loss and gain when cooling	77
7.3.1 Efficiency of tank system	78
7.4 Simulations	79
7.5 Improvements of the cooling state	80
7.5.1 Flow considerations	80
7.5.2 Initial temperature of the active volume	81
7.5.3 Changes to the separation plate	81
7.6 Further experiments	82
8 Conclusion	83
Bibliography	85
Nomenclature	89
Appendix:	
A Calibration and uncertainty	93
A.1 Calibration and uncertainty of temperature sensors	93
A.2 Water velocity of the inter-exchange pump	95
B Program code	99
B.1 Simulation of heat transfer	99
B.2 Plotting of simulations together with measurements	100
B.2.1 Variables for plotting	101
C Labview	105
D Supplementary technical drawings	109
E Supplementary values	111

Did you transport natural gas from the Arctic down to Alberta to boil water to make steam to melt the tar out of the oil-sand reservoirs, and then use more natural gas to make hydrogen to make the tar molecules into gasoline so that North Americans could drive four-tonne vehicles five kilometers to sports clubs to ride 15 minutes on stationary exercise bikes? Did you really do that, Grandpa?

Radio Show, 2003

DR. ROBERT SKINNER

Chapter 1

Introduction

The world's use of energy today is largely based on primary energies which have negative effects on the Earth. United Nations Framework Convention on Climate Change, where 192 countries are members, recognize this [37]. Greenhouse gas emissions need to be considerably reduced in order to work towards a safer climate future. Impacts from greenhouse gases have already been shown with high certainty. Mean temperature has risen and there has been more extreme weather in the later years [1]. Hence, there is a need to change what type of energy we use, from the types emitting greenhouse gases to the types that generates energy directly from the Sun. Many countries have already made commitments through the Kyoto Protocol. This protocol is legally binding for each country and describes measures each country need to fulfill.

Primary energy consumption¹ of the world was 11 740 Mtoe² in 2006. Only 66.2 Mtoe of this where from solar, wind and geothermal energy[18]. This is a small fraction, but energy production based on the Sun has had an annual growth of 30% for more than 10 years, and a growth rate of 20-25% is predicted

¹Primary energy consumption means energy that is in its original unconverted form.

²Million tonnes of oil equivalents, corresponding to 41.87 PJ

to keep up in the upcoming years. Also, the Sun has the potential to cover the world's energy needs using only a fraction of its energy [29]. Having this in mind, there is reason to develop even more and better ways to harvest the Sun's energy.

Heating and cooling of buildings today use a considerable amount of energy, which is mostly based on electricity produced from fossil fuel and fossil fuel used directly. In Norway, for instance, 98% of residential buildings partly or fully use electricity for heating [35]. There is also a large need for cooling in buildings today and mostly this need is also met by electricity. Norway is fortunate to have clean electricity from hydro power and has enough clean energy for both heating and cooling. Many other countries meet their requirements for electricity and heating with electricity from fossil fueled power plants. This method of heating and cooling buildings is inefficient. Transformation of energy from coal and gas to electricity is inefficient [13, 32] and sending it through a power grid have energy loss [31, 38]. Electricity is a high value energy making it suitable for powering machinery, lighting, heating and cooling. Low temperature heat is low value energy. It can not be used to make electricity, but can be used for heating buildings. There is no need to use electricity for heating and cooling buildings, when there are low value energy in the form of heat available. High value energy should be saved for applications that demands it. The Sun provides the heat we need, and it can be collected where it is needed.

To the point of the Kyoto Protocol being fulfilled, solar energy has the potential to do exactly that.

The focus of this thesis is to investigate a specific solar thermal system design that can be used for both solar heating and cooling of buildings. The system is primarily made for heating. Adding small details to the internal workings of the design convert the system into one that can be used for cooling in addition to heating.

Buildings that use solar heating, and buildings that will use solar heating in the future, could also have the benefit of added cooling. If this could replace other means of cooling, there would be no need to acquire other means of cooling the building. This saves money and power, thus making it environmentally friendly. Hence it is important to study this system in order to investigate

such a potential.

The thesis will focus on the behavior of water in the region around a specific design feature, a separation plate, in the tank system. The separation plate help the water remain stratified.

The goals of this thesis is therefore to try to answer these questions:

- How much energy is gained for cooling purposes?
- How well does this tank design utilize cooling?
- How and why does heat travel internally in the tank?
- How does the actual behavior of the tank coincide with theoretical behavior?
- What further changes could be done to the system to increase efficiency?

Chapter 2

Background

Solar energy can be divided into three groups. These are direct solar energy from the Sun's radiation, indirect solar energy from wind, waves and crops, and stored solar energy in the form of fossil fuels. Direct solar energy can be harvested in many different ways, from photovoltaic cells and thermal heat power plants to thermal solar collectors and simple black roofs. This chapter introduces solar collectors and heat storage.

2.1 Energy potential of the Sun

The Sun is a star burning hydrogen and converting it into heat and radiation. The Sun emits $6.2 \times 10^7 \text{ W/m}^2$ from its surface in the form of electromagnetic radiation. Reaching the Earth, this flux of radiation, I_{SC} , is an average of 1367 W/m^2 , the solar constant. At the Earth's surface, this magnitude of the flux has decreased as some of the radiation has been absorbed by the Earth's atmosphere. Nevertheless, the total energy reaching the Earth at the equator is 2.38 MWh/m^2 per year. This value depends on the latitude, but even in parts of Norway this value is about 1 MWh/m^2 . [10, 19]

Chapter 1 briefly introduced world energy use. The total world primary energy

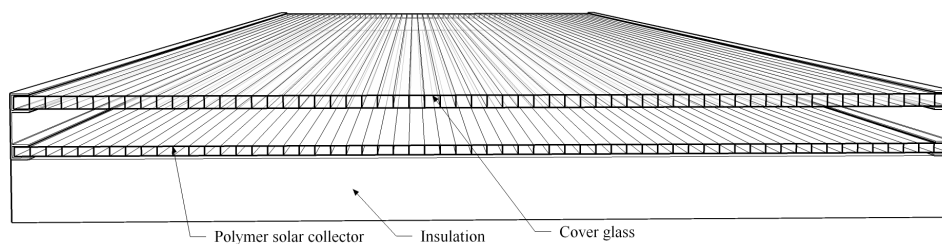


Figure 2.1: A solar polymer collector cut-through. The basic components of the collector are the polymer solar collector, the cover glass and the insulation. The two plates are held apart and in place by brackets. Water flows inside the polymer solar collector from one end to the other. This figure is made using Google Sketchup [14].

use was 11 433 Mtoe and 11 739 Mtoe in 2005 and 2006 respectively[18]. This translates to approximately 1.37×10^8 GWh in 2006. In one year, the Earth receives a total of 1.53×10^{12} GWh, which corresponds to more than 11000 times more energy than we already consume. This shows that there are enough solar energy for the world, today and well into the future. This is a calculation based on the total incoming radiation energy. In reality there are several limits: the atmosphere absorbs some of the incident sunlight, several areas of the Earth are not suited for production of solar energy and the efficiency of converting the energy is not perfect.

2.2 Heat from solar radiation

Harvesting heat from solar radiation is a matter of converting the radiation into heat. A solar collector is a heat exchanger that transforms solar radiant energy into heat. When the Sun's radiation reaches the collector surface, part of the energy is absorbed as heat. The heat is then absorbed by a liquid from inside the collector and transported to a heat storage. The stored heat can later be used for space heating and domestic hot water. This is one of the easiest ways to utilize energy from the Sun. Figure 2.1 show a cut-through of a polymer collector.

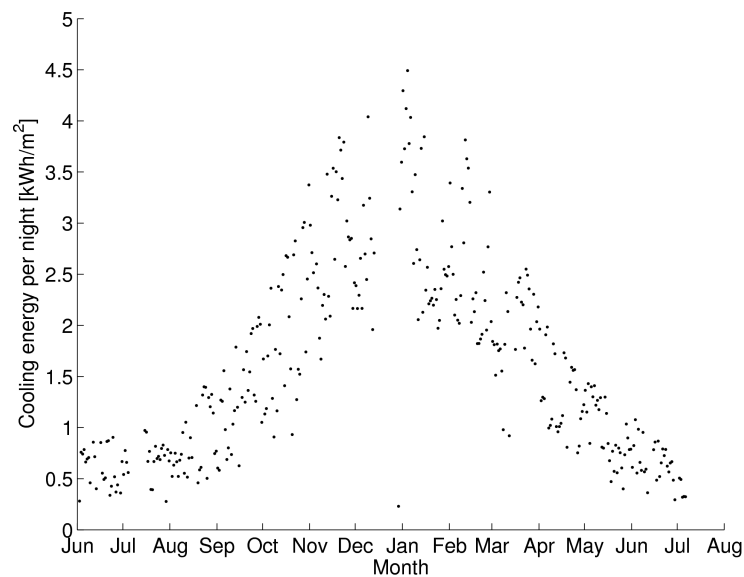


Figure 2.2: Measured values for the energy that is radiated out from a perfect radiator, blackbody, for each night during a whole year. Nights with no net outwards radiation is not represented here. (Source: Degnes-Ødemark [9])

2.3 Collector based cooling

Solar thermal collectors can also be used for cooling. There are two concepts that give them the ability to cool, the first is night sky radiation and the second is convection, which are described in Section 3.2 and 3.3, respectively.

Several studies of night sky radiation have been done. Martin and Berdahl [26] and Berdahl and Martin [3] have made improvements on a work that was started by Berdahl and Fromberg [2]. They have made a formula that can predict night sky radiation based on meteorological data. Degnes-Ødemark [9] has used this formula in his work and has also measured a whole year of night sky radiation at the Sollab. The plot in Figure 2.2 show how much energy that can be utilized per square meter each night.

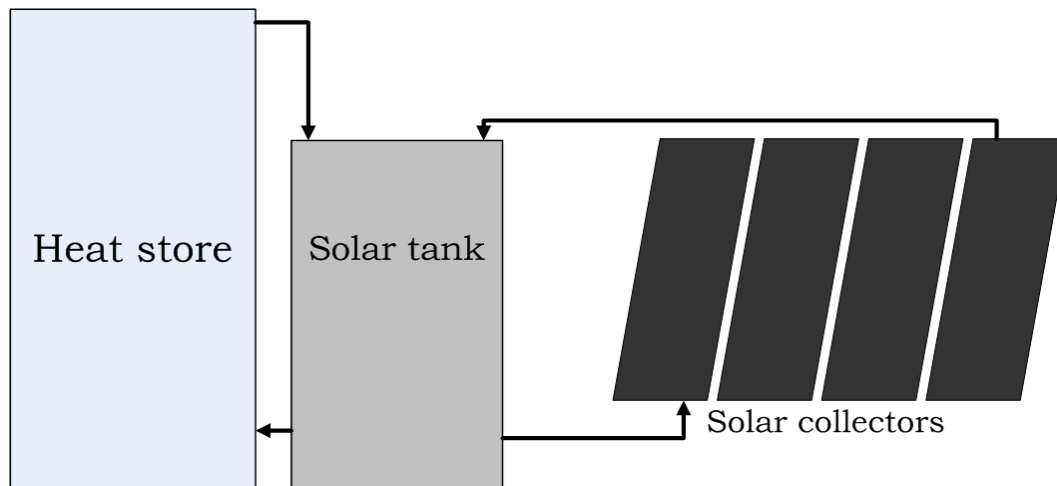


Figure 2.3: The basic components of a solar thermal system.

2.4 Heat storage

An important part of solar thermal systems is storage of heat. During the day there is Sun, but during the night the heating cannot be continued. If the heat collected during the day is needed at night, the heat has to be stored. The system used in this thesis use a heat storage with a physical stratification barrier which is described in Chapter 4.

Experiments have been performed on a system very similar to this earlier. Heian [17] has done experiments where domestic hot water is being consumed during cooling and heating. Before this, Damien and Dorothée [8] improved the stratification of the tank by modifying the water inlets. Other studies of stratification have also been done. Li and Sumathy [24] does a performance study of a stratified tank system with different modifications and Cristofari et al. [7] studies the influence the flow rate has on stratification in a heat store.

Chapter 3

Theoretical background

This chapter will give a theoretical background for the thesis. Included here is theory about energy transfers in different parts of a solar thermal system.

3.1 Blackbody radiation

A black body is an object that is in radiative equilibrium with its surroundings. All radiation that falls onto a black body is absorbed by it. To be in radiative equilibrium it radiates back to the surroundings in accordance to Planck's law, Equation 3.2. A perfect black body is an idealized object, and the radiation from it is described by Stefan-Boltzmann's law

$$R = \sigma_B \cdot A \cdot T^4 \tag{3.1}$$

where σ_B is the Stefan-Boltzmann constant, A is the area that radiates and T is the temperature of the object. Radiation power is proportional to the fourth power of the temperature, making a hot object emit more energy than a cold. The wavelength spectrum of the emitted radiation is given by Planck's law

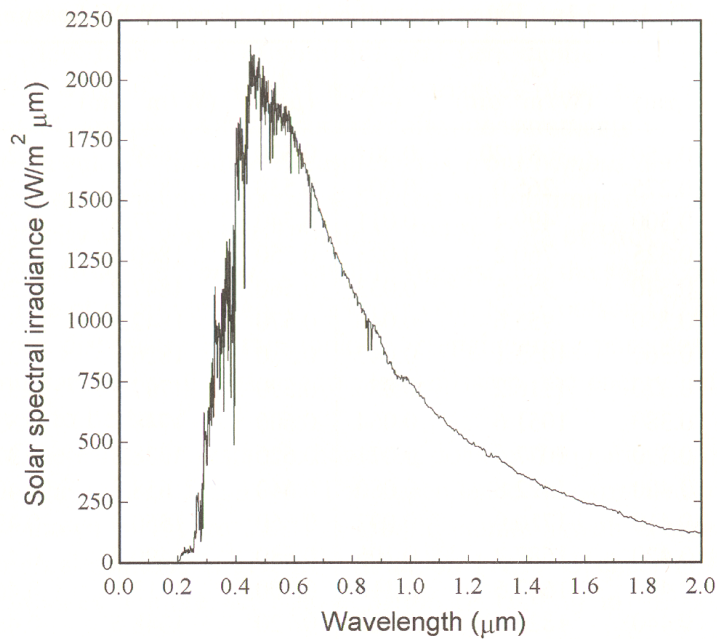


Figure 3.1: The spectral irradiance curve at the mean Earth-Sun distance. If the Sun had been a perfect blackbody it would radiate with a smooth curve like in Figure 3.2. The reason for the deviations is that the Sun does not radiate in perfect accordance with Planck's Law, Equation 3.2. Figure from Duffie and Beckmann [10].

$$E_{\lambda b} = \frac{2\pi hc^2}{\lambda^5(e^{hc/\lambda k_b T} - 1)}. \quad (3.2)$$

h is the Planck constant, k_b is the Boltzmann constant and c is the speed of light. This empirical law gives a maxima, the highest point in Figure 3.1. This maxima is different for objects of different temperatures. The maxima tells us which wavelength the object emits the most energy in. Figure 3.2 shows this curve for two objects. The two objects are blackbodies of 5777 K and 290 K, the temperatures of the Sun and the Earth, respectively. Though the figure is not to scale, the spectral irradiance of two black bodies of different temperatures has the same form. The spectral irradiance of the Sun in Figure 3.1 does not have a smooth curve. It lacks intensity in some of the wavelengths. Hence, the Sun is not a perfect blackbody.

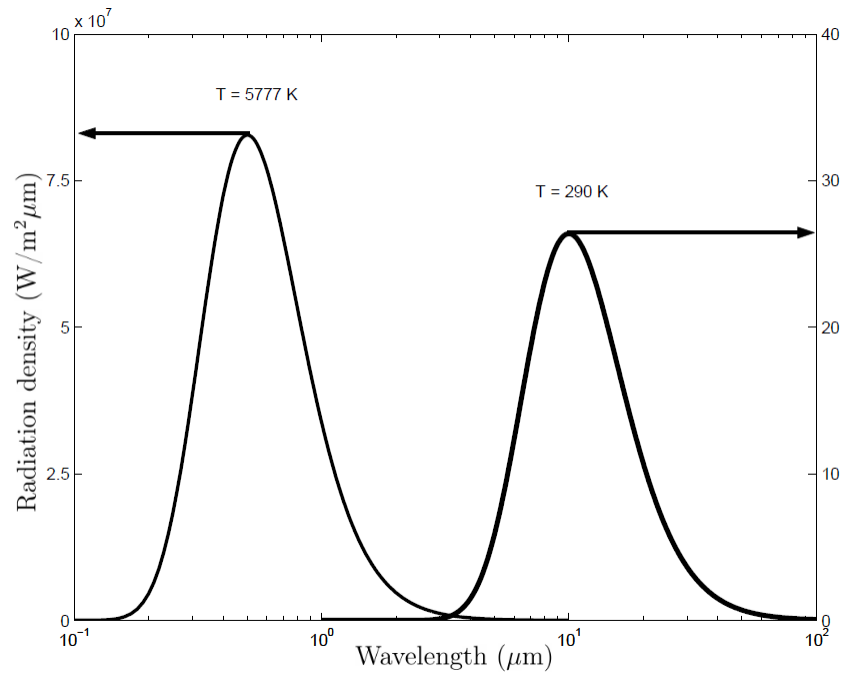


Figure 3.2: Spectral irradiance blackbodies at 5777 K and 290 K, at the surface of the Sun and the surface of Earth, respectively. (Source: Spikkeland [34].)

3.2 Night sky radiation

Night sky radiation involves the concept of Blackbody radiation to make an object cool down. Equation 3.1 expresses that an object of temperature T radiates with the power R . If then, one object radiates more energy than it receives, its total energy is lowered. From Equation 3.9 and 3.10 its temperature will decrease. Figure 3.3 shows the situation where a surface of temperature T_{surf} and emissivity ε can only see the atmosphere of temperature T_{sky} . Assuming that the atmosphere is a perfect blackbody, it is possible to find a formula for how much net radiation will flow between the two surfaces. The rate of energy transfer can be found by using Equation 3.1 for both objects:

$$R_{\text{net}} = A\sigma_{\text{B}}\varepsilon(T_{\text{surf}}^4 - T_{\text{sky}}^4) \quad (3.3)$$

At night, there are several hours with no sunlight, and the only radiation towards Earth comes from the atmosphere. The atmosphere is transparent for some wavelengths as Figure 3.4 shows. Humidity is the largest factor. If

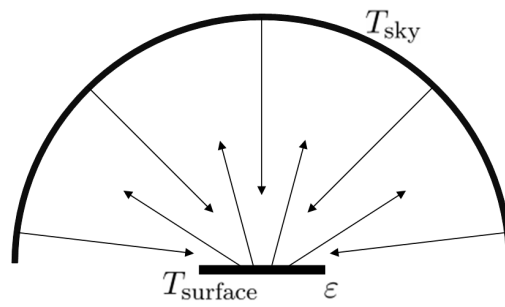


Figure 3.3: The energy exchange between a surface with temperature T_{surf} and emissivity ϵ , and the atmosphere with a temperature T_{sky} .

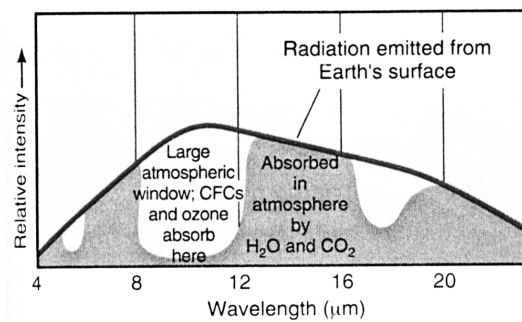


Figure 3.4: Radiation emitted from the surface of the Earth as thick line, and the atmospheric absorption bands showing the atmospheric window. (Source: Botkin and Keller [4].)

there are low relative humidity, radiation from the surface can escape from the Earth. If there are high relative humidity, radiative equilibrium will occur. When that happens the temperature of the atmosphere seen as a blackbody obtains the same temperature, effectively making R_{net} in Equation 3.3 zero.

3.3 Convection

Convection is a process that enables heat to dissipate from a surface, e.g. a solar collector. Convection is not a linear process, hence Equation 3.4 is dependent on the orientation of the surface where convection is taking place.

$$Q = -hA\Delta T \tag{3.4}$$

In Equation 3.4, h is a coefficient that changes as the orientation of the surface of area A changes and Q is the convected power. [19]

3.4 Heat

Heat is energy stored in matter. An increase in the temperature of an object results in increased energy in the object. Heat can travel from one object to another, always trying to even out the temperature difference between the object. Hence heat cannot be stored without insulation of the object where heat is stored. Theory concerning heat is found in Fraden [12] and Schröder [33].

3.4.1 Heat conduction

All materials conduct heat. Materials like water and polymers have poor heat conduction, while copper and aluminum have good heat conduction. Heat conduction in a material is dependent on the heat conductivity constant, k , of the material. The three tanks used in the Sollab are made of stainless steel of type 316L. Values for properties of these materials are given in Table E.2 and E.1 in Appendix E. The heat carrying medium used in this thesis is water. Water has a high heat capacity, which is a good feature for heat stores. Heat conduction is described by the Fourier's Law shown here in its integral form

$$\frac{\partial Q}{\partial t} = -k \oint_S \vec{\nabla} T \cdot \vec{dS}, \quad (3.5)$$

where $\frac{\partial Q}{\partial t}$ is the amount of heat transferred per unit time, k is the materials heat conductivity, $\vec{\nabla} T$ is the temperature gradient and \vec{dS} is an oriented surface area element.

By using the simplification that there is uniformly distributed temperature across equal end surfaces and that the sides are perfectly insulated, the heat flow rate, H , between the surfaces can be expressed as

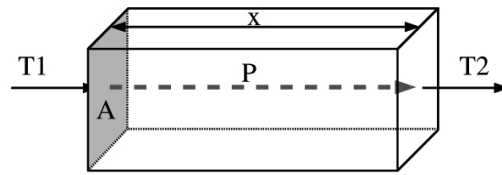


Figure 3.5: A material with cross section A , length x and a temperature difference of $T_2 - T_1$ has a heat flow $H = -UA(T_2 - T_1)$.

$$H = \frac{\Delta Q}{\Delta t} = k \cdot A \cdot \frac{\Delta T}{\Delta x}, \quad (3.6)$$

where A is the cross sectional surface area, Δx is the distance between the ends and ΔT is the temperature difference between the surfaces.

Heat current is often expressed by the overall heat transfer coefficient

$$U = \frac{k}{x}, \quad (3.7)$$

which is also used in construction. Lower value gives lower heat conductivity and hence a more preferred material for an energy saving residence.

Figure 3.5 describes heat conduction. A material with cross section A , a length of x and a temperature difference of $T_2 - T_1$ has a heat flow

$$H = -UA(T_2 - T_1). \quad (3.8)$$

3.4.2 Heat capacity

Heat capacity is the amount of energy an object can hold for each Kelvin the temperature is increased. An object of mass m and with a specific heat capacity c can store a heat capacity of C . The relationship is shown in Equation 3.9,

$$C = cm. \quad (3.9)$$

Specific heat capacities of materials in this thesis are shown in Table E.2 in Appendix E. The specific heat capacity is

$$c = \frac{Q}{m\Delta T}, \quad (3.10)$$

where Q is the heat in Joule, m is the mass and ΔT is the temperature difference that let the material store the energy Q . [33]

3.4.3 Thermal expansion

Water expands when it is heated above or cooled below 4 °C. In this thesis the temperature of the water never drops below 4 °C. Furthermore, the temperature of the water is in the range of 4 to 75 °C in this thesis.

Linear thermal expansion of a material can be expressed as

$$\frac{\Delta L}{L_0} = \alpha_L \Delta T_E, \quad (3.11)$$

where ΔL is the change in length, L_0 is the original length, α_L is the thermal expansion coefficient and ΔT_E is the temperature difference of the material. A material with a positive thermal expansion coefficient will therefore increase in length if it is heated. The definition of the linear thermal expansion coefficient is

$$\alpha_L = \frac{1}{L_0} \frac{\partial L}{\partial T}, \quad (3.12)$$

a fractional change in length for each fractional change in temperature divided by the original length. The volumetric thermal expansion coefficient α_V is three times the linear thermal expansion coefficient α_L ,

$$\frac{\Delta V}{V_0} = 3\alpha_L \Delta T_E = \alpha_V \Delta T_E. \quad (3.13)$$

The new volume of a material that has been heated is therefore

$$L_1 = L_0(1 + \alpha_V(T_2 - T_1)), \quad (3.14)$$

where T_1 and T_2 is the temperature before and after, respectively. Thus, hot water has a larger volume than cold water. During expansion, a material's weight does not increase since no mass is added or removed. The only change is the volume. In effect, the material's weight per volume decreases. In a tank of water with no turbulence, cold water will fall to the bottom and warm water will rise to the top. This concept is applied in the tank design. When water is heated, it will rise to the top of the tank, leaving the coldest water at the bottom for further heating.

Chapter 4

Experimental setup and methods

In Chapter 2, a general description of solar thermal systems was presented. This chapter will give a detailed description of the specific setup studied in this thesis. The tank system and design are described in Section 4.2. Following it is a description of the auxiliary parts and information about the equipment used in this chapter is found in Section 4.7 on page 31. The system for gathering data by the use of computer logging in Section 4.8 is followed by a description of the methods that has been used.

4.1 Overview

The experiments were performed at the Sollab, which is a small building outside the Physics Department at UiO¹. Its purpose is to study solar heating and radiative cooling applications in buildings. For the experiments conducted in this thesis an experimental setup, which represents a complete solar thermal system, were set up here for the experiments. The system consists of collectors on the roof, a solar tank with an integrated domestic hot water (DHW) tank, a floor tank and a floor integrated water loop. The collectors on the roof heat

¹University of Oslo

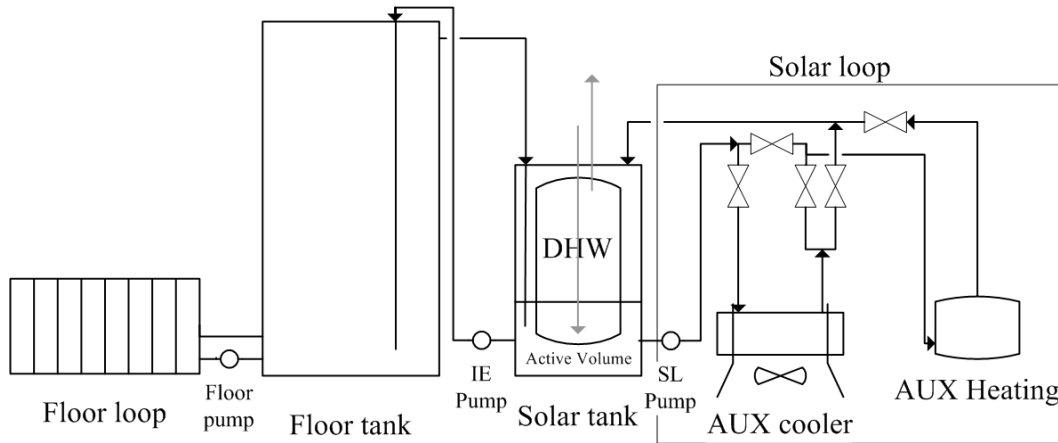


Figure 4.1: The components of the solar thermal system at the Sollab.

the system during the day and cool it during the night using night sky radiation as mentioned in Section 3.2, while insulated steel tanks filled with store the energy. The floor loop that is attached is used to heat or cool the Sollab.

For these experiments, the collectors on the roof, for heating and cooling purposes, were not yet ready. Instead, an external fan based fin cooler, auxiliary cooler, were mounted outside. Cooling was done by circulating water outside the Sollab and through the auxiliary cooler. For heating, the collectors have been replaced by a DHW heater for better reliability. This also results in the ability to achieve a flux of energy that can be controlled precise with defined start conditions. Using auxiliary components make the system independent of weather or time of day.

Figure 4.1 shows how all the parts are connected. The constituents in the figure from left to right are floor loop, floor pump, floor tank, inter-exchange pump, solar tank, solar pump, auxiliary cooler and auxiliary heater.

4.2 The tank system

The experimental setup consists of three tanks. Figure 4.3 represents a technical drawing of the tanks with their dimensions. To better visualize the system, Figure 4.4 is drawn in three dimensions. Important details are also marked and named. Throughout this chapter references to Figure 4.4 are made with

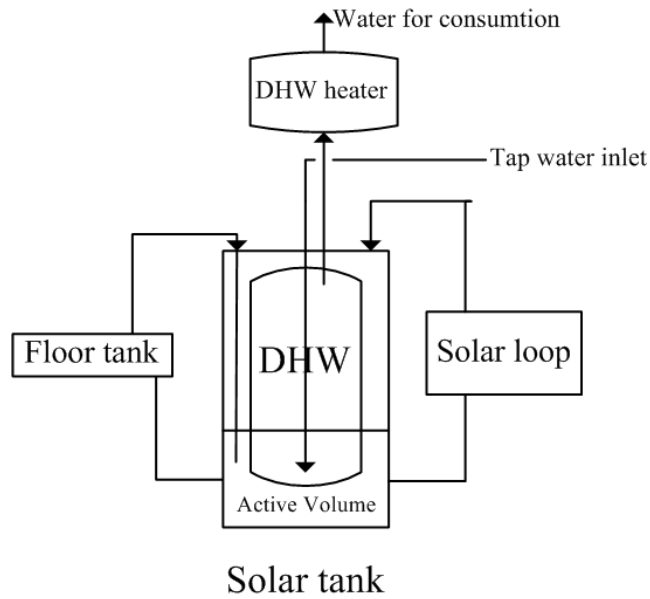


Figure 4.2: The system solar thermal system at the Sollab with an added DHW for extra heating of the DHW in the solar tank. The extra DHW above the solar tank is not installed at present.

parentheses; an example of this is the floor tank(a).

Figure 4.3 is a technical drawing of the system with measurements of all the parts in mm. The floor tank is the tallest tank(a). The solar tank, (k), is the smaller rectangular tank. Inside it is the DHW tank, (k), which is resting on a supporting ring, (e).

4.2.1 Internal DHW tank

The purpose of the DHW tank in a system in use is to provide hot water for domestic purposes. The volume of the tank is 200 l. Water in the DHW tank is separated from water in all other parts of the system. In this thesis there are no active tapping of water. No DHW is consumed, hence it has volume only dependent on thermal expansion. Thus, the system is in this respect passive.

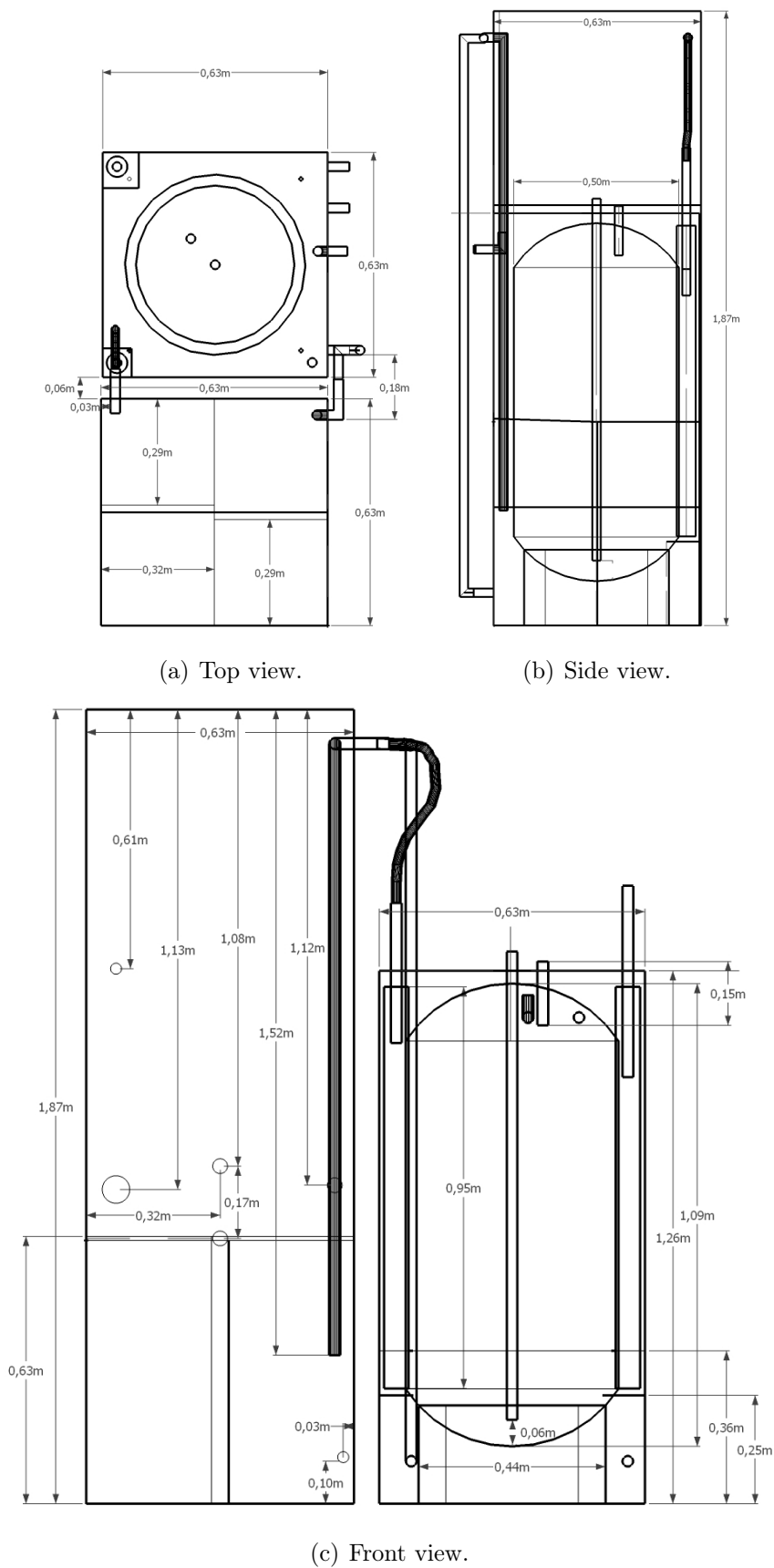


Figure 4.3: The tank system inside the Sollab. Figure is made using Google Sketchup [14].

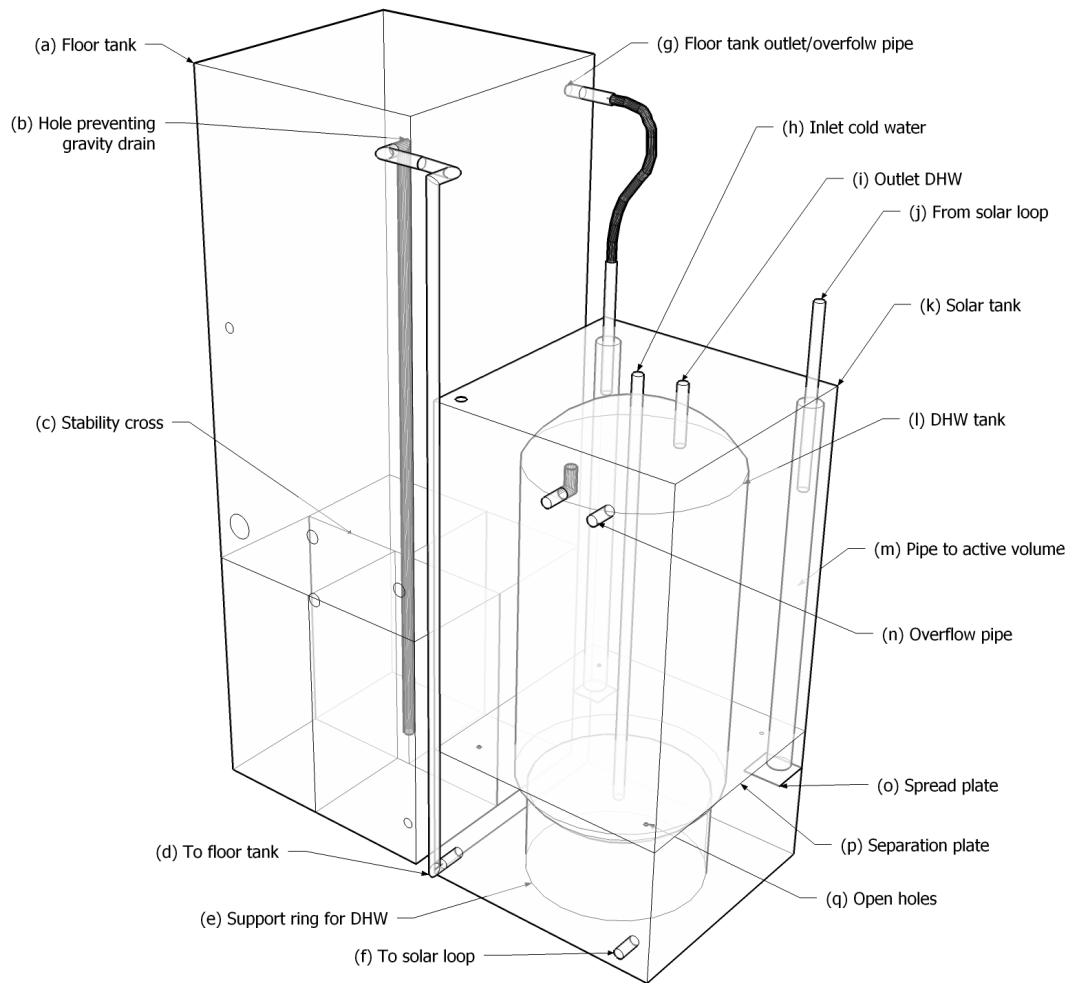


Figure 4.4: Details of the tank system. The different details are referred to in the text with its letter in parentheses e.g. floor tank(a). This figure shows the tanks without insulation and housing.

4.2.2 Solar tank

The solar tank is used as additional DHW storage, a volume buffer and for storing water looped in the simulated collectors. Its total volume is 500 l, and it contains 449 l of water including the DHW. The expansion of the tank as water extends the walls outwards, is not taken into account, but discussed as an uncertainty in Section 4.10.2. The solar tank is divided into two compartments, excluding the internal DHW tank. In the bottom compartment, the active volume, there are two inlets, (d) and (f), and two outlets, (g) and (j). The outlets lead the water to the pumps. One pump, the inter-exchange pump, lead water into the floor tank tank, while the other pump lead water into the solar loop. The two pipes leading into the solar tank come from the overflow in the floor tank and the return from the solar loop. When the inter-exchange pump lifts water into the floor tank, the water rises, and reaches an overflow pipe, (g), which brings the water back down into the lower compartment in the solar tank. The active volume has high mixing due to water always flowing in and out, creating turbulence. Therefore even temperature in the whole of the active volume is assumed.

In the top compartment, the upper volume of the solar tank, the water is at rest, almost not affected by the turbulent water in the active volume. A separation plate(p) make sure the compartments are separated. There are four holes(q) with a diameter of 10 mm in the separation plate and glitches between the plate and the DHW tank. These holes are deliberately put there to have the opportunity to insert temperature sensors. The separation plate has a hole with room for the DHW tank. The DHW tank is not welded to or tightly fitted into the hole. Instead the openings between the DHW tank let water flow up and down as needed. The water has to be able to move up and down as the water expands and compacts due to thermal expansion. In addition, the solar loop has an actual volume of water inside it when the solar loop pump is running. When the solar loop pump is not running the solar loop is empty and all its contents drains into the solar tank. The floor tank also fills up above the overflow pipe, using water from the solar tank. Some of the heated water in the solar tank will therefore be dragged down into the active volume when starting the inter-exchange pump or the solar loop pump. Because of this, the volume in the solar tank is not constant.

Water entering the active volume first enters the solar tank and comes into a wide pipe(m). This pipe is present to make sure no air bubbles are transported down to the active volume. Air bubbles in the active volume would have found their way out up through the top compartment of the solar tank. Air bubbles traveling upwards in water are contributing to mixing it. To keep the water in the compartment as layered as possible, no air should be allowed to enter the active volume from below. A thin pipe with high water velocity would let some air bubbles follow the water all the way down. Therefore a wider pipe which in turn has lower water velocity is placed to lead water down to the active volume. [5, 8]

Spread plates(o) are placed at the bottom of the pipes leading down into the active volume. This ensures that the water that is entering has horizontal and not vertical movement. Despite the above measures, if air enters the active volume and finds its way to the pumps, the pumps could stop or in worst case be damaged. The plates prevent air from entering the pumps, keeping the air in the top horizontal water layer.

When the system is in the heating state of poeration, the water in the bottom of the active volume is the coldest. Therefore the water to the solar loop is taken from the bottom to maximize the energy gain. Colder water gives a colder collector. A cold collector radiates and convects less energy to the surroundings than a warm collector, as is shown in Section 3.1. The solar tank including the DHW tank should have the warmest water, hence the floor tank gets the coldest of the hot water, also from the bottom of the active volume. This might seem contradictory to the assumption that the temperature in the active volume is equal in the whole volume, but the temperature of the water at the moment it enters the active volume will be different from the temperature of the active volume until it is mixed.

4.2.3 Floor tank

The floor tank is a larger storage of water with a volume of 0.704 m^3 or 704 l. This is based on the measured size of the tank. Since the floor tank is for floor heating and cooling, the temperature is lower than in the solar tank. A working temperature for the floor tank is down to about $15 \text{ }^\circ\text{C}$ for cooling purposes.

The temperature should not go below the dew point temperature, T_{dp} . At this temperature water from the air, air humidity, will condensate on the tank and could cause water damages. For heating purposes the tank can go up to about 60 °C. It is important to note that the floor tank is not an expansion of the DHW water store. It is present for house heating, not for domestic use. 60 °C is a high temperature for this use, and should be considered the maximum temperature rather than the normal working temperature.

The volume of 704 l of water expands 3.8 l when heated from 20 to 40 deg C. Another volume uncertainty is the expansion in as the water press on the tank walls. The stability cross(c) that is placed inside the floor tank has been evaluated by Hamazaoui et al. [16]. Stability calculations were conducted for two types of inner support for the floor tank, and implementation of the cross was done by welding. Their work showed that there was less deformation of the walls than their stability calculations had predicted. The authors concluded that the stability cross worked well.

4.2.4 Pumps

There are three pumps in the system. There are one pump for the floor loop, one inter-exchange pump between the two main tanks, and one between the solar tank and the simulated collectors. The system is designed to use only water. Water has a high heat capacity, 4.1819 kJ/kgK², making it a good medium for heat storage and transport. Transport means the transfer of heat between heat store, solar tank and collectors. Water is also readily available, cheap, easy to handle and environmentally friendly.

The water velocity was controlled by valves. The valve for the solar loop was tweaked until the preferred circulation velocity was reached by looking at the digital flow-meter.

²Heat capacity of water is also often written with other useful units, 1.1616 kWh/m³K.

Table 4.1: The table depicts all possible flows in the system, where n describes one of the 7 settings of the inter-exchange pump. The calculated volume flow for each setting is shown in units of m^3/h . Uncertainties of each flow is also listed. This table is a short version of Table A.4.

n	Flow(m^3/h)	Uncertainty(m^3/h)
1	0.128	± 0.007
2	0.200	± 0.009
3	0.24	± 0.01
4	0.29	± 0.01
5	0.35	± 0.02
6	0.36	± 0.02
7	0.40	± 0.03

4.3 Solar loop

The Solar loop consists up of a DHW heater, an external cooler and a flow-meter. Instead of solar collectors, a small DHW heater supplies heat to the system. All of the pipes in the loop are isolated to maintain as little heat loss as possible. The simulated collector is referred to as the solar loop. Valves are used to control the flow direction. Three possible directions can be achieved. The first loop is to only let the water flow through the auxiliary cooler. The second is only through the DHW heater and the third is through both. Before the collectors on the roof were decided to be left out of the loop, the roof collectors were used to cool together with the auxiliary cooler to maximize the cooling output. After the actual solar collectors on the roof were left out, the third option had no application.

4.3.1 External auxiliary cooler

Since the actual solar thermal collectors are not used, a device to cool water was needed. In this thesis an external Fincoil water to air cooler was used. Water is looped out through copper loops with fins, and the fan ensures that energy dissipate to the air. The energy flux is dependent on the difference between ambient temperature and the water temperature, and the flow velocity of the water.

4.3.2 Auxiliary heater

Due to the absence of collectors, a source of hot water is required. Therefore, a domestic hot water heater from Oso was installed in the solar loop. The heater produces 2 kW and had the ability to heat water to between 55 and 80 °C. A knob inside the panel of the heater was manipulated with a screwdriver to change the desired maximum temperature.

4.4 Normal operating state for heating

A normal operating state for the system is when it is used in a domestic situation. The system produces DHW for such purposes. Hence, there should always be enough hot water for that. If there at some point is no more hot water or not hot enough water, DHW are being consumed too fast, or the system is not dimensioned for the specific usage. The heating of DHW is done fully or partly by the sun. When there is not enough sun to heat the DHW tank to a desired temperature, the internal or external DHW heater continues the heating. Figure 4.2 shows how an external DHW heater can be installed. No extra DHW heater is installed in this experimental setup. The internal tank as it is in this experimental setup is shown in Figure D.1 in Appendix D.

When using solar heat, water from the solar loop enters the active volume and heats it. Water in the active volume then transfers the heat up in the solar tank partly by heat conduction and partly by transport of water through the gaps between the separation plate and the DHW tank. The transfer of heat will only be in an upwards direction if the water above the separation plate or in the DHW tank is colder than that of the active volume. The most preferable is to have only heat conduction. This is because movement in the water above the separation plate will create turbulence and hence the stratification of the tank will be disturbed.

There is no exchange of water from the active volume to the DHW tank. The DHW tank will be heated by conduction of heat from the active volume. If the water at the bottom of the DHW tank is heated too fast, the hot water could travel up in the tank, creating some degree of mixing and hence loss of stratification. Normally the transfer of heat from the solar collectors, to

the water, to the active volume and to the DHW tank will be continuous without large peaks in temperature. Therefore, there will be none or very little disturbance of the stratification in the DHW tank.

When DHW is consumed, cold water enters at the bottom of the DHW tank through the pipe(h) leading from the top of the DHW tank and down to the bottom, displacing the topmost and hottest water and making it exit through the outlet(i) at the top. The new cold water will stay at the bottom and by that keeping the stratification in the DHW tank.

4.4.1 Operating state for cooling

The main purpose of this thesis is to study the tank design when it is used for cooling. The cooling state of the system is when the solar loop removes heat from the system rather than adding heat. This happens at night when the collectors are able to remove heat from the system by the use of night sky radiation or convection. The solar pump and the IE pump run when the system is used to remove heat from the floor tank. Even when cooling, hot water is needed in the DHW tank. The separation plate creates an almost enclosed volume below it. As long as the water from the solar loop during cooling is colder than the water above the separation plate there is no convection up into the top chamber of the solar tank. So, if there is exchange of water it should only be because of flow caused by the inlets and outlets. The turbulence of the water in the active volume can cause water to transport some water up and down relative to the separation plate. There are, however, heat conduction from the top chamber down to the active volume.

The water in the part of the DHW tank that is below the separation plate will also be cooled by heat conduction. Heat is conducted from the DHW tank into the active volume. The water in the DHW tank will therefore be cooled down. Having the coldest water at the bottom of the DHW tank, there will still be stratification. Knowing this, and that water has low heat conductivity, the temperature of the water in the part of the DHW that is above the separation plate will not fall below the temperature of the water at the same height in the top compartment of the solar tank. This is assuming that no DHW is consumed and that the water returning from the solar loop is colder than the

water entering it.

4.5 Temperature monitoring

Monitoring and logging of the experiments is the most important task. Results from the Sollab come from the sensors placed in the system. Hence, it is important to place the sensors at good positions. There are several aspects to consider when placing sensors. Too many sensors make them obsolete, too few sensors cause low resolution and disappearing details. Below, the sensors are presented, followed by an explanation of the computer logging.

4.6 Temperature sensors

Temperatures are measured using thermocouples. All sensors in this thesis are thermocouples that measure temperature unless otherwise stated. A thermocouple is a contact sensor based on the Seebeck effect. It consists of two wires of different metals that are in contact with each other. This produces a voltage that can be measured. Thermocouples have a characteristic of 10 to 40 $\mu V/^\circ C$ depending on the type of sensor, meaning that for each degree the temperature changes, the voltage changes accordingly. The sensors are of type T. A type T sensor is made from a wire of copper and a wire of constantan, and is used because it is resistant to corrosion in moist environments. The producer gives the accuracy of the sensors to be $\pm 1.0^\circ C$ in a temperature range of $-25^\circ C$ to $+100^\circ C$.

A thermocouple is a relative sensor. It can only measure the difference in temperature between two junctions, or couples. The first junction is the twisted sensor tip itself and the second junction is the contact points over which the voltage is measured. The temperature of the second junction needs to be measured by an absolute sensor. The absolute measured temperature together with the voltage measured for the thermocouple, is used to calculate the temperature of the thermocouple. The terminal connector block of type TBX-68T from National Instruments [30] used in this thesis has an absolute temperature sensor for this purpose, a thermistor with an accuracy of $0.5^\circ C$.

Since the sensors are not linear, they were calibrated in the full temperature range they were used. Calibration showed that the sensors had a better accuracy than the producers stated them to have. This was, however, within a different temperature range. In the temperature range of 0 °C to 70 °C, the uncertainty³ of the measurements is $\pm 0.36^\circ\text{C}$. One standard deviation σ_T is 0.22 °C, meaning that 68% of the measured values will be within $\pm 0.22^\circ\text{C}$. Two of the sensors had a problem that sporadically made them measure a temperature that was far from the mean temperature. Later this was found to be a problem with the specific channel on the connector block, not the sensor itself. Therefore it should be mentioned that the median⁴ is $\pm 0.08^\circ\text{C}$. Calibration is done for all sensors and the procedure and tables are shown in Appendix A. [12, 21]

The sensor placement was decided on the basis of the total number of sensors available and the importance of accuracy in certain areas in the tank system. Two terminal connector blocks were used to connect all the sensors to the computer. Each connector block can read 15 sensors. One sensor on each connector block logged the block's own temperature, an absolute temperature sensor. Thus, there were 28 sensors available for placement in the tank system. Figure 4.6 shows how the data acquisition works. First the sensors have a physical response, then the connector block sends the voltage to the PCI⁵ card inside the computer and converts the voltage into a digital signal.

Figure 4.5 shows the placement of the sensors in the three tanks. All dimensions are in millimeters, the small black disks are sensors and the respective names on the sensors are the same as used in the resulting plots and description. Sensors in the solar tank and in the DHW tank are placed close to each other near the separation plate, making the vertical resolution high in this area. When cooling the floor tank, the active volume is used as an interim storage for the water, before it enters the floor tank. Therefore, when using a tank design with a separation plate as low as 36 cm above the bottom, the energy loss needs to be studied as closely and precise as possible. Sensors in the solar tank and the DHW tank are placed at the same heights, so that it is

³Uncertainty is the maximum deviation from the real value. In this case the real value is determined by a spirit thermometer.

⁴The median is here the median of the maximum deviations from the real value of each sensor.

⁵Peripheral Component Interconnect

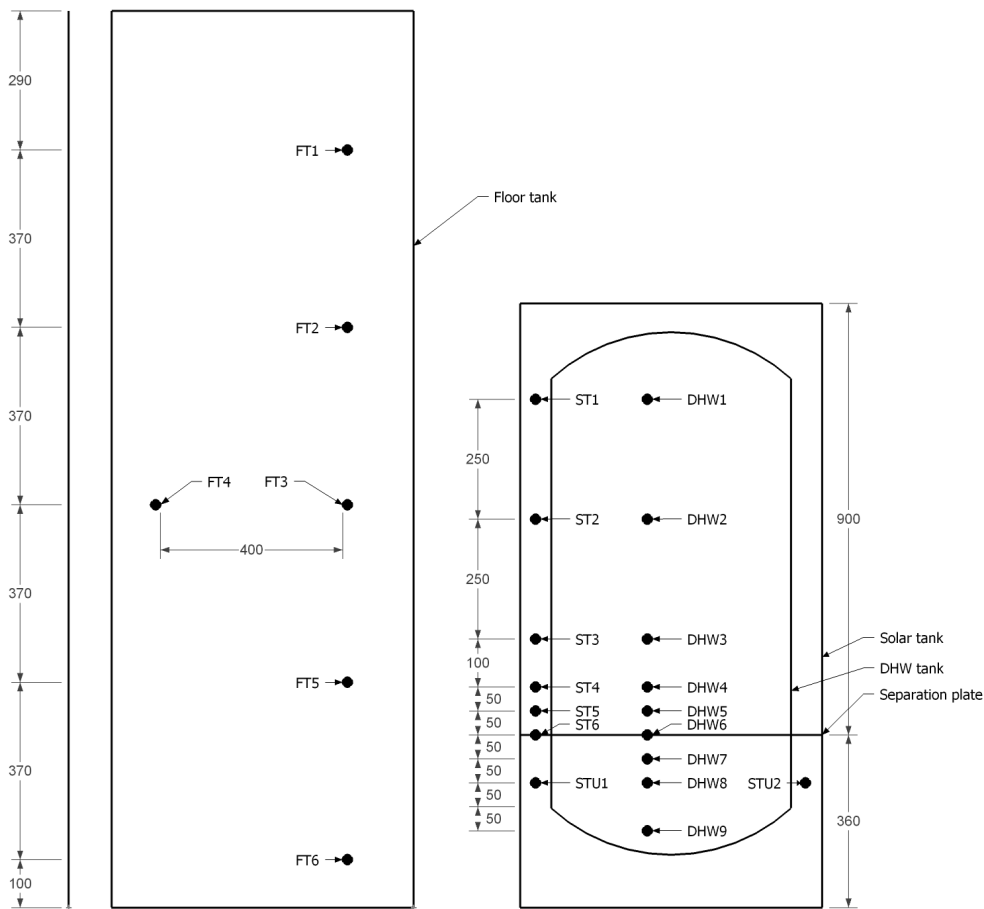


Figure 4.5: Sensors are placed in intervals from top to bottom in all three tanks. All dimensions are in millimeters. The small black points are sensors. The sensor named ST_6 is placed 5 mm above the separation plate.

possible to look at the energy transport between the tanks, and to study the temperature layers in the tanks.

The active volume has two sensors because the water is so turbulent that an average of these is a good enough measure of the temperature. The floor tank has six sensors, where two of the sensors in the floor tank are at the same height, but at different horizontal positions. This is to see if there is difference in temperature, which needs to be taken into considerations when calculating the energy in the tank.

A method for measuring which could require considerable less sensors is the calorimetric method. This method has often been applied by our research

group [28]. The reason for not using this method is that it is important to have a high vertical resolution around the separation. It needs to be high enough to look at energy fluxes in this particular tank design. The calorimetric method considers the system as a calorimeter to find the energy that is gained or used. It considers the whole system, whereas the goal in this thesis is to look at internal temperature differences.

4.7 List of equipment

For easy reference, equipment and specifications are listed below.

- Water circulation pump (Internal exchange and floor loop) [15]
Producer: Grundfos
Type: UPS 25-60 B 180
Class: H
Max pressure: 10 bar
Power consumption: (40 - 100) W / (0.2 - 0.44) A (in 7 steps)
- Water circulation pump (Solar loop)
Producer: Grundfos
Type: UPS 25-80 B 180
Class: F
Max pressure: 10 bar
Power consumption: 245 W, 1.04 A
- Domestic hot water heater.
Producer: *Ozo*.
Type: RD 30
Power: 2 kW. (Measured: 1.9 kW)
- Flowmeter (Solar loop)
Producer: Enermet
Type: 9V-MP115
Voltage, freq., power: 230 V; 50 Hz, 10 VA
- Auxiliary cooler [11]
Producer: Fincoil

Type: SOLAR Junior G-5-1-500-1400-1

Volume (water): 8 l

- Thermocouple [20]
Producer: Labfacility Ltd (UK)
Type: T
Wires: Copper (Cu) and constantan (Cu-Ni alloy)
Accuracy: ± 1.0 K (from manufacturer)
- Terminal connector block
Producer: National Instruments
Type: TBX-68T
Inputs: 25
- PCI-card
Producer: National Instruments
Type: 4351

4.8 Hardware and logging software

There is a long chain of events when measuring a temperature. First, a sensor has a physical response to the temperature around it, and then the signal is conducted through the connector block collecting all sensors and sending it further to a data card which interprets the voltage into digital signals that computer software can read. Once set up, it is very manageable. When the data has been saved to a computer data file, the interpretation and visualization of the results can be done.

4.8.1 LabVIEW

The computer software LabVIEW⁶ [6] is used to log the temperatures of the system. Amongst other things, it does data acquisition and simulation in

⁶LabVIEW - Laboratory Virtual Instrumentation Engineering Workbench - Version 7.1.

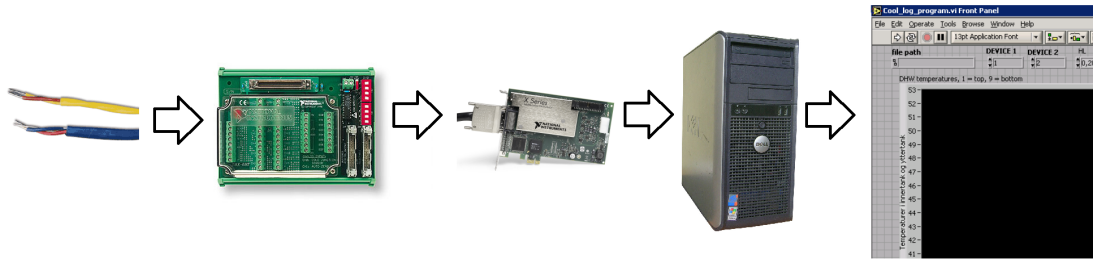


Figure 4.6: Collecting of measurement data. A response from a sensor is sent to the connector block. From there the voltage from the sensors is sent collectively to an internal computer card. The card translated the voltages into digital signals and sends them to the software for logging.

physics and electronics. Combined with data cards and sensor connection blocks it can be used to collect experimental data used in this thesis.

LabVIEW does not collect data by itself. A program in the LabVIEW programming language has to be made. In LabVIEW, such a program is called a *virtual instrument*. The program has to compensate for sensor calibration and hardware manufacturer specifications. After that the calibration of the sensors in their environment needs to be corrected for. The programs interface is shown in Figure C.1 in Appendix C. The top row in the program lets the user decide on start parameters. All these parameters are constant as seen in the figure, except of the time step. Trying out different time steps, 30 seconds was the shortest time step the hardware could handle. Time steps lower than this resulted in 30 seconds time step anyway. In addition to this, when studying the data gathered in details, it is found that every now and then the system jumps one more second ahead. This could be because the system does not report every 30 seconds exactly, but rather 30 seconds plus a fraction of a second. No explicit reason for this has been found. This is taken into account in later calculations.

The internal workings of the program, the program "code", is shown in Figure C.2 in Appendix C. At the left side, outside the program loop, is the input of all the sensors. The first column of gray outlined boxes calculates the temperature of the sensors from the voltage the sensors are measuring. To make the system correct, every sensor has to be calibrated individually. The boxes doing the calibration are marked with "calibration" above them. After obtaining the correct, calibrated and compensated temperatures, they are plotted in the

Chapter 4: Experimental setup and methods

2008	10	21	09	04	31	944,076431	73,905582	73,986543	73,797777	73,904390	73,948813	73,942000
2008	10	21	09	04	48	944,110722	73,866680	73,929615	73,878929	73,887053	73,901881	73,918038
2008	10	21	09	05	12	944,215299	73,870653	73,945114	73,797554	73,935420	73,864720	73,880795
2008	10	21	09	05	42	944,381260	73,857807	73,942193	73,811054	73,924280	73,865094	73,910837
2008	10	21	09	06	12	944,683074	73,879376	73,915904	73,843953	73,899689	73,884913	73,958715
2008	10	21	09	06	42	944,858948	73,845266	73,965946	73,865874	73,882187	73,890440	73,929645
2008	10	21	09	07	12	945,061994	73,859686	73,949011	73,875267	73,866930	73,886699	73,955560
2008	10	21	09	07	42	945,280757	73,864538	73,929127	73,752099	73,855309	73,875082	73,950511
2008	10	21	09	08	12	945,394861	73,848890	73,971208	73,853065	73,884150	73,882534	73,920074
2008	10	21	09	08	42	945,586533	73,836615	73,940836	73,799858	73,913056	73,840715	73,912777
2008	10	21	09	09	12	945,874741	73,852924	73,952156	73,817691	73,886520	73,873392	73,917504
2008	10	21	09	09	42	945,975844	73,836987	73,903296	73,849452	73,818011	73,839441	73,873592
2008	10	21	09	10	12	946,148477	73,804455	73,963157	73,779416	73,904079	73,843252	73,938392

Figure 4.7: A part of a data raw file as LabVIEW outputs it.

Table 4.2: Measurements from data files, cronologically, but split into three table to make room for all of them. *ST* = Solar Tank, *FT* = Floor tank, *DHW* = Domestic hot water, *I* = Input, *O* = Output, *V* = Voltage, *ref* = reference, *Dev* = Device.

(a) Part one

Value	Year	Month	Day	Hour	Minute	Second	$Vref_{Dev1}$	DHW_1	DHW_2	DHW_3	DHW_4	DHW_5
Unit	(YYYY)	(MM)	(DD)	(h)	(m)	(s)	(μ V)	($^{\circ}$ C)	($^{\circ}$ C)	($^{\circ}$ C)	($^{\circ}$ C)	($^{\circ}$ C)

(b) Part two

Value	DHW_6	DHW_7	DHW_8	DHW_9	ST_I	ST_O	FT_I	FT_O	TA	$Vref_{Dev2}$	ST_1	ST_2
Unit	($^{\circ}$ C)	($^{\circ}$ C)	($^{\circ}$ C)	($^{\circ}$ C)	($^{\circ}$ C)	($^{\circ}$ C)	($^{\circ}$ C)	($^{\circ}$ C)	($^{\circ}$ C)	(μ V)	($^{\circ}$ C)	($^{\circ}$ C)

(c) Part three

Value	ST_3	ST_4	ST_5	ST_6	ST_{I1}	ST_{I2}	FT_1	FT_2	FT_3	FT_4	FT_5	FT_6
Unit	($^{\circ}$ C)	($^{\circ}$ C)	($^{\circ}$ C)	($^{\circ}$ C)	($^{\circ}$ C)	($^{\circ}$ C)	($^{\circ}$ C)	($^{\circ}$ C)	($^{\circ}$ C)	($^{\circ}$ C)	($^{\circ}$ C)	($^{\circ}$ C)

program's interface and saved to a data file.

The data files contain 36 columns of values. This is more than the 30 sensors mentioned above. The additional 6 values are year, month, date, hour, minute and second. In Table 4.2 is a list of the different value names, in the order they appear in the files. In Figure 4.7 is a part of a raw file from LabVIEW.

One problem that occurred when analyzing results was that the indoor temperature was not directly logged. It was logged through the values $Vref_{Dev1}$ and $Vref_{Dev1}$. From these, the temperature had to be calculated through the solution of the cubic equation. All values for the room temperature are an average of the two sensors, thus minimizing the uncertainty and obtaining a better value.

4.9 Methods

Methods used in this thesis are presented here. Ways to interpret the results are needed, and they are described here. The theory in this section is deduced from the theory in Section 3. Programming is done using the programming language Python.

4.9.1 Weighting of sensors

Table 4.3 lists the temperature sensors and the volume they each measure. Calculation of the volumes is done by first dividing the tank into vertical domains. This can be done taking advantage of the principle from Section 3.4.3. It is possible to divide the tank into horizontal layers because each layer only transports down when the tank is stratified.

4.9.2 Calculation of heat loss and gain

In each experiment, the gained energy in the heat store was calculated along with the loss in the solar tank. The values are calculated on the basis of the temperature change in each tank and the tank's volume. The energy gain and loss of each partial volume of each tank, shown in Table 4.3, were calculated and added together. Equation 3.10 is used to make a sum that adds up all layers of water in the tank

$$Q_{\text{total}} = \sum_i^n cm_i(\Delta T)_i, \quad (4.1)$$

where Q_{total} is the heat lost from the tank measured in the unit of Joule, m_i is the i 'th mass, c is the heat capacity and n is the total number of volumes.

Table 4.3: Volume of water for each sensor, e.g. sensor FT₁ measures the temperature of 79.4 liters of water.

Sensor	Volume	Volume(l)	Volume(m ³)
FT ₁	V ₂₂	79.4	0.0794
FT ₂	V ₂₁	146.9	0.1469
FT ₃	V ₂₀	73.4	0.0734
FT ₄	V ₁₉	73.4	0.0734
FT ₅	V ₁₈	146.9	0.1469
FT ₆	V ₁₇	113.1	0.1131
ST ₁	V ₁₆	32.5	0.0325
ST ₂	V ₁₅	50.1	0.0501
ST ₃	V ₁₄	35.1	0.0351
ST ₄	V ₁₃	15.0	0.0150
ST ₅	V ₁₂	10.0	0.0100
ST ₆	V ₁₁	5.0	0.0050
DHW ₁	V ₁₀	31.8	0.0318
DHW ₂	V ₉	49.1	0.0491
DHW ₃	V ₈	34.4	0.0344
DHW ₄	V ₇	14.7	0.0147
DHW ₅	V ₆	9.8	0.0098
DHW ₆	V ₅	9.8	0.0098
DHW ₇	V ₄	9.8	0.0098
DHW ₈	V ₃	14.7	0.0147
DHW ₉	V ₂	12.2	0.0122
ST _{U1}	V ₁	50.6	0.0506
ST _{U2}	V ₀	50.6	0.0506

4.9.3 Heat loss

The heat loss of the solar tank is the loss from the water inside it, through the walls and insulation and into the room and walls. Using Equation 3.6 and Equation 3.10 results in an expression for the overall heat loss for the solar tank. Rearranging Equation 3.10 to

$$Q_H = cm_s \Delta T_Q, \quad (4.2)$$

with m_s and ΔT_Q being the mass of water in the solar tank and the temperature change needed for the material to absorb or emit the amount Q_H of heat. Then, rearranging Equation 3.6 and inserting Q_H in the place of ΔQ ,

$$\begin{aligned} \left(\frac{kA}{\Delta x} \right) &= \frac{\Delta Q}{\Delta t \Delta T_{st}} \\ &= \frac{cm_s \Delta T_Q}{\Delta t \Delta T_{st}}, \end{aligned} \quad (4.3)$$

where ΔT_{st} is the temperature difference between the solar tank and the room. This gives a new value, a coefficient for the heat loss. The new value, $\left(\frac{kA}{\Delta x} \right)$, is made up of three properties of the tank. These properties cannot be found explicitly as separate constants because the thickness of the walls is not equal all around the tank. Furthermore, there are also corners where insulation is suddenly thicker, and the walls of the tank face the room at three sides. The other three sides face the outside wall, the heat store and the floor. Hence the new value should not be considered as the product of three values, but rather a value that defines a property of the solar tank.

4.9.4 Simulation of heat transfer

Simulating the heat loss in an enclosed tank of water can be done with a discretization of Equation 3.6 and use of Equation 3.10. Since the water in the tank is considered to be at rest for this simulation no more than one dimension is needed. This simulation will be of the solar tank. The tank is equal in depth and width, so the only iterations needed are along the z -axis, upward, and in

time. The tank is being split into volumes of area A and height dL . Each piece has an energy defined by Equation 3.10 by defining ΔT to be equal to its absolute temperature. This energy changes linearly with its temperature. Figure 4.8 show the discretization at time $t=0$. Each volume is represented by a point on a one dimensional line. At time $t=1$ the energy will be

$$\begin{aligned}
 Q_i &= Q_i + Q_{i-1} - Q_{i+1} \\
 T_i \cdot c \cdot m &= T_i \cdot c \cdot m - \frac{k \cdot A}{dL}(T_i - T_{i-1}) + \frac{k \cdot A}{dL}(T_{i+1} - T_i) \quad (4.4) \\
 T_i &= T_i + \frac{k \cdot A}{dL \cdot c \cdot m}(T_{i-1} + T_{i+1} - 2 \cdot T_i).
 \end{aligned}$$

Transitions used are

$$\begin{aligned}
 Q_i &= c \cdot m \cdot \Delta T = c \cdot m \cdot T_i \\
 Q_{i-1} &= H_{i-1} \cdot t = -\frac{k \cdot A}{dL}(T_i - T_{i-1}) \quad (4.5) \\
 Q_{i+1} &= H_{i+1} \cdot t = -\frac{k \cdot A}{dL}(T_{i+1} - T_i).
 \end{aligned}$$

Equation 4.4 shows that the temperature can be calculated using °C and not absolute temperature, K. Since all of the parameters are constants, the only thing changing over time is the temperature T . c and m in the equation are the specific heat of water and the weight of a single discrete volume:

$$m = AdL \cdot 1000[kg]. \quad (4.6)$$

Using this, Equation 4.4 can be further simplified into

$$T_i = T_i + \frac{k}{dL^2 \cdot c \cdot 1000}(T_{i-1} + T_{i+1} - 2 \cdot T_i). \quad (4.7)$$

A small program is made using the programming language Python. Ideas and concepts for the program was found in *A Heat Transfer Text Book* [25] and *A Primer on Scientific Programming with Python* [22]. Equation 4.7 is used by the program to calculate the heat conduction. The program takes different

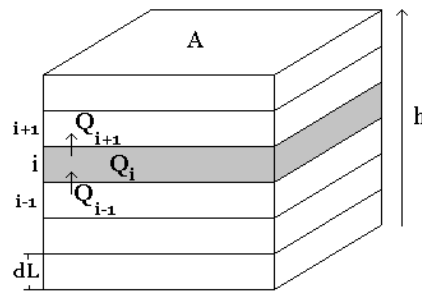


Figure 4.8: A discretized model of a part of the the tank. The tank is split into horizontal parts. Each part has a temperature. Based on the temperature of each part, the heat conduction between each part can be calculated for a series of time-steps.

inputs to be able to accommodate for different initial conditions of the solar tank. These options are the step length dL in meters, the runtime in hours, the length of the time steps in seconds, the temperature of the top volume, the temperature of the active volume and the height of the separation plate in meters. An example of an output is shown in Figure 4.9. The input parameters are put on top of the figure in the respective order mentioned above.

The cross-section of the walls of the tank, including the solar tank and the DHW tank, have an area of 40.9 cm^2 . This is only true where the cross-section of the tank has a radius of 25 cm. The tank is made from steel⁷ which has a thermal conductivity of 16.2 W/mK . Comparing this to the cross-section area of the water which is 0.37 m^2 , where water has a thermal conductivity of 0.609 W/mK , it is found that the steel is the cause of 25% of the heat conduction in the tank. In the program, this is compensated for by altering the thermal conductivity constant of water. The total heat conductivity constant for 40.9 cm^2 of steel and 0.37 m^2 of water is found to be 0.76 W/mK , which is used in the simulation.

4.10 Uncertainties

Uncertainties are listed in Table 4.4 along with explanations of the values.

⁷Steel type: 316L

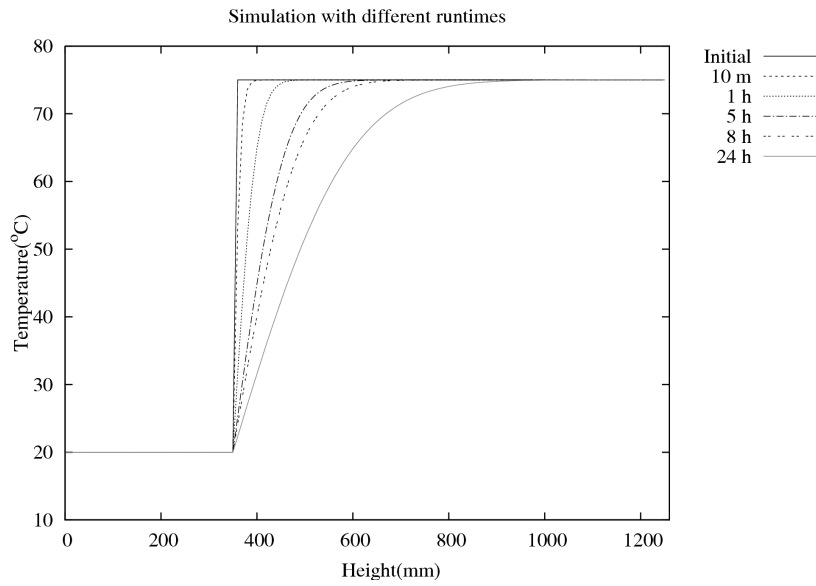


Figure 4.9: An example of a simulation of the heat transfer in the water in the solar tank. The plots are the temperature of the water versus the height in the tank. In the simulations, it is also assumed that the water is at rest.

4.10.1 Temperature sensors

All sensors and uncertainties regarding the temperature sensors are considered in the uncertainty calculations. The thermistor on the terminal block, the spirit thermometer, the immersion bath and the thermocouples have uncertainties. The calibration of the temperature sensors showed that they had an uncertainty of ± 0.4 °C. Appendix A.1 gives the details of the calibration.

4.10.2 Volume of tanks

The estimate of the uncertainty of the volume of the tanks is based on two things. The first is the uncertainty in the measured dimension of the tanks. The uncertainty is better than ± 1 mm in each direction. The volume uncertainty is

$$\begin{aligned}
 \Delta V_{ST} &= 0.001 \text{ m}(0.63 \text{ m} 0.63 \text{ m} + 0.63 \text{ m} * 1.13 \text{ m} * 2) \\
 &= 0.0018207 \text{ m}^3 \approx 2 \text{ l} \\
 \Delta V_{FT} &= 0.001 \text{ m}(0.63 \text{ m} 0.63 \text{ m} + 0.63 \text{ m} * 1.80 \text{ m} * 2) \\
 &= 0.0026649 \text{ m}^3 \approx 3 \text{ l}.
 \end{aligned}
 \tag{4.8}$$

The uncertainty in the volumes because of expansion of the tank walls is estimated to be 8 and 5 l for the floor and solar tank respectively. This is based on a project work done by Hamazaoui et al. [16]. After the filling of the tank the physical deformation of the tank was found. The tanks were measured before and after filling, and were found to increase 7 mm in circumference. The volume was not measured directly. My estimation is a calculation based on the circumference, area and volume of a cylinder with an increased radius of 7 mm.

Table 4.4: Uncertainties of the equipment and sensors used in this thesis are listed here.

Item	Uncertainty	Comment
Thermistor on terminal block	$\pm 0.5 \text{ }^\circ\text{C}$	Removed by calibration of the thermocouples.
Immersion bath	$\pm 0.4 \text{ }^\circ\text{C} \pm 0.5\%$	Removed by use of spirit thermometer.
Spirit thermometer	$\pm 0.05 \text{ }^\circ\text{C}$	Can be read as accurate as $0.1 \text{ }^\circ\text{C}$. Ice water is used as reference for true zero $^\circ\text{C}$.
Thermocouple	$\pm 1 \text{ }^\circ\text{C}$ $\pm 0.4 \text{ }^\circ\text{C}$	Producer rating After calibration. See Appendix A.1 for details.
Volume of FT	$\pm 3 \text{ l}$ $\pm 8 \text{ l}$	Estimated uncertainty because of dimensions of the tank Estimated uncertainty because of tank wall expansion
Volume of ST	$\pm 2 \text{ l}$ $\pm 5 \text{ l}$	Estimated uncertainty because of dimensions of the tank Estimated uncertainty because of tank wall expansion
IE pump flow		Evaluated in Appendix A.2. See Table A.4.
Solar loop flow	$0.005 \text{ m}^3/\text{h}$	Display of Enermet flowmeter show two decimals, e.g. 0.36.

4.10.3 Conductive heat loss

The heat loss from the solar tank that is caused by conduction into the room can be described by Equation 6.4 when the temperature is even throughout the whole tank. This could not be calculated into the results because the tanks do not have a uniform temperature during the cooling experiments, the tanks are stratified. Since this is not calculated into results, it is instead set to be an uncertainty. There will be additional heat loss because of this.

Chapter 5

Experiments

The experiments were done to log the temperatures of the tank system during cooling. The temperatures are measured at 28 positions using 28 temperature sensors. The sensor placements are shown in Figure 4.5.

This chapter describes the execution of the experiments in Section 5.1. In addition a list of the experiments and a description of the resulting plots are presented in Section 5.2 and 5.3, respectively.

Chapter 6 present the resulting plots and details of the temperatures in the tank system.

5.1 Execution of the experiments

The experiments were conducted as follows. First the solar tank and the DHW tank was heated to a desired temperature with the solar loop using only the DHW heater. Upon reaching the desired temperature, the DHW heater was stopped, the fan of the auxiliary cooler was started and the flow in the solar loop was changed to include only the auxiliary cooler. When the temperature of the active volume reached below the temperature of the floor tank, the

Table 5.1: List of measurement series from the Sollab.

Experiment	Date	Filename	Period (<i>from - to</i>)	Lines
1	21.10.2008	<i>08.10.21.dat</i>	2008-10-21 09:04 - 2008-10-22 14:03	3479
2	27.10.2008	<i>08.10.25.dat</i>	2008-10-25 10:29 - 2008-10-28 09:54	8691
3	28.10.2008	<i>08.10.28.dat</i>	2008-10-28 09:55 - 2008-10-30 16:29	6551
4	11.08.2009	<i>09.08.11.dat</i>	2009-08-11 16:13 - 2009-8-15 16:18	11531

IE pump was started. The system was in this state of operation until the experiment ended.

5.2 Experiment list

The experiments took place in the Sollab and were conducted in September and October of 2008. In Table 5.1 the present measurement series are listed and described. Some experiments started days before and ended days after the actual used data. That is why the dates and filenames do not coincide in the table.

5.3 General description of plots

All the plots are shown in Section 5.4. The plots are also shown in the results, Chapter 6, when they are needed. Plots shown in Chapter 6 are not removed from Section 5.4. Plots are made with the programming language Python using the plotting software Gnuplot¹.

5.3.1 Temperature plots

Each experiment from Table 5.1 is represented by four temperature plots, which are the temperature monitoring in Figure 5.1, 5.2, 5.5, 5.6, 5.9 and

¹Gnuplot is a powerful open-source plotting software.

5.10. There is one plot for each tank, and an additional plot for the inlet, outlet, indoor and ambient temperature measurements. The legend shows the labels of the sensors, which are defined in Figure 4.5. The plots display the temperature in °C versus time in seconds. The vertical lines mark changes to the volume flow. That is, at each vertical line there is a change in where the water enters and leaves the tank system and where it originates from. These changes are: turning on or off the domestic hot water heater, auxiliary cooler or the inter-exchange pump. To better describe the events, the time between the vertical lines are marked by roman numbers, e.g. **I,II**. The actions at each vertical line is presented in Table 5.2.

*Table 5.2: List of actions taken during the experiments. The roman numbers, **I**, span the time and actions that happen during that time.*

Date	Period	Time	Actions
21/10			Solar tank temperature is 74 °C
	I	09:50	Auxiliary cooler ON ^a
			Solar loop flow is 0.36 m ³ /h
	II	10:30	IE pump ON
			IE flow is 0.24 m ³ /h
	16:16	Auxiliary cooler OFF	
27/10			Solar tank temperature is 50 °C
	I	13:45	Auxiliary cooler ON
			Solar loop flow is 0.34 m ³ /h
	II	14:14	IE pump ON
			IE flow is 0.24 m ³ /h
	16:41	IE OFF	
28/10			Solar tank temperature is 50 °C
	I	13:54	Auxiliary cooler ON
			Solar loop flow is 0.36 m ³ /h
	II	16:20	IE pump ON
			IE flow is 0.24 m ³ /h
	17:45	Auxiliary cooler OFF	

^aTurning on the auxiliary cooler also implies stopping the DHW heater and switching the solar loop's valves from heating to cooling.

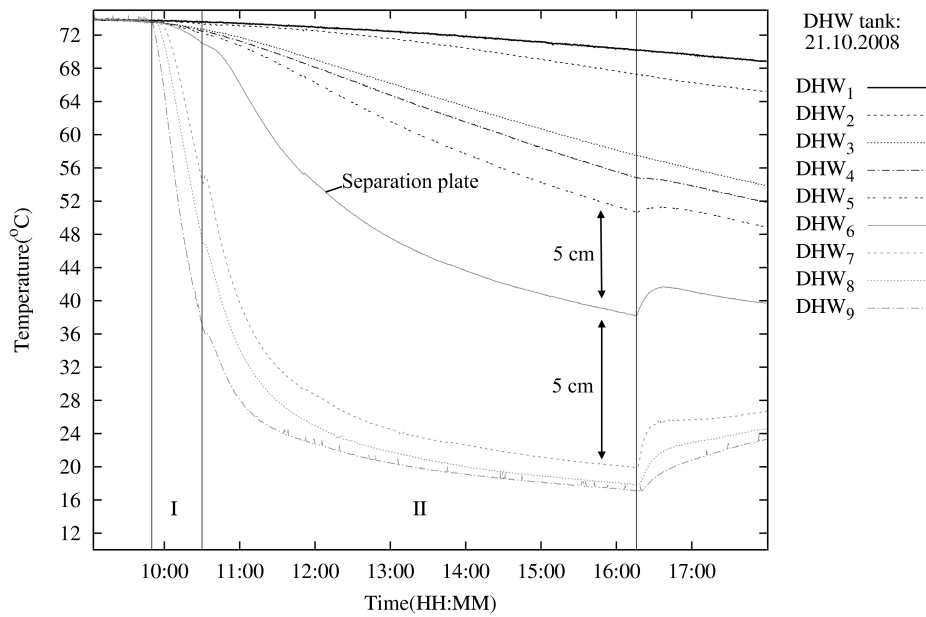
5.3.2 Stratification plots

The next type of plots shows the temperature of each layer in the tanks. These plots are 5.3, 5.7 and 5.11. There are three plots for each experiment, one for each tank. All plot lines are the temperature in °C versus the height of the placement of the sensors inside the tank at a certain time defined in the legend. The time between one plot line and the next is one hour. The x-axis of the plots is the height of the tanks in mm and ranges from 0 mm to 1260 mm. There are three vertical lines in the plots. These represent from the left to the right, the bottom of the solar tank, the separation plate and the top of the solar tank. The vertical lines are placed at 110 mm, 360 mm and 1200 mm, respectively.

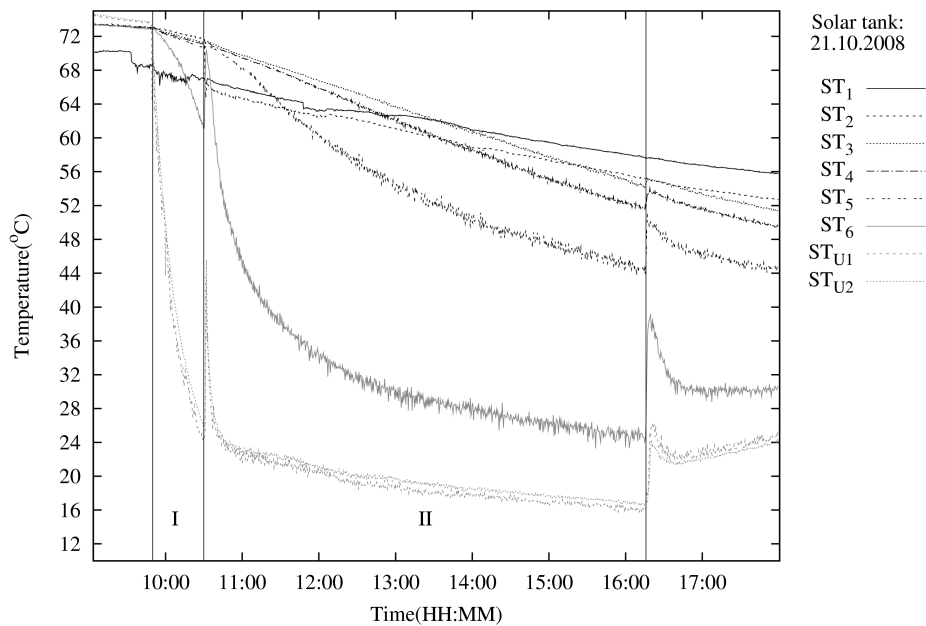
5.3.3 Temperature change plots

Figure 5.4, 5.8 and 5.12 show the temperature change of each layer. There are three plots for each experiment, one for each tank. The temperature change plotted is measured by the sensor shown at the x-axis. The temperature change is measured in °C.

5.4 Resulting plots

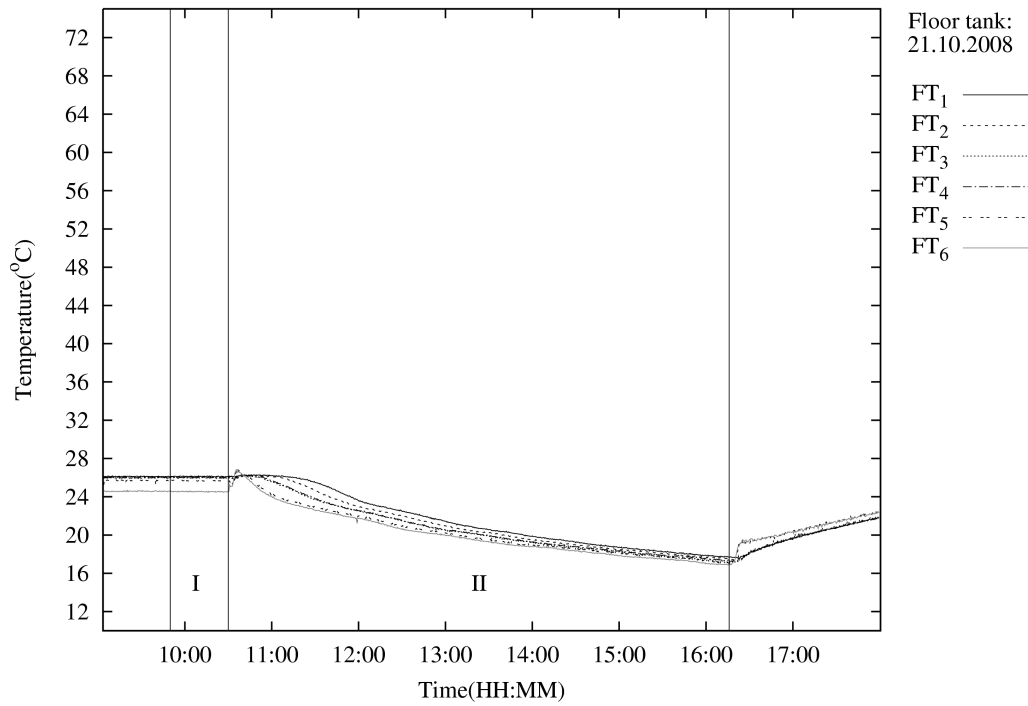


(a) DHW tank.

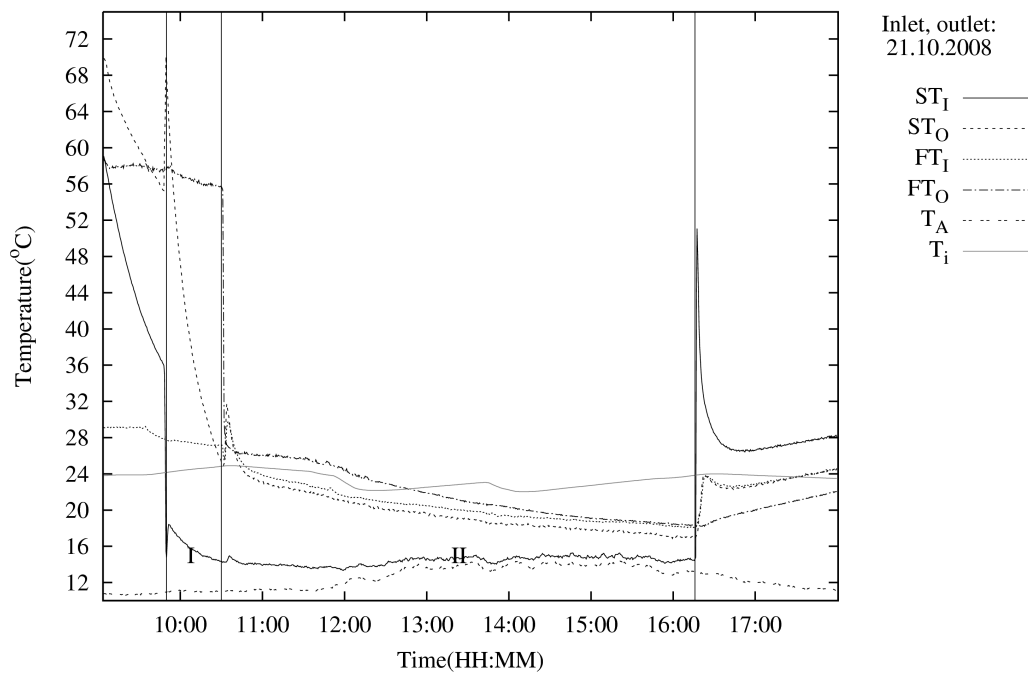


(b) Solar tank.

Figure 5.1: A cooling experiment, showing two periods marked with **I** and **II**, respectively. Each period is between two vertical markers. Exact position of the markers are found in Table 5.2. Period **I** is when the auxiliary cooler is running, thereby cooling the active volume, and period **II** is when the IE pump is running in addition to the auxiliary cooler.

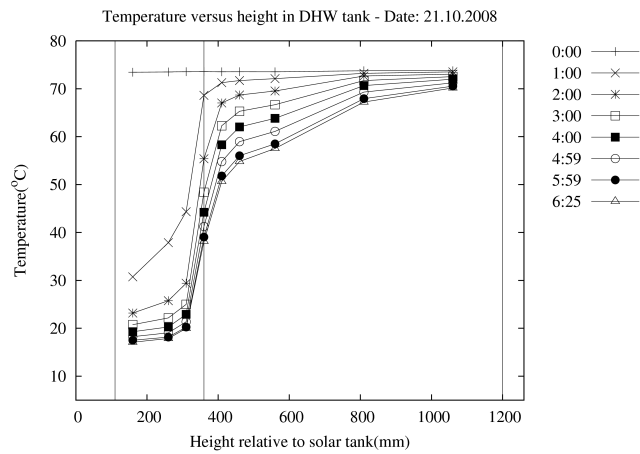


(a) Floor tank.

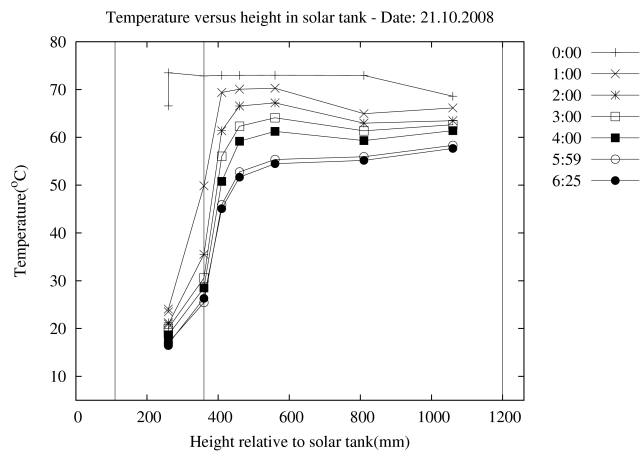


(b) Inlet, outlet, ambient and indoor temperature.

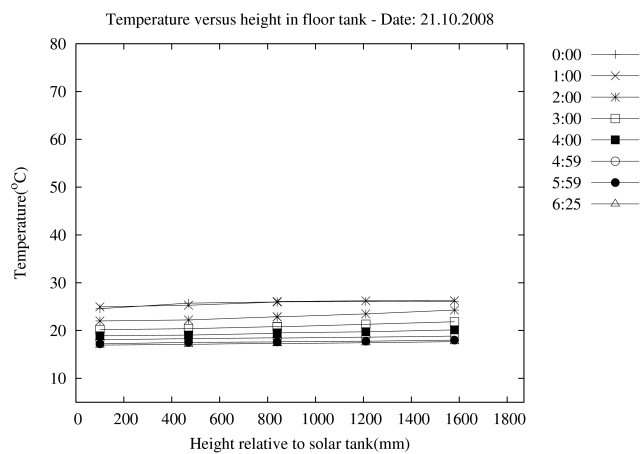
Figure 5.2: See Figure 5.1 on the preceding page for description.



(a)

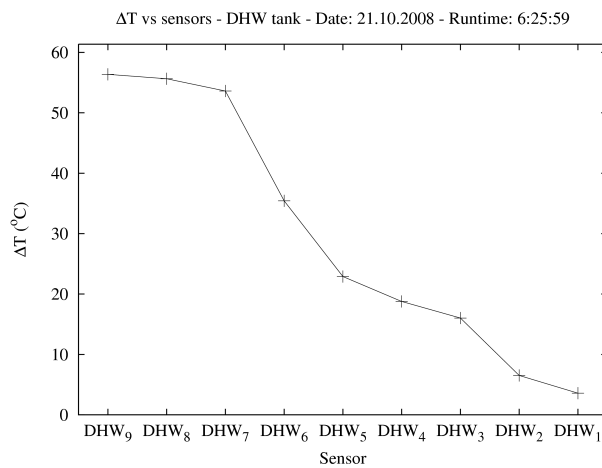


(b)

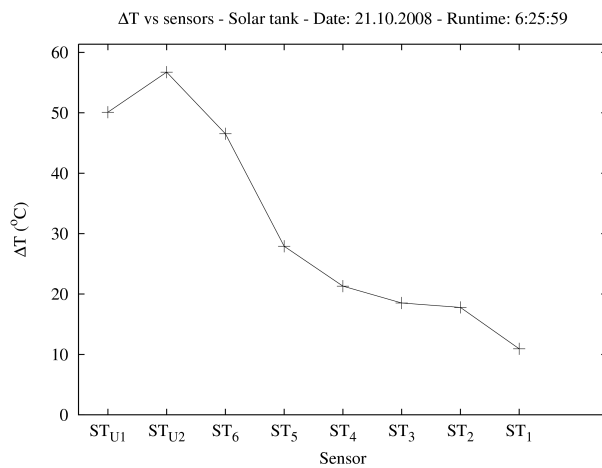


(c)

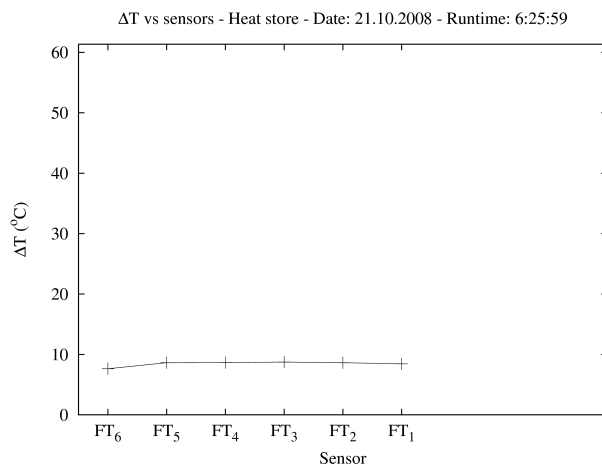
Figure 5.3: Each plot line show the temperature at the height of each sensors in the tanks. The first plot line, the top plot line, is the temperatures at the start of the cooling experiment. The subsequent plot lines show the temperature at a later moment found in the legend.



(a)

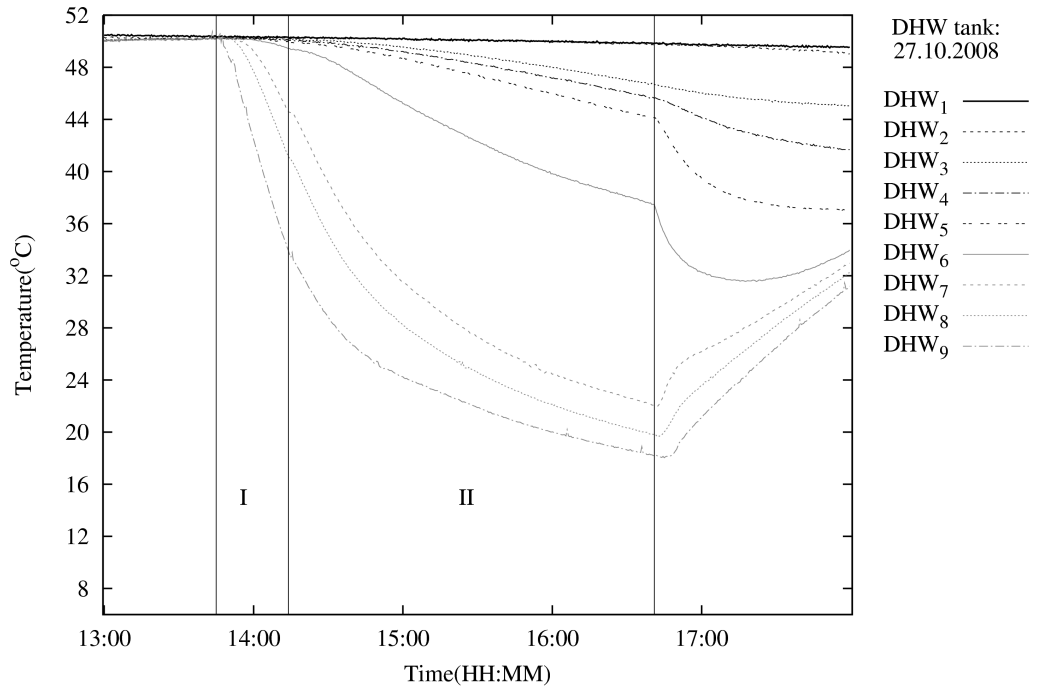


(b)

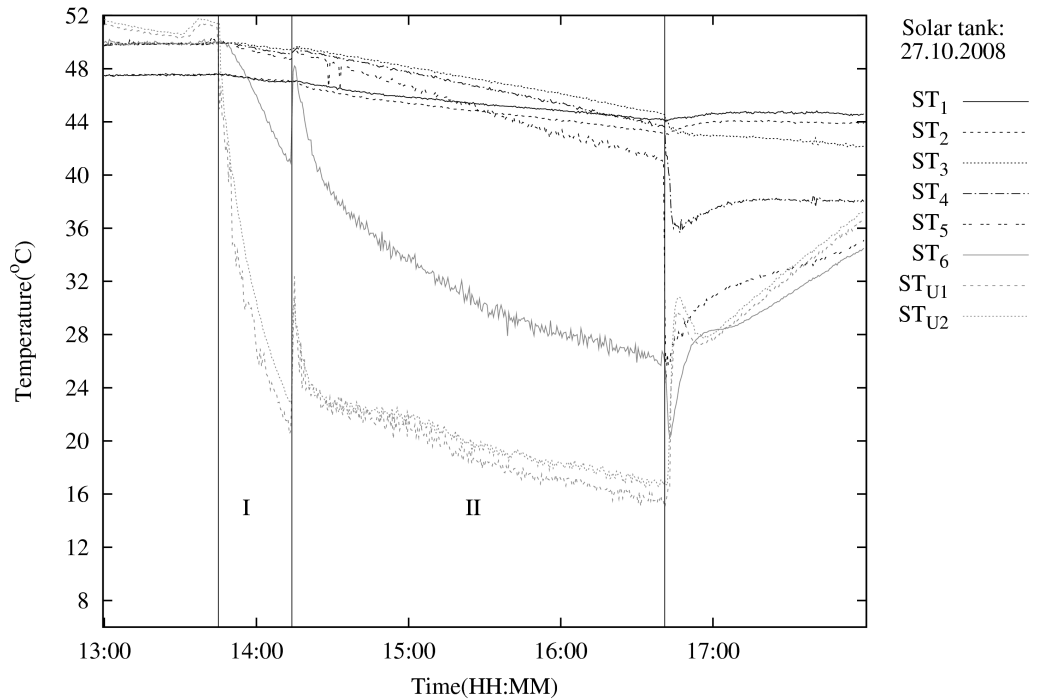


(c)

Figure 5.4: The temperature difference measured by each sensor between start and stop of the cooling experiment. The figure does not have absolute height on the x-axis.

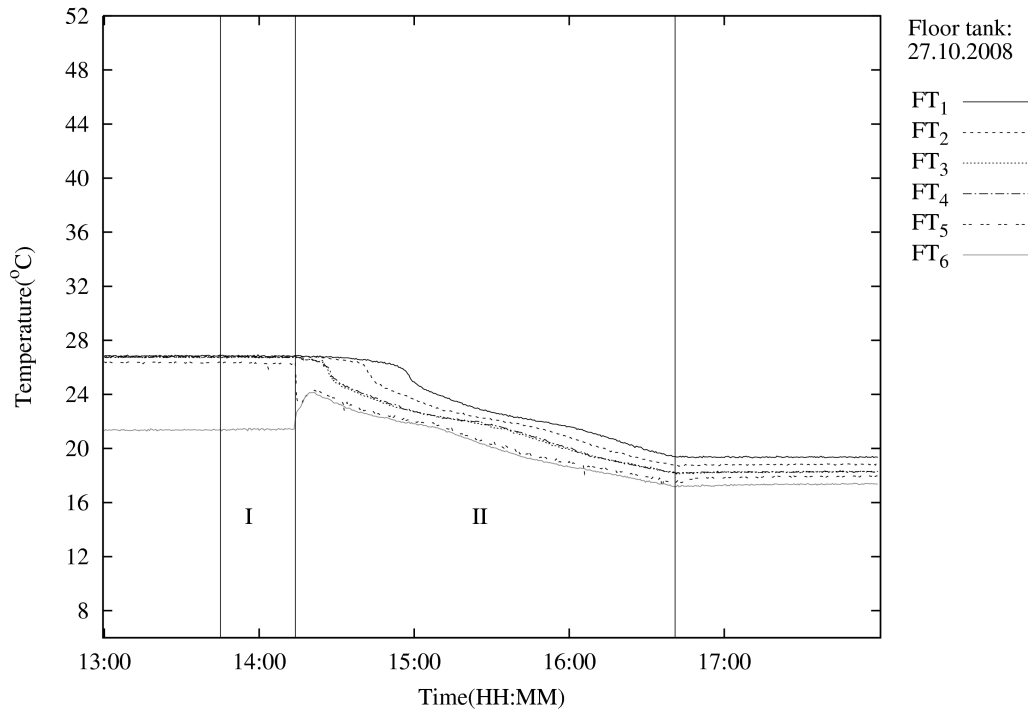


(a) DHW tank.

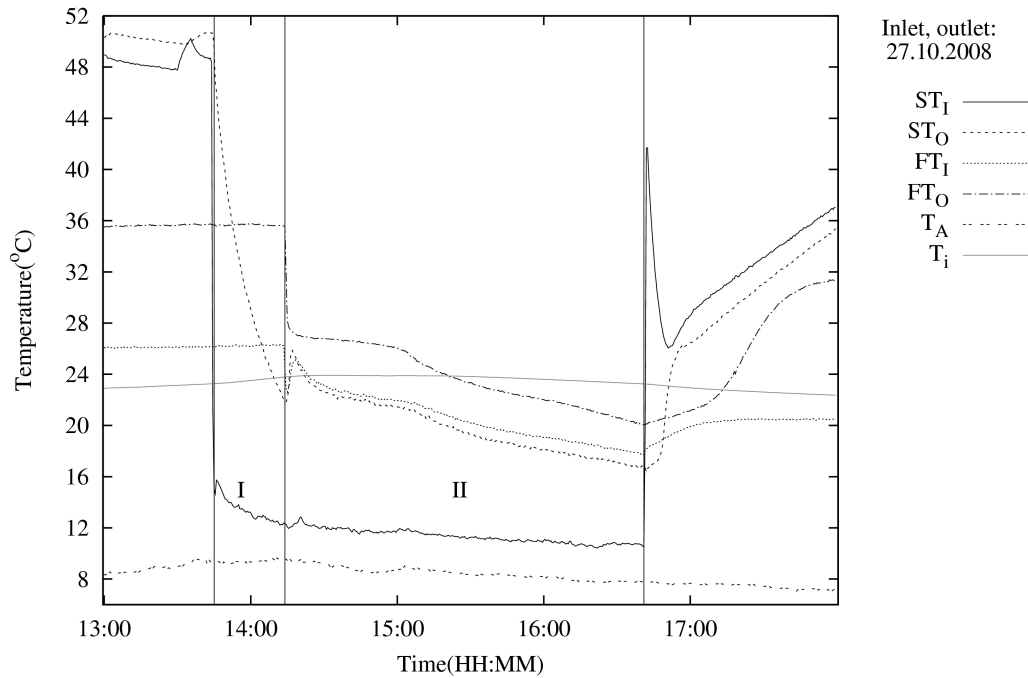


(b) Solar tank.

Figure 5.5: See Figure 5.1 on page 47 for description.



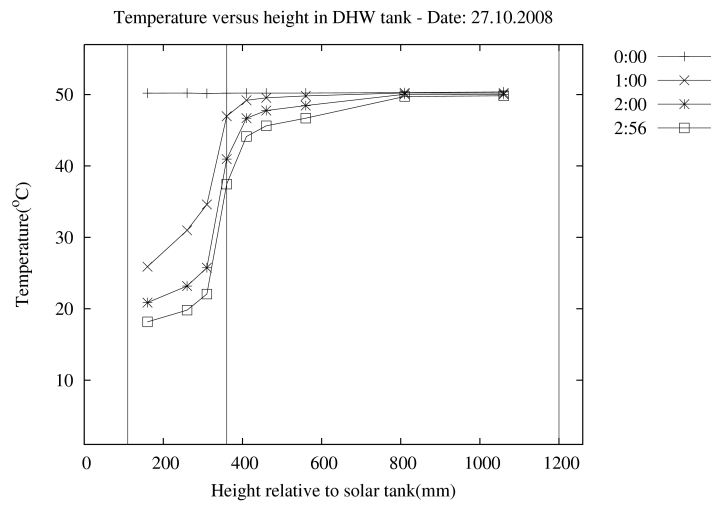
(a) Floor tank.



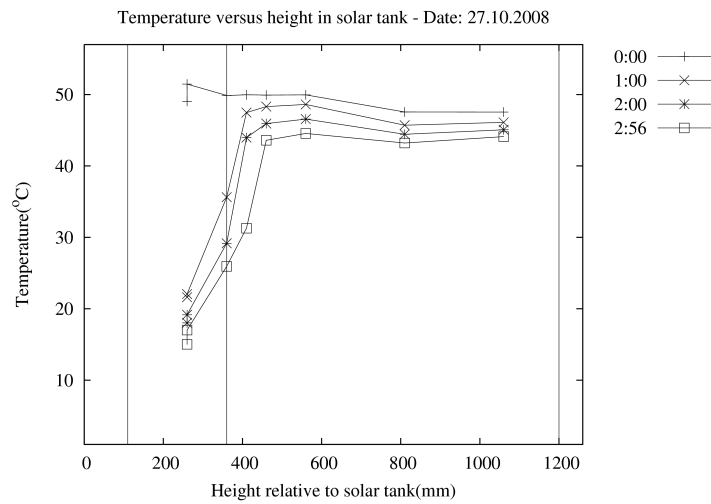
(b) Inlet, outlet, ambient and indoor temperature.

Figure 5.6: See Figure 5.1 on page 47 for description.

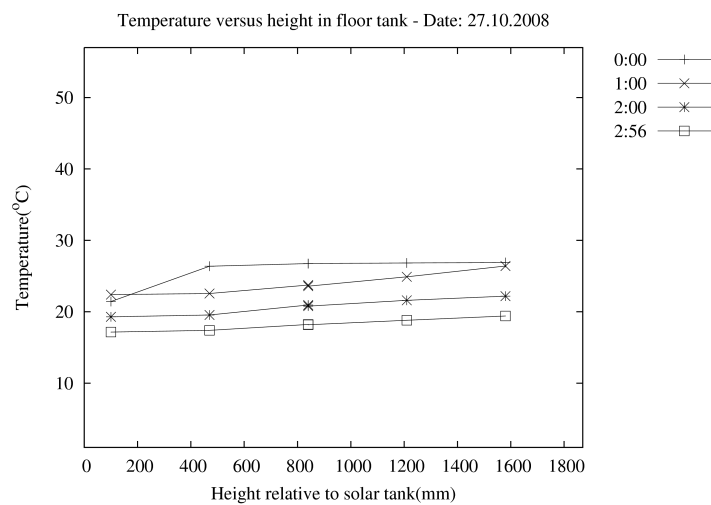
5.4 Resulting plots



(a)

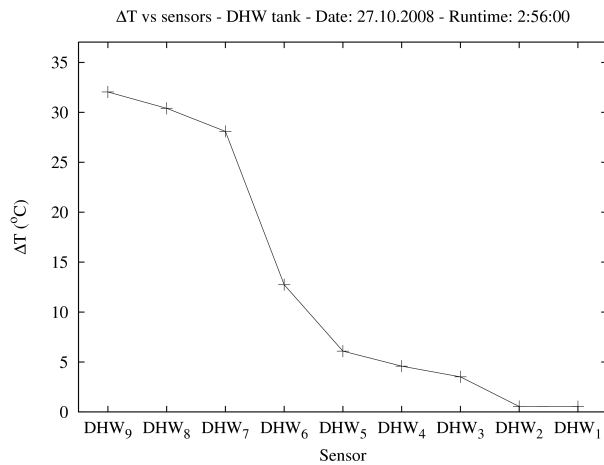


(b)

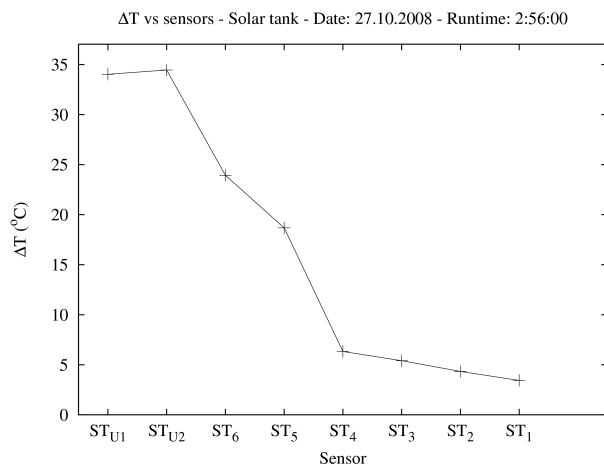


(c)

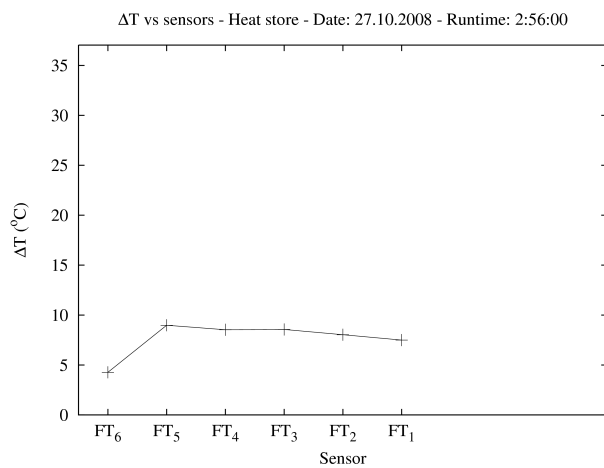
Figure 5.7: See Figure 5.3 on page 49 for description



(a)

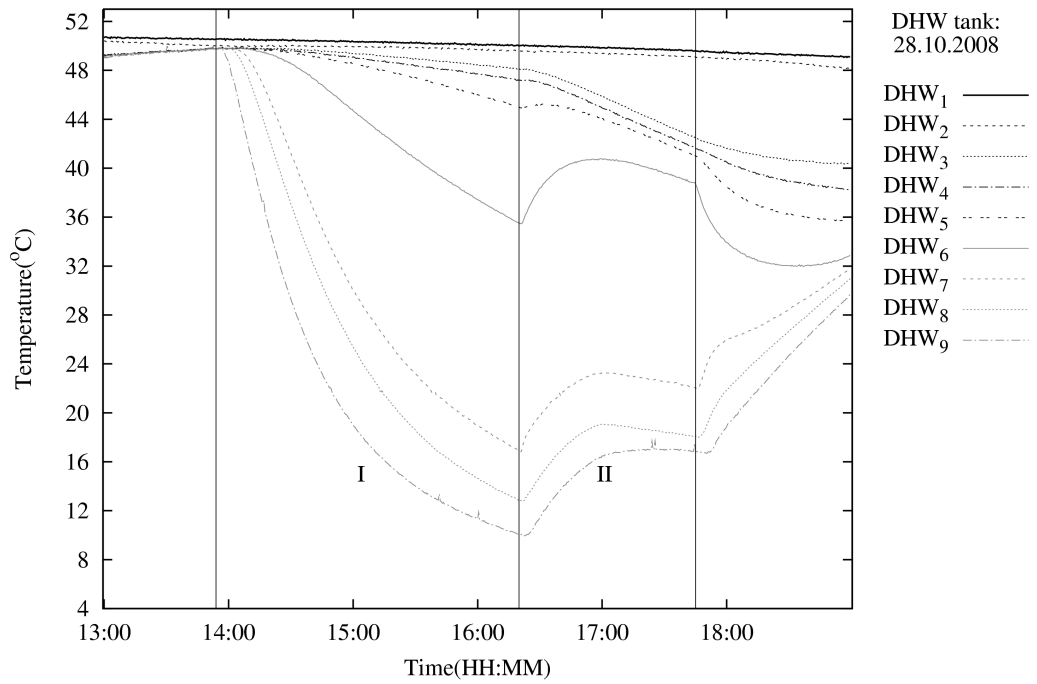


(b)

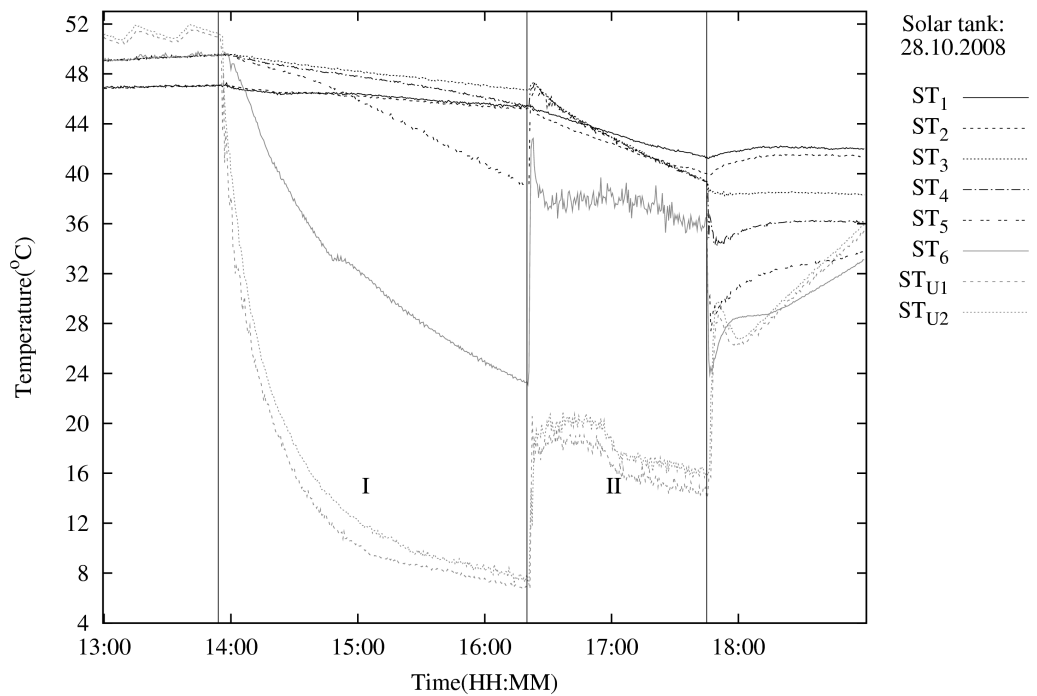


(c)

Figure 5.8: See Figure 5.4 on page 50 for description.

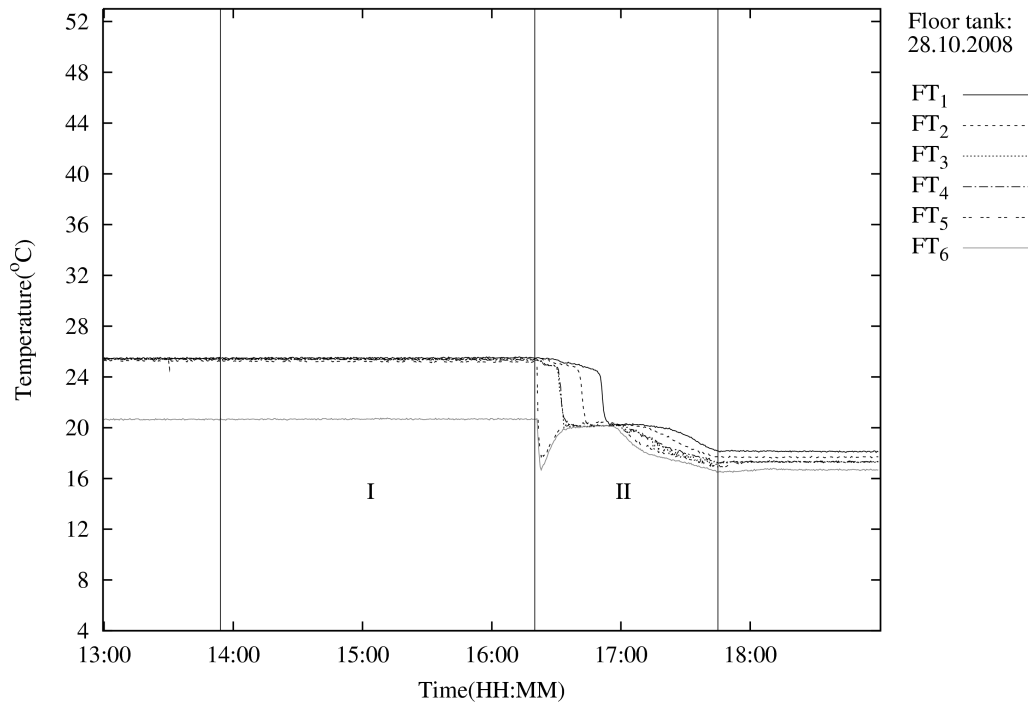


(a) DHW tank.

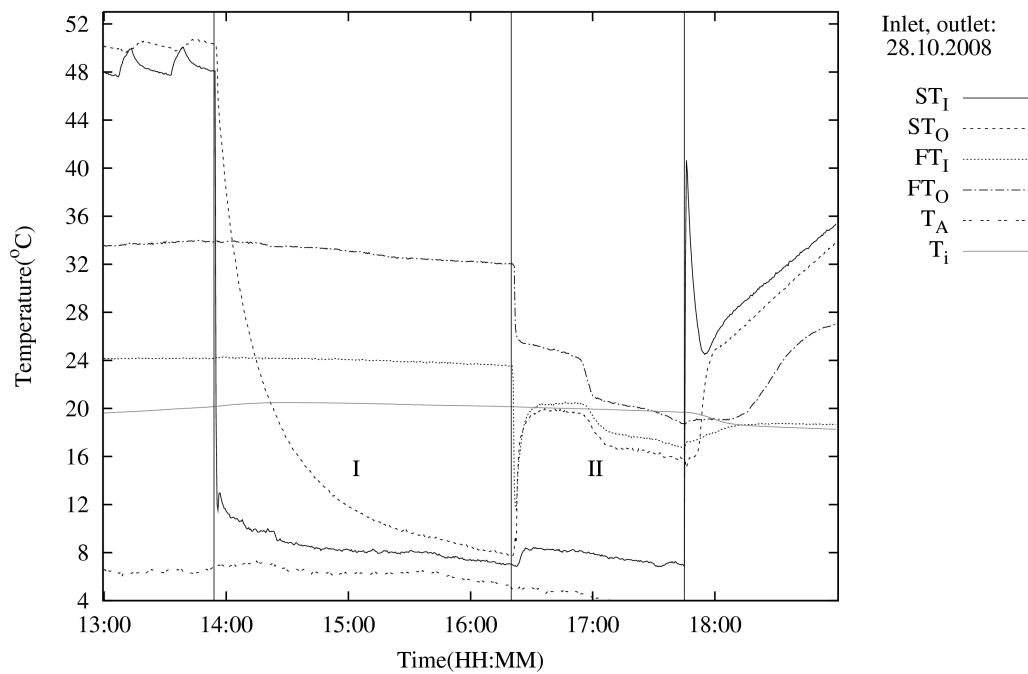


(b) Solar tank.

Figure 5.9: See Figure 5.1 on page 47 for description.



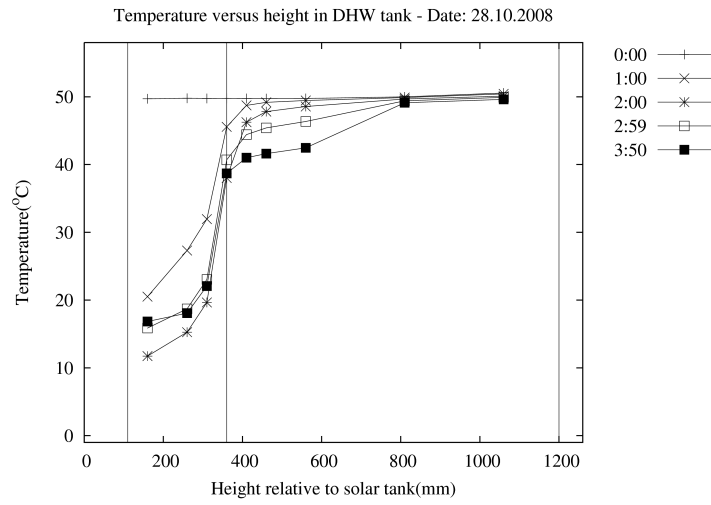
(a) Floor tank.



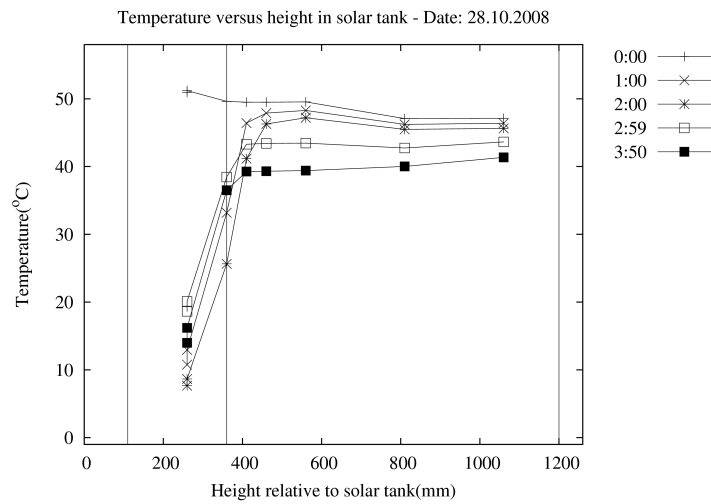
(b) Inlet, outlet, ambient and indoor temperature.

Figure 5.10: See Figure 5.1 on page 47 for description.

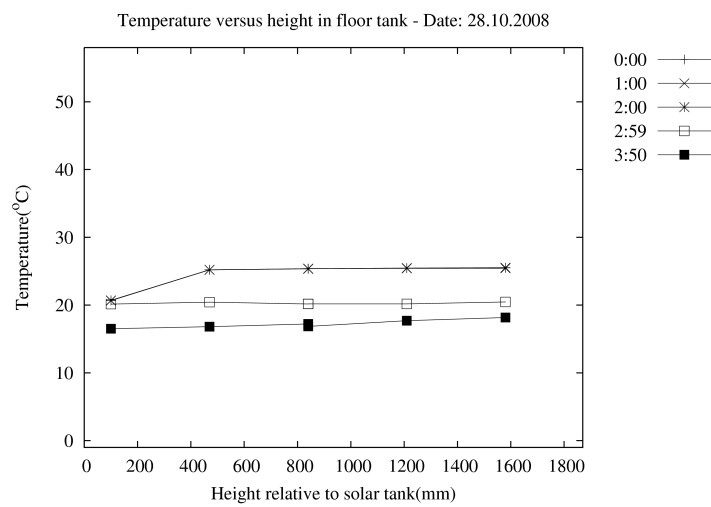
5.4 Resulting plots



(a)



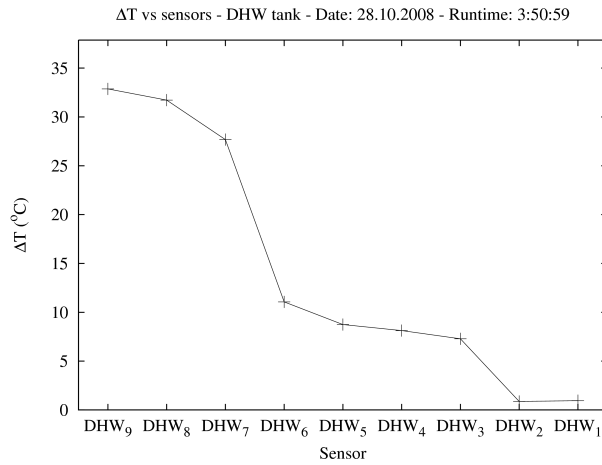
(b)



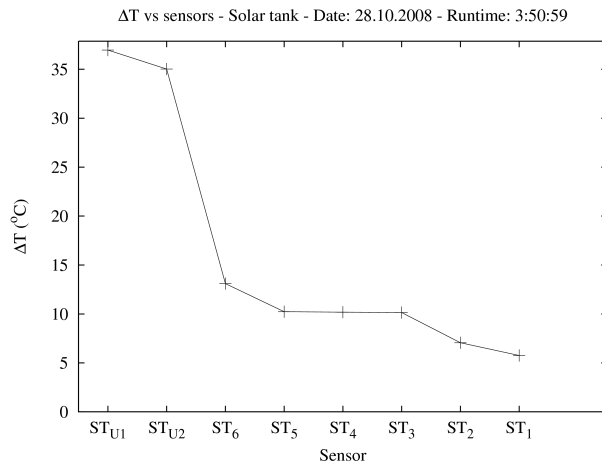
(c)

Figure 5.11: See Figure 5.3 on page 49 for description

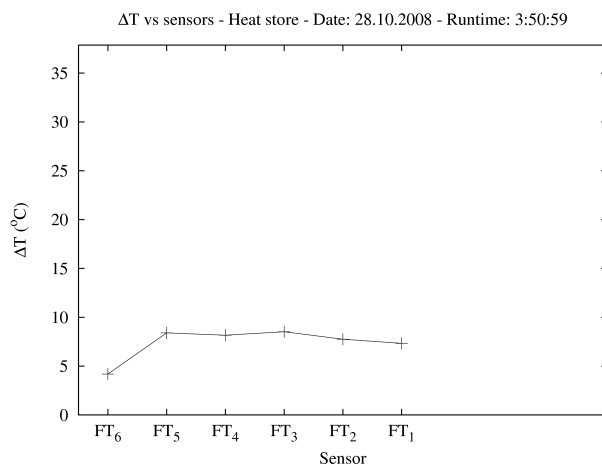
Chapter 5: Experiments



(a)



(b)



(c)

Figure 5.12: See Figure 5.4 on page 50 for description.

Chapter 6

Results

The results evaluates the plots from Section 5.4 and point out the most important details in the plots.

6.1 General temperature plot

The temperature plots for all the experiments have the same general characteristics. Figure 6.1 show the plot for the first experiment. All plot lines are the temperatures measured by the sensors in the DHW tank. The top plot line is measured by the top most sensor and the bottom plot line is measured by the bottom most sensor. None of the plot lines in the DHW tank cross during any of the experiments. When no plot lines cross each other during the experiment, the tank is stratified during the whole experiment.

6.1.1 DHW tank

Sensor DHW₆ is placed at the exact height of the separation plate. The plot line measured by the DHW₆ sensors is marked with "Separation plate" in Figure 6.1. Two double headed arrows are also placed in the figure. These show

how far these sensors are placed from each other. Sensor DHW₇ is placed 5 cm below sensor DHW₆ and sensor DHW₆ is placed 5 cm below sensor DHW₅. The measured temperature difference between the layers with sensor DHW₇ and DHW₅ is between 30 °C and 40 °C during most of the experiment. In the two other experiments' plots of the DHW tank, the measured temperature difference is not as large between the same two sensors. This is because the two other experiments started cooling when the solar tank reached 50 °C and the first experiment, on 21.10.2009, started cooling when the solar tank reached 74 °C. The temperature gradient between the two layers containing sensor DHW₅ and DHW₇ is therefore between 3 °C/cm and 4 °C/cm. That is, the temperature increases 3-4 °C each centimeter from the bottom to the top of the volume between these two layers.

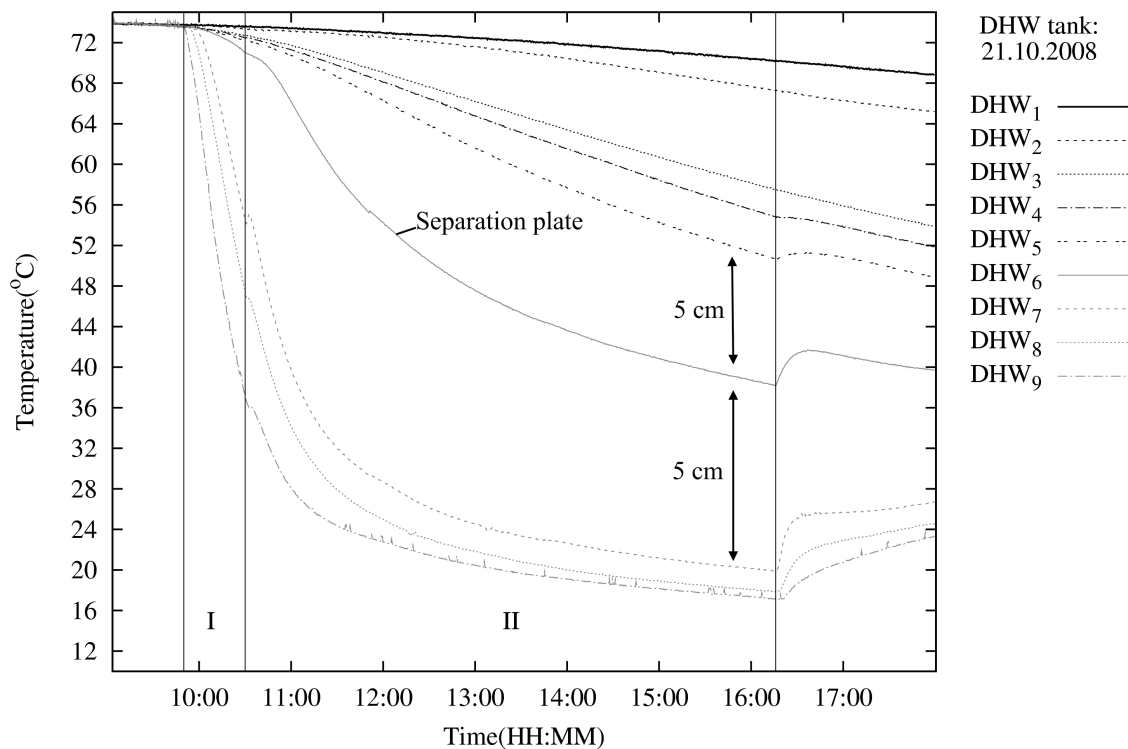


Figure 6.1: A cooling experiment, showing two periods marked with **I** and **II**, respectively. Each period is between two vertical markers. Exact position of the markers are found in Table 5.2. Period **I** is when the auxiliary cooler is running, thereby cooling the active volume. Period **II** is when the IE pump is running in addition to the auxiliary cooler.

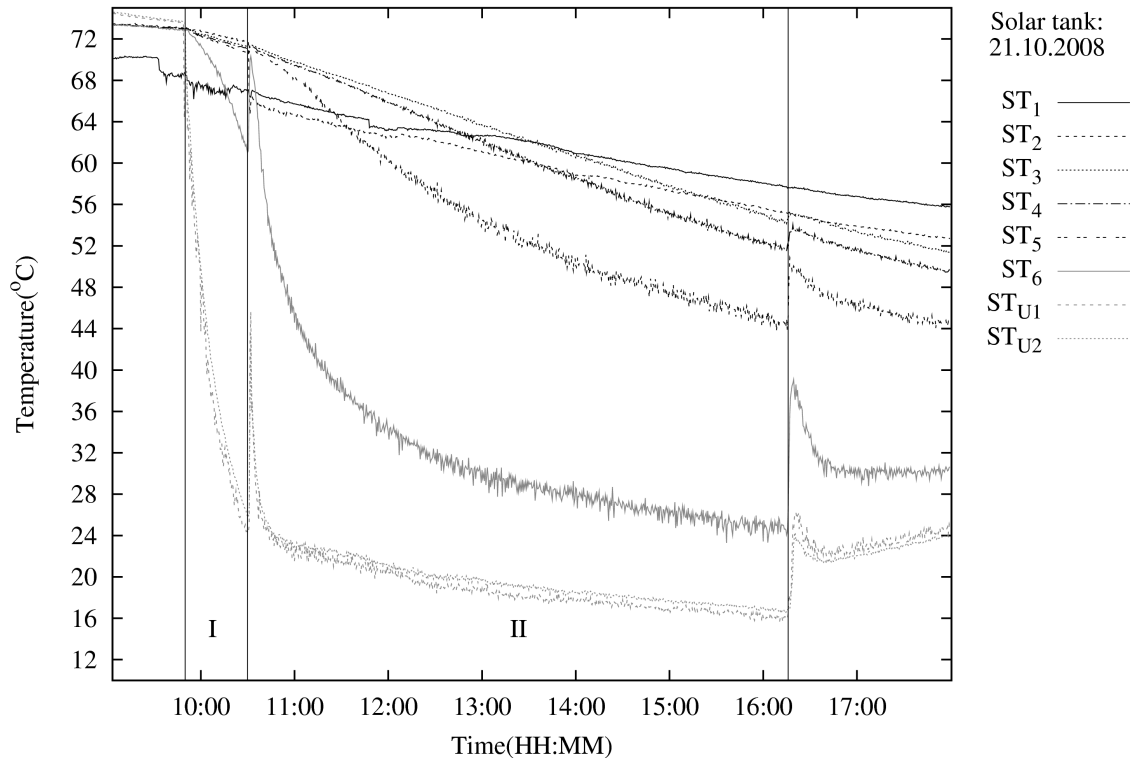


Figure 6.2: A plot of the solar tank from the first cooling experiment. The two sensors placed below the separation plate is sensors ST_{U1} and ST_{U2} . See also the description of Figure 6.1.

6.1.2 Solar tank

Figure 6.2 shows a plot of the temperatures in the solar tank. The plot is from the same experiment as Figure 6.1. The temperature plot lines in the plot in Figure 6.2 is not as smooth as the plot lines in the plot of the DHW tank. The DHW tank has no turbulence because no water enters or leaves it. The solar tank has four inlets and outlets. This creates turbulence which leads to the oscillating temperature measurements of the sensors placed there. Sensor ST_{U1} and ST_{U2} are placed 10 cm below the separation plate. The temperatures measured by these sensors are shown in the two bottom most plot lines. In the solar tank stratification of the water can be observed. The sensor 5 cm above the separation plate, ST_5 , measures a temperature of 20-25 °C above the temperature measured by sensor ST_6 , 1 cm above the separation plate. The temperature measured by sensor ST_5 is oscillating within approximately 2 °C. The ST_6 sensor is placed 1 cm above one of the holes (q) in the separation plate

shown in Figure 4.4. Sensor ST₆ is oscillating within approximately 3 °C.

6.1.3 Deviating sensors

The plot lines for sensors ST₁ and ST₁ in the plot in Figure 6.2 does not follow the trend of the other plot lines. Before the start of period I ST₂ follow the temperature of the other sensors, but sensor ST₁ measures a temperature that is 6 °C lower than the other sensors. After the inter-exchange pump starts when period II begins, the temperature of sensor ST₂ also drops. The temperatures measured by sensors ST₁ and ST₂ follow a different decline than the other sensors. In the plots for the solar tank in the other two experiments, Figure 5.5(b) and 5.5(b), the measurements for both sensors ST₁ and ST₂ start at a lower temperature than the measurements for the rest of the sensors.

6.2 Heat layers - stratification

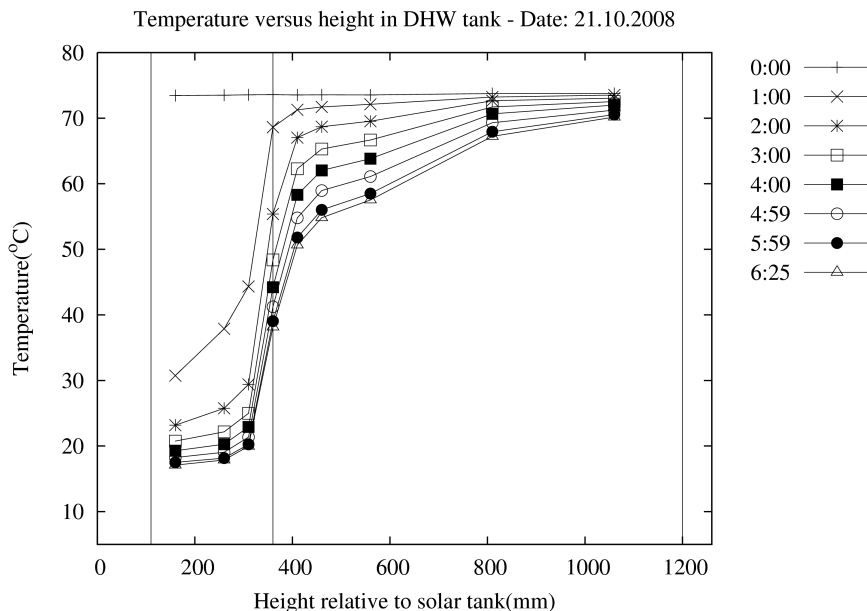


Figure 6.3: Each plot line show the temperature at the height of each sensors in the DHW tank. The first plot line, the top plot line, is the temperatures at the start of the cooling experiment. The subsequent plot lines show the temperature at a later moment found in the legend.

Section 3.4.3 states that water will arrange itself in layers with the warmest water on top and the coldest water at the bottom, assuming that the water is at rest. Figure 6.3 show that the temperature of the water in part of the of the DHW tank that is below the separation plate drops faster than the temperature of the water above the separation plate. For each step upwards, the temperature drops slower. Upwards in the tank is from left to right in the Figure 6.3. At the bottom the temperature drop is 56.3 °C and the two top sensors have temperature drops of 6.5 °C and 3.6 °C. This is also shown in Figure 5.4(a). This figure shows the total temperature drop that each sensor measures during the cooling period of the experiment.

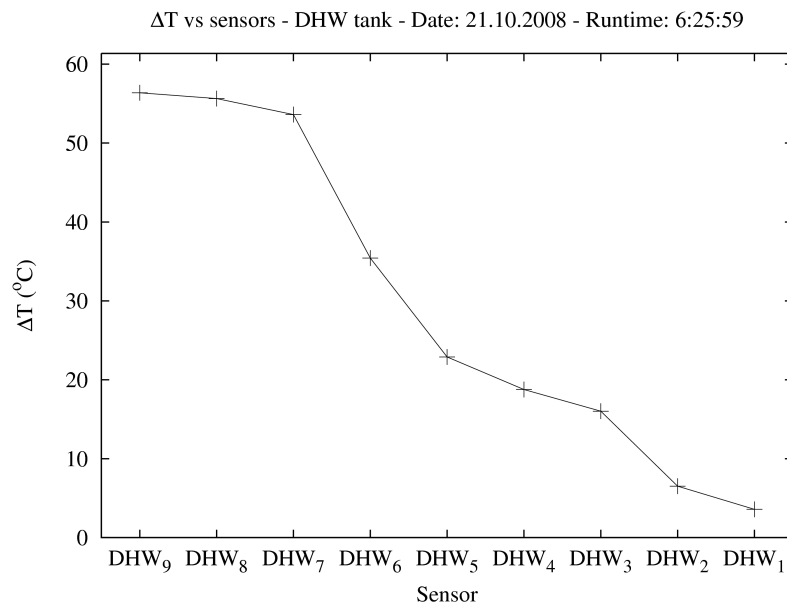


Figure 6.4: The temperature difference measured by each sensor between start and stop of the cooling experiment. The figure does not have absolute height on the x-axis.

Figure 6.3 and 6.4 also show that there is a difference in how fast the temperature drops above and below the separation plate. The temperature drops 53.6, 35.4 and 22.9 °C at respectively 5 cm below, 0 cm below and 5 cm above the separation plate. That is, the difference in temperature drop over 10 cm is 30.7 °C.

Table 6.1: Initial conditions given to the Python program. Two runs are done for each experiment with different parameters. The dates refer to which experiments are simulated. The height is the placement of the separation plate in meters above the bottom of the solar tank.

Date	Type	$dL(m)$	Time(h)	Step(s)	$T_{init,t}(^{\circ}C)$	$T_{init,b}(^{\circ}C)$	Height(m)
21.10.2008	b	0.01	6.42	30	74	20	0.36
	a	0.01	6.42	30	74	20	0.31
27.10.2008	b	0.01	2.93	30	50	20	0.36
	a	0.01	2.93	30	50	20	0.31
28.10.2008	b	0.01	3.85	30	50	20	0.36
	a	0.01	3.85	30	50	20	0.31

6.3 Simulated theoretical and measured heat transfer

Section 4.9.4 developed a method of simulating heat transfer. Equation 4.7 was derived from the equations for heat transfer and heat capacity. The method used the programming language Python to model the solar tank. The program can be run with different options so that it can be used to fit different initial conditions. It can therefore be used to compare the actual temperature profile with the theoretical temperature profile.

Initial conditions for the program were set to values similar to the ones in the experiments. Table 6.1 show the inputs given to the program for simulations of the DHW tank. Two simulations were done for each experiment. One where the separation plate is put at the height it actually is and one where the separation plate is put 5 cm below the actual position of separation plate. This is done because the temperature in the DHW tank at the height of the separation plate is below the temperature of the active volume. The temperature of the active volume $T_{init,b}$ is set to be an the average of the temperature measured in the active volume. The temperature $T_{init,t}$ of the volume above the separation plate is set to the temperature the solar tank and the DHW tank had when the cooling period started.

The plots in Figure 6.5 and 6.5 show the resulting simulations and the actual

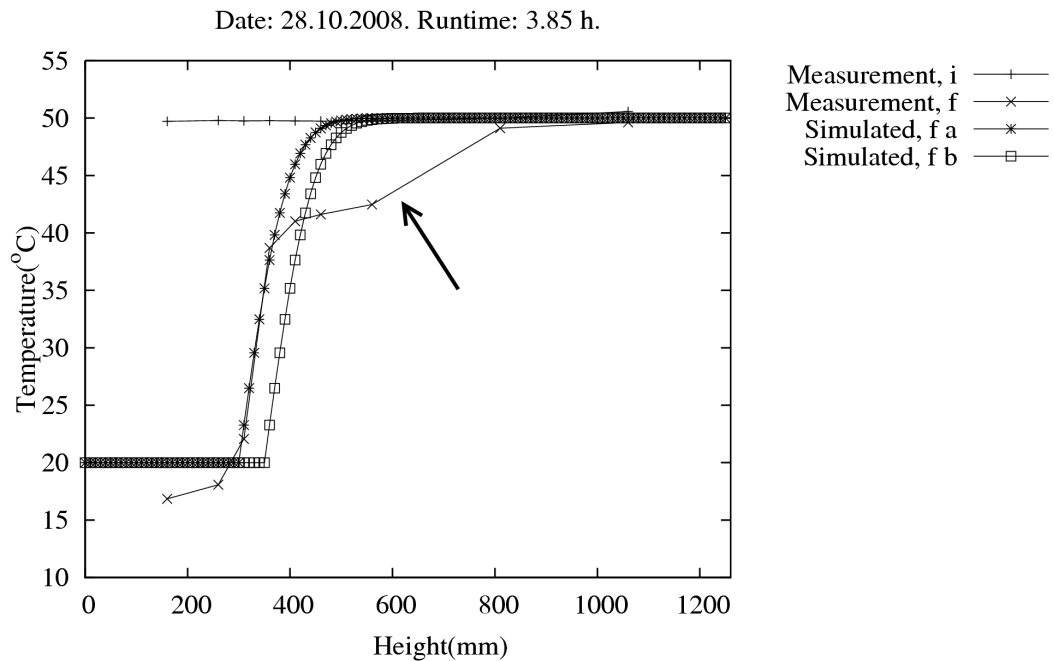


Figure 6.5: These plots, this and the two plots in Figure 6.6, show the temperature profile measured in the DHW tank, from the sensor at the lowest point and up to the sensor at the highest point. The two lines following the measured line are simulations of the heat transfer in the same tank, and with initial conditions set to those of the actual experiment. Initial conditions are found in Table 6.1.

measurements together. All three plots show the same characteristics. Both simulated plot lines follow the trend of the temperature profile in the DHW tank. Simulation of type a fits better than simulation of type b. In all plots the measured temperature profile of the tank dips down, see arrow in Figure 6.5. Except from the dip, the simulated temperature profile fit the results to some extent.

6.4 Calculated energy gain and loss

From each experiment, the gained energy in the heat store was calculated, along with the loss in the solar tank. During cooling the definition of gain and loss is defined like this:

- Energy loss in the solar tank and the DHW tank is the energy that is lost because of heat conduction and convection from the water above the separation plate to the water below the separation plate. From there the energy is transported to the outside through the auxiliary cooler.
- Energy gain, or cooling gain, is the amount of heat that has been transferred out of the floor tank into the active volume and from there transported to the outside through the auxiliary cooler.
- Total gain is the energy loss from the solar tank subtracted from the energy gained for cooling.

The values are calculated on the basis of the temperature change in each tank and the tanks volume. The energy change of each partial volume of each tank, shown in Table 4.3, were calculated and added together using Equation 4.1. Table 6.2 shows the findings. In none of the experiments were there any total energy gained. The experiment of 27.10.2008 had the smallest total loss of 1.26 kWh. The experiment with highest total loss was the experiment of 21.10.2008, with a total loss of 7.73 kWh.

Table 6.2: Energy gain and loss for the cooling experiments.

Date	Energy gain (kWh)	Energy loss (kWh)	Total gain (kWh)
21.10.2008	6.208	13.936	-7.728
27.10.2008	5.613	6.872	-1.258
28.10.2008	5.406	7.708	-2.302

Table 6.3 show the cooling power also taking into account the energy consumed by the solar loop pump. The solar loop pump uses 245 W. This is also a source of heat that needs to be dissipated outside in the auxiliary cooler. In contradiction to Table 6.2, Table 6.3 also shows the total amount of heat that has been removed from the two tanks. The power of the IE pump is also excluded from the calculations because it does not have linear power consumption and is not on during the whole cooling experiment. In addition to these energy aspects, the fan of the power of the auxiliary cooler is 0.59 kW. This is not taken into consideration in Table 6.2, but the system requires 0.59 kW of power to have the cooling power needed. The reason for not

putting it in Table 6.2 is that cooling power not necessarily depends on a fan. The cooling could be based solely on night sky radiation.

Table 6.3: This table holds the total energy the auxiliary cooler has dissipated to the outside air, including the energy consumed by the solar pump. The last column is the mean cooling power included the pump power. The power of the IE pump is not included as it varies non-linear with its settings and is not turned on for the whole experiment.

Date	Cooling gain (kWh)	Heat loss (kWh)	Total cooling (kWh)	Cooling power. (kW)
21.10.2008	6.208	13.94	21.71	3.38
27.10.2008	5.613	6.872	13.20	4.51
28.10.2008	5.406	7.708	13.99	3.91

When using this method of cooling, there is one inevitable loss. The active volume of the solar tank has to be used for energy exchange between the floor tank and the solar loop. The lost is then the energy lost when cooling of the active volume. The minimum energy that is lost is

$$Q_{\text{lost}} = mc(\Delta T)_{\text{lost}}, \quad (6.1)$$

where $(\Delta T)_{\text{lost}}$ is the temperature change from the start of the cooling period to the end of the cooling period. With a temperature difference of 30 °C and 54 °C, the minimum heat loss from the active volume is 4.97 kWh and 8.27 kWh, respectively. These values are time independent.

6.4.1 Efficiency of tank system

In this thesis the power of the cooling device is not interesting. The interesting aspect is the internal efficiency of the system. The efficiency of the tank system, the solar tank and the floor tank is the energy gained by cooling divided by the energy lost from the solar tank. Using this definition the efficiency of the tank system is

$$\eta = \frac{E_{\text{gained}}}{E_{\text{lost}}}. \quad (6.2)$$

Chapter 6: Results

Table 6.4: Temperature drop in the tanks. The drop in temperature of each sensor during the cooling period of the experiment are listed here and are plotted in Figure 5.4, 5.8 and 5.12.

Date	DHW ₉	DHW ₈	DHW ₇	DHW ₆	DHW ₅	DHW ₄	DHW ₃	DHW ₂	DHW ₁
21.10.2008	56.4	55.6	53.6	35.4	22.9	18.8	16.0	6.5	3.6
27.10.2008	32.0	30.4	28.1	12.7	6.1	4.6	3.5	0.5	0.5
28.10.2008	32.9	31.7	27.7	11.1	8.7	8.1	7.3	0.9	0.9

	ST _{U2}	ST _{U1}	ST ₆	ST ₅	ST ₄	ST ₃	ST ₂	ST ₁
21.10.2008	50.1	56.7	46.5	27.9	21.3	18.5	17.8	10.9
27.10.2008	34.0	34.4	23.9	18.7	6.3	5.4	4.3	3.4
28.10.2008	37.0	35.0	13.1	10.2	10.2	10.1	7.1	5.8

	FT ₆	FT ₅	FT ₄	FT ₃	FT ₂	FT ₁
21.10.2008	7.6	8.6	8.6	8.7	8.6	8.4
27.10.2008	4.3	9.0	8.5	8.6	8.0	7.5
28.10.2008	4.2	8.4	8.2	8.5	7.7	7.3

η is a unit-less value that is a number higher than zero. If there are more energy gained than lost the value is above 1. If the value is 2 the energy gained is twice as large as the energy lost. Two other efficiencies that can be used is

$$\eta_{\text{pf}} = \frac{E_{\text{gained}}}{E_{\text{pf}}}$$

and

$$\eta_{\text{p}} = \frac{E_{\text{gained}}}{E_{\text{p}}}.$$
(6.3)

η_{pf} is the energy gained as cooling in the floor tank divided by the power used by the pump and the auxiliary cooler's fan. η_{p} is the same, but without the power consumed by the fan. The values for the efficiencies are shown in Table 6.5.

6.4.2 Heat loss

The experiment on 11.08.2009 was done to find the energy loss in the solar tank. Loss is a measure of how much energy is lost from a system. Here, it is a

Table 6.5: This table has the calculated efficiencies for the system. The different efficiencies are explained in the text.

Date	Efficiency η	Efficiency η_{pf}	Efficiency η_p
21.10.2008	0.45	1.16	3.95
27.10.2008	0.82	2.29	7.82
28.10.2008	0.70	1.81	6.16

measure of how fast energy dissipates from the tank at any given time. During an experiment, or a commercial tank system in a house, there will be loss to the surroundings, the room in which the tank is placed. From the theory in Section 3.4.1, heat transfer from one mass to another, is dependent on the temperature difference, the distance the heat needs to travel, the area it travels through and a material specific constant. Logging of the indoor temperature is done indirectly through voltages proportional to the temperature. Indoor temperature is an average of two sensors one meter apart, making the values more accurate. The overall tank temperature is given by an average of all the sensors with a relative weighting of each sensor. Table 4.3 gives the volumes each sensor is measuring and by dividing each volume with the total solar tank volume, the relative weighting was found. A specific value for the tanks area and insulation thickness is not a straight task to find. Therefore an analytical approach is taken.

Figure 6.7 show the weighted mean temperature of the solar tank as a function of time. The temperature is plotted during a period of 4 days, 4 minutes and 44 seconds. The other two plotted lines are the indoor temperature of the Sollaband and the mean temperature over the same period. As seen in the figure, the temperature has a slightly downward sloping exponential curve.

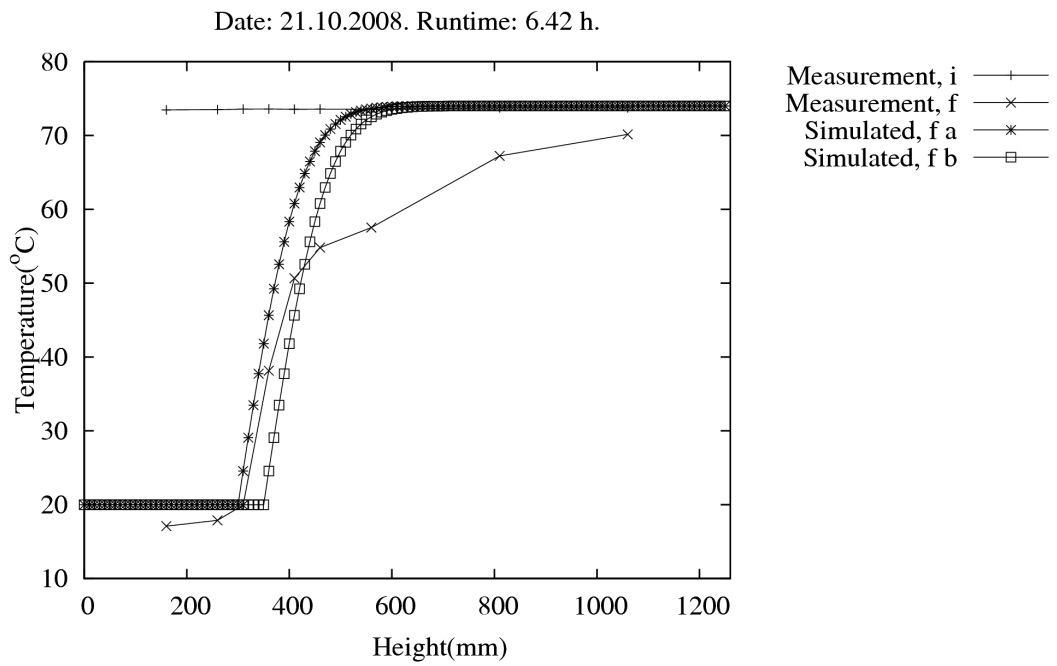
A problem became evident when using Equation 4.3 to calculate $\left(\frac{kA}{\Delta x}\right)$ for the system. It is not linear for ΔT_{st} . Therefore the line was discretized into eleven parts. Each part was used to calculate a value for $\left(\frac{kA}{\Delta x}\right)$. Table 6.6 shows the values. Using linear regression, the temperature dependent formula for the total heat loss coefficient was found to be

$$\left(\frac{kA}{\Delta x}\right) = 7.14 \times 10^{-5} \Delta T_{st} + 0.00149. \quad (6.4)$$

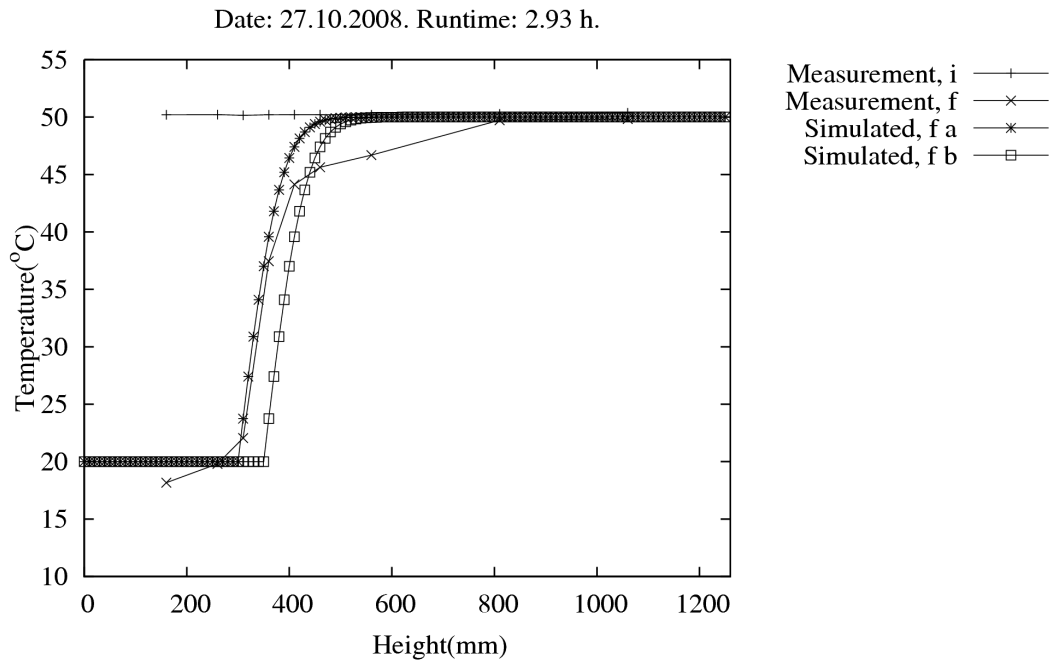
Table 6.6: Calculated $\left(\frac{kA}{\Delta x}\right)$ (W/K) from experimental results. Time is in steps of 30 seconds, making it easier to correlate with Figure 6.7.

Time (From-to 30 s)	$\left(\frac{kA}{\Delta x}\right)$ (W/K)
100-1000	0.004035
1000-2000	0.003920
2000-3000	0.003801
3000-4000	0.003718
4000-5000	0.003645
5000-6000	0.003647
6000-7000	0.003492
7000-8000	0.003357
8000-9000	0.003378
9000-10000	0.003244
10000-11000	0.003282

6.4 Calculated energy gain and loss



(a)



(b)

Figure 6.6: See caption of Figure 6.5 for description.

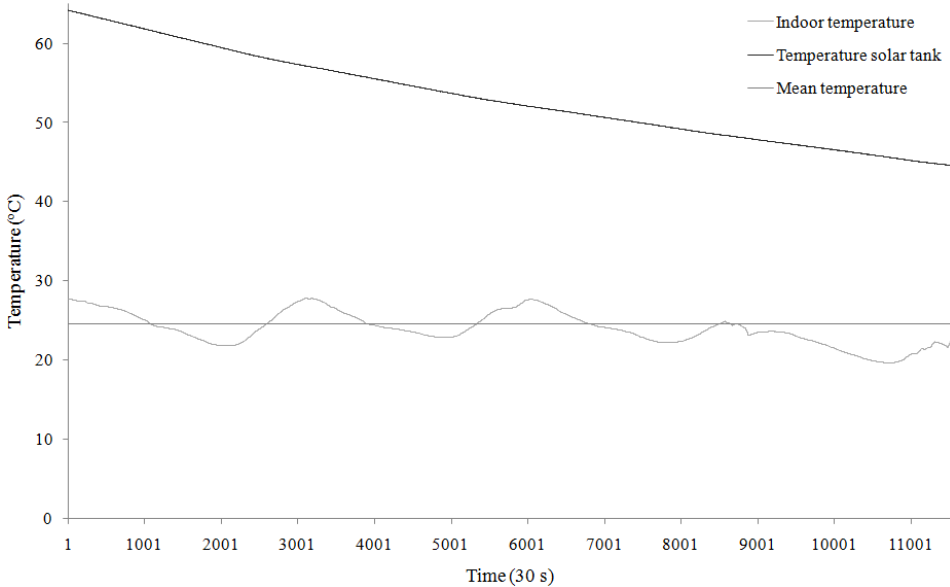


Figure 6.7: This plot show the temperature of the solar tank as it is cooling down.

Chapter 7

Discussion

Several aspects of the results are interesting to discuss. There were also problems along the way which is discussed and used for interpretation of the experiments. The main focus of the discussion is the stratification of the solar tank and the DHW tank. Also, some improvements for further experiments are discussed.

7.1 Practical problems

When performing practical experiments, there can always be things does not work out as planned. The experiments in this thesis are no exception and below is a description of what went wrong.

7.1.1 Cracked cooler

The auxiliary cooler is placed outside. The heat carrying medium in the solar loop is water. The system is designed to use clean tap water without any additives like a coolant. This means that the auxiliary cooler has to be drained when the ambient temperature drops below zero °C to avoid freezing of water

and possible destruction of the cooler. Somehow, all the water inside the cooler had not been fully drained. The cooler's copper pipe had burst at several places. When the spring came, the damages were uncovered, and the cooler were found to not be repairable. When results had been analyzed and found to be inadequate, the winter had destroyed the auxiliary cooler, preventing further experiments. Therefore the experiments listed in Chapter 5 are the only experiments that have been found to be good enough to analyze. More results are available, but with an experimental execution that did not coincide with the goal of the thesis.

7.1.2 Sensors not submerged in water

The next problem that was found was that two sensors were not fully submerged during the experiments. A description of this is made in Section 6.1.3. Two of the sensors in the solar tank, ST_1 and ST_2 , were deviating from the expected behavior. They measured a temperature lower than they would if they were functioning correctly. The warmest water should be measured by the sensor closest to the top of the tank since no other problems with the stratification in the top of the tank were found. The other sensors measured a temperature profile that suggested that the temperature was highest at the top and lowest at the bottom. The first conclusion was that the sensors stopped working properly. This posed the problem that the full temperature profile of the solar tank could not be found.

No experiments could be performed in the Sollab during the winter. Therefore a system check was done before leaving the Sollab to itself for the winter. When checking the water level in the tanks, the solar tank lacked several liters of water. Approximately 60 ± 5 liters of water were needed to refill it to its overflow pipe. When the sensors had been calibrated on June 17, 2008, the system was filled with water until the water reached the overflow pipe. After this, no water was refilled until after the experiments. Hence, about 60 l of water had evaporated over a period of 4 months and 11 days. This seems like a very large volume, but no leaks in the system were found elsewhere. The value is supported by the plots in Figure 6.2 and 5.5(b). The plot in Figure 6.2 shows that sensor ST_2 measures a temperature below the other sensors after the inter-exchange pump between the solar tank and the floor tank is started,

but not before. This indicates that it was submerged before the inter-exchange pump was started, but not after. The plot in Figure 5.5(b) shows that sensor ST_2 measures a temperature below the other sensors even before the inter-exchange pump is started. This indicates that sensor ST_2 is not submerged at any time after and including October 27, 2008. Table 4.3 show that sensor ST_1 measure the temperature of 32.5 l of water and sensor ST_2 measure the temperature of 50.1 l of water. Since the only volume that is lost is that above the height of sensor ST_2 , the amount of water that had evaporated was then larger than the water in the solar tank above the height of ST_2 .

$$V_{\text{evap}} > 32.5 \text{ l} + \frac{50.1}{2} \text{ l} = 57.55 \text{ l} \approx 58 \text{ l} \quad (7.1)$$

The problems with sensors ST_1 and ST_2 are therefore concluded to be caused by them not being submerged due to a not fully filled solar tank. Solutions to this is to enclose the top of the tank with damp proof course and also refill the tanks with regular intervals.

The DHW tank did not need to be refilled even though it had open pipes. Closed pipes would have created pressure when the water was heated or cooled.

7.2 Stratification

There are several details in the results that suggest that there are a high degree of stratification in the solar tank and the DHW tank. The floor tank is also stratified to some extent. This section will be a discussion around the stratification of each of the three tanks.

7.2.1 DHW tank

Stratification of the DHW tank is important, because the water that is to be consumed should be as hot as possible. The water that is consumed comes from the upper volume of the tank. The warmest water is in the upper volume of the tank when the tank is stratified. If the water in the tank is not stratified during cooling, heat will be transferred to the active volume. Since there are

no other flows in the DHW tank except when new cold water enters at the bottom, the only factor that affects the stratification in the DHW tank is the solar tank.

A stratified solar tank will keep the DHW tank stratified. The warmest water in the solar tank will be in the upper volume and the coldest will be in the bottom volume. Having the same situation in the DHW tank, the heat transfer in the tanks would only be by heat conduction and it would only be in a vertical direction. A fully mixed solar tank would therefore disturb the stratification in the DHW tank.

The results show that there is a high degree of stratification in the DHW tank. The plot of Figure 6.1 show this. Furthermore, the plot in Figure 6.3 show the time dependence of the stratification. Even with the full volume of the active volume being cooled to below 20 °C, the volume of the DHW tank that is above the separation plate has a strong temperature gradient. Section 6.1.1 finds the temperature gradient to be 3-4 °C per centimeter during most of period **II** of the first cooling experiment.

7.2.2 Solar tank

The stratification of the solar tank is dependent on the design of the tank system. The separation plate is in place to ensure that turbulent water in the active volume does not disturb the upper volume of the solar tank. The plot in Figure 6.2 support this. Sensor ST₆ is placed 1 cm above the separation plate, that is approximately the same height. The temperature measured by sensor ST₆ is not equal the temperature of the active volume. It is 8 °C higher than the temperature of the active volume. Temperature sensors at higher positions in the solar tank also suggest that the separation plate is doing its job, namely keeping the stratification in the top volume of the solar tank.

As mentioned in Section 6.1.2 the sensors signals in the solar tank are oscillating. The sensors behave normal when the pumps of the inter-exchange and the solar loop are turned off. This suggests that the turbulence created by the pumps affects the water in the upper volume of the solar tank as well. There are as mentioned in Section 4.2.2 several places in the separation plate where water can travel vertically between the active volume and the upper volume

of the solar tank. There are four 10 mm holes in the plate which are meant to be used for sensors. Two of the holes are used for sensors and thereby almost closing them. There is also a glitch all the way around the DHW tank between the DHW tank and the separation plate. The separation plate is not welded onto the DHW tank when the design was made. The DHW tank was lowered down into the solar tank through a hole in the separation plate. Knowing that water can travel vertically between the active volume and the upper volume of the solar tank, that there is turbulence in the active volume and that the temperature in the upper volume is oscillating, it is concluded that flow in the active volume creates turbulence in the upper volume. Therefore, turbulence in the active volume disturbs the stratification in the solar tank. As mentioned above, the stratification of the DHW tank is affected by the stratification of the solar tank. Hence, flow in the active volume affects stratification of the DHW tank.

7.2.3 Floor tank

The floor tank is also stratified. The difference between the warmest and coldest water is not as large as in the solar tank though. Figure 5.7(c) contains a plot that shows the stratification. The warmest water is at the top and the coldest water is at the bottom, which is as expected since cold water from the active volume of the solar tank enters at the bottom of the floor tank. When the system is in cooling mode, this is also what we want to have; the warmest water from the top of the floor tank flows down to the active volume of the solar tank.

7.3 Energy loss and gain when cooling

An important feature of a system that is supplying heating and cooling to a building is that it has a net energy gain from the cooling and the heating. Section 6.4 present the definition of energy loss and cooling gain.

From the data that has been collected, a calculation of the energy loss and the cooling gain has been done, and thereby also the net energy gained or lost. In

all the experiments conducted, more energy was lost than gained. This means that the energy gained by cooling of the floor tank, where gained energy is the heat that is lost from the floor tank, is less than the heat that is lost from the solar tank during the same period. In the case of the experiment of 27.10.2008, the net loss is 1.3 kWh during the simulated night of 2 hours and 56 minutes. Unfortunately, this is not the result I believed I would get. From the point of view of these results, it seems like there is little potential in the design.

On the other hand, the loss is not so large if we compare to the cooling energy that is gained. The loss is only 18% more than what has been put into heating of the solar tank and the DHW tank. Looking at the energy from the point of view of having converted heat into cooling the loss is 18%, a conversion factor of 0.82. This is of course only if we see the system as a way of converting heat into cooling. What the system should do is to actually gain more cooling than it loses heat.

On the other hand, what has happened is that solar energy has been transformed into cooling energy. But this is only true if the heat in the solar tank comes from solar heating through solar collectors. So if the same collectors were used for radiative cooling, the cooling would be a free addition to the system. No heat pump or fin cooler would need to be purchased.

Another important note is that a large part of the heat lost from the solar tank is actually inevitable. If the system is to be used, the loss of energy which can be calculated using Equation 6.1 will in fact be lost.

The energy that had to be dissipated through the auxiliary cooler was between 13.2 kWh and 21.7 kWh. If this should be dissipated only by night sky radiation by using collectors without cover sheets, 30-40 m² of collectors is needed. This is based on Figure 2.2, but not taking into account the emissivity of the collectors or the fact that the collectors are also convecting heat to the air.

7.3.1 Efficiency of tank system

Table 6.5 show the calculated efficiencies of the system. First, looking at the efficiency η , we see that it does not make much sense. The sense it does make is that it tells us that the energy gained by the system is negative and small

compared to the energy dissipated through the auxiliary cooler.

The most interesting efficiency is the one in the last column of the table, namely η_p . Several things need to be known before using these values. The only energy used is the energy needed to run the pump, or pumps. The energy lost as heat from the solar tank and DHW tank is not taken into account here because this heat is assumed to come from solar heating, and hence it is not energy we need to use any auxiliary heater to get. Having established the defense for the high efficiency, which is approaching $\eta_p = 8$, we can start giving the setup credit for being good. Good in the sense that it can be used to cool a floor tank that can be used to cool a building.

7.4 Simulations

To find out how the heat conduction in the solar tank and the DHW tank coincide, a simulation was done. The simulation is a simplification of the physical tank system. The algorithm and programming is explained in Section 4.9.4. The resulting plots are shown in Section 6.3. Since the simulation does not take into account any movement of the water and that it uses a stationary boundary condition at the height of the separation plate, we have to discuss the deviations from the results.

The temperature in the volume of the DHW tank that is below the separation plate follows the simulated temperature profile well. Figure 6.5 show this. Simulation a show a better fit than simulation b. Simulation a are done with a lower separation plate than simulation b. When the simulations reach the height of the separation plate the coherence stops. The measured temperature profile dips down. This happens consistently in all plots, and the dip is also larger for the plot in Figure 6.6(a). Hence, the longer a cooling experiment lasts, the more heat is lost from above the separation plate. The explanation for this is found in Section 7.2.2. The stratification in the upper volume of the solar tank is disturbed by the turbulence in the active volume of the solar tank.

The top of the solar tank has two temperature sensors that are not submerged in water. This fact together with the simulated plots shows that the simulation

is accurate. In the plots in Figure 6.5 and 6.6(b) the top two sensors only measure a small decrease in the temperature during the experiments. This means that the only heat transfer in the part of the DHW tank above the height of sensor ST_2 is only by conduction. The conduction of heat through water is very slow and hence the observed small temperature drop. This shows that from the height and up, the only heat transfer.

7.5 Improvements of the cooling state

From the experimental results of this thesis there are several things that could have an effect on the efficiency of the system.

7.5.1 Flow considerations

We have established that turbulence in the active volume of the solar tank disturbs the stratification in the upper volume of the solar tank. The turbulence is created by the flow of the solar pump and the IE pump. If the pumps were set to a lower flow it would lead to less loss because of disturbance of the stratification in the upper volume of the solar tank. The downside of lowering the speed of the pumps is that they would not transport heat as quickly from the floor tank to the auxiliary cooler. This means that the total energy gain may not change much. Nonetheless, a series of experiments should be done to find out if this could increase the total energy gain.

Another series of experiments that could be done is using different flow velocities for the two pumps. The flow speed of the solar loop pump and the IE pump could be changed with respect to each other. The reason for suggesting this is based on the simulations presented in Section 6.3 and the theory about heat conduction presented in Section 3.4.1. If the temperature in the active volume is as high as possible, the heat conduction from the top volume to the active volume of the solar tank will be as low as possible. Convection will also have a lower effect on the temperature above the separation plate. Using this information, the best way to achieve a temperature that is as high as possible in the active volume is to use a lower flow in the solar loop than between the

solar and the floor tank.

7.5.2 Initial temperature of the active volume

There are also things that are affecting the initial temperature of the active volume. An important reason is be the consumption of DHW. When DHW is consumed for domestic purposes, cold water enters in the bottom of the DHW tank. I am also assuming that fresh water is 5-10 °C. The water will first fill the lowest parts of the DHW tank. Heat from the active volume will therefore be transferred into the DHW tank if it is warmer than the new water. In effect, the active volume gets a lower temperature. This means that the loss from the solar tank will be less than if this was not the case. The cold water is water that has to enter the system, hence using it for cooling is an energy gain for the system.

Further experiments should therefore be conducted with the addition of the consumption of DHW.

7.5.3 Changes to the separation plate

Having seen that the holes and glitches in the separation plate enables the turbulence in the active volume to disturb the stratification of the upper volume, it is possible that changes to the holes can increase the total energy gain of the cooling experiments. If we were to use only one small hole to decrease the flow in the solar tank it would cause problems when the solar collectors have to be filled and drained. The new solar collectors to be placed on the roof has an internal volume of 30 l, excluding pipes, that will fill with water when the solar loop is running. Therefore it seems like a bad idea to make the total opening in the separation plate as small as possible. Instead the holes could be placed as far away from the inlets as possible while sealing the glitch between the DHW tank and the separation plate.

Another change may be to lower the separation plate again. This way the inevitable loss of all the heat in the active volume would decrease. On the other hand, it is important that the heat exchange between the active volume

and the DHW tank is large enough to conduct as much heat as possible from the active volume to the DHW tank during heating. Heating experiments should be done before and after moving the separation plate to see if the heat exchange is large enough.

7.6 Further experiments

Further improvement to the experiments is to place the sensors using what is learned in this thesis. There are more sensors in the floor tank than what is needed. The temperature difference measured by the different sensors is small. In particular, the two sensors at the same height in the floor tank measure a temperature difference that is insignificant for use in calculations.

In this thesis it is assumed that the active volume of the solar tank has high mixing and therefore two sensors measure a good estimate of the temperature. To be surer about the temperature, more sensors could be used in the active volume.

Chapter 8

Conclusion

The tank concept, with a separation plate at 36 cm, has been found to be an adequate way to utilize the system for both cooling and heating. The gain in cooling energy of one night is in the range of 5.4 kWh to 6.2 kWh. At the same time, the heat loss from the solar tank is in the range of 6.9 kWh to 13.9 kWh. Some of this loss is inevitable in most cases, but with optimization of the system based on the results, this performance could be increased. An increase in performance could come from moving the separation plate further down.

The theoretical heat transfer simulations revealed that the stratification was to some extent disturbed. The stratification of the tanks was present, but it could be improved.

It is also concluded that the heat loss from the solar tank during cooling is caused by turbulence in the upper volume, which in turn is caused by turbulence in the active volume. This interaction, and hence the heat transfer, between the volumes occur because water is allowed to travel through the openings in the separation plate. The heat transfer could be minimized by sizing and positioning the openings differently.

Bibliography

- [1] B.C. Bates, Z.W. Kundzewicz, S. Wu, and J.P. Palutikof. Climate change and water. Technical report, 2008. Technical Paper of the Intergovernmental Panel on Climate Change.
- [2] Paul Berdahl and Richard Fromberg. Thermal radiance of clear skies. *Solar Energy*, 29(4):299–314, 1984.
- [3] Paul Berdahl and Marlo Martin. Emissivity of clear skies. *Solar Energy*, 32(5):663 – 664, 1984.
- [4] B. D. Botkin and E. A. Keller. *Environmental Science - Earth as a living planet*. John Wiley & Sons, Inc., New York., 5th edition, 2005.
- [5] Lise Boye-Hansen and Simon Furbo. Solvarmeanlæg med tømning. *Laboratoriet for Varmeisolering, Technical University of Denmark*, 1995.
- [6] National Instruments Corporation. Labview, 2009. <http://www.ni.com/labview/>.
- [7] C. Cristofari, G. Notton, P. Poggi, and A. Louche. Influence of the flow rate and the tank stratification degree on the performances of a solar flat-plate collector. *International Journal of Thermal Sciences*, 42(5):455 – 469, 2003.
- [8] Lelandais Damien and Pain Dorothée. Study of a heating and cooling system thanks to solar energy. Master’s thesis, University of Oslo, June 2006.
- [9] Henning Degnes-Ødemark. A study of night sky radiation, an heating and cooling of buildings with solar thermal collectors. Master’s thesis, University of Oslo, October 2009.

Bibliography

- [10] John A. Duffie and William A. Beckmann. *Solar engineering of thermal processes*. Wiley, New York :, 3rd ed. edition, 2006.
- [11] *Fincoil SOLAR Junior/Junior R Manual*. Fincoil, 2005.
- [12] Jacob Fraden. *Handbook of modern sensors*. Springer Science + Business Media, LLC, 2004.
- [13] General Electric. H system*. Internet(January 2009): http://www.ge-energy.com/prod_serv/products/gas_turbines_cc/en/h_system/index.htm.
- [14] Google. Sketchup, 2009. <http://sketchup.google.com>.
- [15] *UPE series 2000*. Grundfos, 1997.
- [16] Abdelkarim Hamazaoui, Khalid Dadi, and Kristian Hauglie. Hovedopp-gave: Varme- og kjølesentral for bygg ved hjelp av solfangere. 05 2006.
- [17] Svetlana Heian. Thesis in progress. Master's thesis, University of Oslo, 2009.
- [18] IEA.org. International energy agency. Internet(January 2009): http://www.iea.org/Textbase/stats/balancetable.asp?COUNTRY_CODE=29, 2009. URL http://www.iea.org/Textbase/stats/balancetable.asp?COUNTRY_CODE=29.
- [19] Øivin Holter, Finn Ingebretsen, and Hugo Parr. *Fysikk og Energiressurser*. Universitetsforlaget AS, 1998.
- [20] *LabFacility Base Metal Thermocouple Extention & Compensating Wires And Cables*. Labfacility Ltd.
- [21] *Thermocouple, resistance thermometer and thermistor theory and practice*. Labfacility Ltd., 2009. http://www.labfacility.co.uk/pdf_library/.
- [22] Hans Petter Langtangen. *A Primer on Scientific Programming with Python*. 2009.
- [23] *Lauda Immersion Thermostat E 100*. Lauda, 2005.

- [24] Z. F. Li and K. Sumathy. Performance study of a partitioned thermally stratified storage tank in a solar powered absorption air conditioning system. *APPLIED THERMAL ENGINEERING*, 22(11):1207–1216, August 2002.
- [25] John A. Lienhard IV and John A. Lienhard V. *A Heat Transfer Text Book*. Phogiston Press, 3rd edition, 2008.
- [26] Marlo Martin and Paul Berdahl. Characteristics of infrared sky radiation in the united states. *Solar Energy*, 33(3-4):321 – 336, 1984.
- [27] MathWeb. Matweb - material property data, May 2009. Internet(May 2008): <http://www.matweb.com>.
- [28] Michaela G. Meir, John Rekstad, M. Peter, L. Henden, and B. Sandnes. Determination of the performance of solar systems with the calorimetric method. *SOLAR ENERGY*, 73(3):195–207, 2002.
- [29] Oliver Morton. Solar energy: A new day dawning?: Silicon valley sunrise. *Nature*, 443:19–22, September 2006.
- [30] National Instruments Corporation. National Instruments, 2009. <http://www.ni.com/>.
- [31] Graham Philips. Internet(January 2009): <http://climatetechnology.gov/library/2003/tech-options/tech-options-1-3-2.pdf>, November 2003.
- [32] Hans-Dieter Schilling. How did the efficiency of coal power stations evolve, and what can be expected in the future? Internet, 2005. <http://www.sealnet.org/s/8.pdf>(January 2009).
- [33] Daniel V. Schröder. *An Introduction to Thermal Physics*. Addison Wesley Longman, 2000.
- [34] Gunn Spikkeland. Ulike metoder for å bestemme energiutbyttet i et solvarmeanlegg. Master’s thesis, University of Oslo, 2005.
- [35] SSB.no. Fortsatt lavt strømforbruk i husholdninger. Internet(December 2008): <http://www.ssb.no/husenergi/1>.
- [36] John R. Taylor. *An Introduction to Error Analysis*. University Science Books, 2nd ed. edition, 1997.

Bibliography

- [37] United Nations Framework Convention on Climate Change. UNFCCC, 2009. <http://unfccc.int/>.
- [38] U.S. Climate Change Technology Program. Internet, 2000. <http://www.powerwatch.org.uk/energy/graham.asp>(January 2009).

Nomenclature

A	Area of a blackbody[m ²]
α_L	The linear thermal expansion coefficient [1/K]
α_V	The volumetric thermal expansion coefficient [1/K]
C	Heat capacity [J/K]
c	Specific heat capacity [J/kg K]
c	Speed of light
δF	Uncertainty of flow of IE pump [m ³ /h]
DHW	Domestic hot water
ΔL	Change in length of a material as the temperature change [m]
∂L	Fractional change in length of a material [m]
dL	Step length of simulation [m]
δt	Uncertainty of time measurement during calibration of IE pump [s]
∂T	Fractional change in temperature of a material [K]
ΔT_E	Temperature change of a material [K]
$\Delta T_{st}t$	Temperature difference between the solar tank and the room [K]
ΔV	Change in volume of a material as the temperature change [m ³]
δV	Uncertainty of measured water volume during calibration of IE pump [m ³]
ΔV_{FT}	Uncertainty of volume of floor tank [l]

Nomenclature

ΔV_{ST}	Uncertainty of volume of solar tank [l]
E_{gained}	Energy gained by cooling of floor tank [kWh]
E_{lost}	Energy lost is solar tank because of cooling [kWh]
E_p	Energy used by the solar pump [kWh]
E_{pf}	Energy used by the solar pump and auxiliary fan [kWh]
η	Internal efficiency
η_p	Efficiency of cooling
η_{pf}	Efficiency of cooling
F	Flow of the IE pump [m^3/h]
FT	Floor tank
H	Heat flow [W]
h	The Planck constant [$6.626\ 068\ 96(33) \times 10^{-34}$ Js]
IE	Inter-exchange, name of pump between solar tank and floor tank.
I_{SC}	The solar constant [1367 W/ m^2]
k	The material's heat conductivity [W/mK]
$\left(\frac{kA}{\Delta x}\right)$	Total heat transfer coefficient for the solar tank [W/K or J/sK]
k_b	Boltzmann constant [$1.3806503 \times 10^{-23} \text{m}^2 \text{kg}/\text{s}^2 \text{K}$]
λ	Wavelength [m]
L_0	Original length of a material [m]
Mtoe	Million tonnes of oil equivalent. [1 Mtoe = 41.87 PJ]
m_s	Mass of water in solar tank [kg]
$\frac{\partial Q}{\partial t}$	The amount of heat transferred per unit time [W]
R	Radiated effect [W]
\vec{dS}	An oriented surface area element [m^2]

σ_B	The Stefan-Boltzmann constant [$5.670 \times 10^{-8} \text{ W/m}^2\text{K}^4$]
σ_T	Standard deviation
ST	Solar tank
∇T	The temperature gradient [K/m]
T	Temperature of a blackbody [K]
t	Measured time of water flow during calibration [s]
$T_{\text{init,b}}$	Initial temperature of active volume in simulations [$^{\circ}\text{C}$]
$T_{\text{init,t}}$	Initial temperature of above the separation plate in simulations [$^{\circ}\text{C}$]
T_{sky}	Sky temperature [$^{\circ}\text{C}$]
T_{surf}	Surface temperature [$^{\circ}\text{C}$]
toe	Tonnes of oil equivalent. [1 toe = 41.87 GJ]
U	The overall heat transfer coefficient [$\text{W/m}^2\text{K}$]
V	Volume of measured water during calibration [m^3]
V_0	Original volume of a material [m^3]
Δx	Distance between the surfaces heat travel [m]

Appendix A

Calibration and uncertainty

Calibration of the equipment is important to ensure validity of the results. The calibration also gives the uncertainty. Uncertainty theory used in this section is found in An introduction to Error Analysis [36].

A.1 Calibration and uncertainty of temperature sensors

The calibration was done 17.06.2008. The temperature sensors were calibrated using a Lauda Immersion Thermostat E 100 [23]. Before calibration all the sensors were cut in length to reach the places they were to measure the temperature. All the sensor tips were twisted and soldered together. The sensors were then fastened to the terminal connector block. The sensors were gathered to a bundle and inserted in the water bath of the immersion thermostat. The first temperature to calibrate for were 0 °C. A mixture of ice and water were used as a reference for 0 °C. Ice and water in co-existence is by definition 0 °C at atmospheric pressure. The other temperatures, 25, 40, 50 and 60 °C, were obtained by heating with the immersion thermostat. The digital thermometer which is built into the immersion thermostat was not trusted. Instead, a spirit thermometer with an accuracy of 0.05 °C, were used. Reading the thermometer could not be done more accurate than 0.1 °C. The spirit thermometer is assumed to be correct within ± 0.05 °C since the spirit thermometer showed

Chapter A: Calibration and uncertainty

Table A.1: The maximum uncertainty, the standard deviation and the median of the uncertainties for all the sensors at different temperatures. All values in the table have the unit °C.

Temperature:	0	25	40	50	60
Max uncertainty:	0.310	0.317	0.320	0.361	0.270
Max stddev:	0.180	0.211	0.218	0.207	0.145
Median:	0.072	0.070	0.078	0.083	0.078

Table A.2: The maximum uncertainty, standard deviation and median of the uncertainties for all the sensors in the temperature range from 0 to 60 °C. All values in the table have the unit °C.

Maximum uncertainty:	0.361
Maximum stddev:	0.218
Median:	0.083

0.0 °C in ice water.

The temperatures were logged with the same LabVIEW program as the other measurements in this thesis, but without the calibration. The gathering of data lasted for about 10 minutes for each temperature. Table A.1 show the maximum uncertainty, the standard deviation and the median of the uncertainties for each temperature. The maximum uncertainty is the largest difference between measured temperature and the average of the measured temperature over the 10 minutes. The average of the temperatures is in the calibration offset to fit the actual value given by the spirit thermometer. The median is in Table A.1 set to be the median of the maximum uncertainty of each sensors at the given temperature.

Table A.2 show the maximum uncertainty, the standard deviation and the maximum median of the uncertainties for all the sensors and all the temperatures.

The uncertainty in Table A.2 are taking into account the thermistor on the terminal connector block because this uncertainty is taken into account when calibrating the sensors. The uncertainty in Table A.2 does not take into ac-

A.2 Water velocity of the inter-exchange pump

count the uncertainty of the spirit thermometer. The maximum uncertainty of each sensor is therefore

$$\begin{aligned}\delta T &\approx \delta T_{\text{calibrated}} + \delta T_{\text{spirit}} \\ &\approx 0.361 \text{ }^\circ\text{C} + 0.05 \text{ }^\circ\text{C} \\ &\approx 0.411 \text{ }^\circ\text{C} \\ &\approx 0.4 \text{ }^\circ\text{C}\end{aligned}\tag{A.1}$$

Using the same set of measurements, the calibration constants for each sensor were found. The curve fit for the sensors is a second degree polynomial curve fit. The theory of the thermocouples makes them linear, but the curve fit was better for the measured series when using second degree polynomial curve fit. Hence, there are three constants for each sensor. The formula for the calibration is

$$T_{\text{cal}} = c_1 + c_2 T_{\text{mes}} + c_3 T_{\text{mes}}^2.\tag{A.2}$$

All calibration constants are shown in Table A.3.

A.2 Water velocity of the inter-exchange pump

There was no flow-meter attached to the IE loop. To know how the flow of the water that flows from the active volume of the solar tank to the floor tank the velocity of the water needs to be measured. In the absence of a flow-meter that could do the task, the water volume versus time had to be measured manually.

The IE pump has seven settings for the velocity. The velocity is dependent on the pressure. The pressure is dependent on the height the water is lifted. Therefore the pump had to be calibrated for the specific setup.

The IE pump was started with no other parts of the system running. Water entered the floor tank and the water level in the tank increased. This happens

Chapter A: Calibration and uncertainty

Table A.3: Calibration constants for the sensors. These values are used in the LabVIEW program.

Device	Sensor	c_3	c_2	c_1
1	2	-5.90601302190569E-05	1.00209522924830	0.0198731731897367
	3	-0.000108264643772855	1.00664843381972	0.0713945217039627
	4	-0.000153335961154224	1.00872785182783	0.105250223569127
	5	-0.000136182765728027	1.00881191927520	0.0264679678663058
	6	-0.000130653537870709	1.00760990318092	0.136128072330898
	7	-0.000116747441874061	1.00750037467854	0.191516502963389
	8	-8.61575967909126E-05	1.00546062942294	0.118843220888799
	9	-0.000144773873511218	1.00906162392028	0.0523506637668112
	10	-0.000169066823648857	1.01240113428012	-0.0006361321096368
	11	-0.000142665703491355	1.00870575974482	0.113967188558904
	12	-0.000144356309125536	1.01002626935003	0.0005285236926182
	13	-0.000175703119407339	1.01160603001737	0.147365422816249
	14	-0.000104911118002427	1.00718162492842	0.0651875424735364
	15	-9.97270089427707E-05	1.00693781117236	0.188917877911056
	2	2	-6.91824855617651E-05	1.00460553707816
3		-9.88283771566138E-05	1.00641122240851	0.253189978291751
4		-0.000110697371805784	1.00763372789859	0.164024946896734
5		-0.000110936682936899	1.00817348503383	0.177469395747428
6		-0.000103279756063456	1.00825975826692	0.0985640644025550
7		-0.000162093966171914	1.01139411450001	0.165303786976797
8		-0.000131229934603404	1.00944976021507	0.104973715605925
9		-0.000119196666213181	1.00804389575723	0.398867853446438
10		-7.77604164570044E-05	1.00486390428676	0.311857190104625
11		-0.000101760256760119	1.00728889735336	0.336482888940365
12		-0.000135819598117640	1.00893171677569	0.265857174897450
13		-0.000125414834575682	1.00780195671163	0.373924868037049
14		-0.000251073733979480	1.02053334034631	-0.414893639602505
15		-0.000146806226874692	1.01036852351864	0.209899139803375

A.2 Water velocity of the inter-exchange pump

because the outlet lets out more water the higher the pressure is. After a while the height will converge to the point where the amount of water entering the floor tank equals the amount of water exiting it. When the height of the water in the floor tank had stabilized the outlet from the floor tank was led onto a tray. Water was filling the tray for 10-20 seconds for each velocity setting on the pump. The water volume was then measured. Results from the procedure are listed in Table A.4.

The uncertainties of the flows need to be calculated for each flow. The uncertainty of the time comes from the stopwatch and the use of it. Errors in pushing the clock and stopping the water at the exact time is estimated to be within 0.5 s. The error in measuring is estimated to 20 ml, or 0.02 l, because of the use of measuring glass accurate to 10 ml. This way the error is less than that stated in Table A.4. The total uncertainty of two values being divided or multiplied is

$$\begin{aligned} \frac{\delta F}{|q|} &\leq \frac{\delta t}{|t|} + \frac{\delta V}{|V|} \\ &\Downarrow \\ \delta F &\leq \left(\frac{\delta t}{|t|} + \frac{\delta V}{|V|} \right) |q|. \end{aligned} \tag{A.3}$$

where δF is the uncertainty of the flow, F is the flow, δt is the uncertainty of the time, t is the time, δV is the uncertainty of the volume and V is the volume of the measured water. This results in an uncertainty that can be calculated for each flow setting in the IE pump. The uncertainties are shown in the last column in Table A.4. Uncertainty is rounded to one significant figure.

Table A.4: Measured values for the time and volume for each setting n on the IE pump. The calculated volume flow for each setting is shown in units of l/s, l/m and m^3/h . Values for the flow measured in m^3/h is rounded to the first digit that is uncertain.

n	Time(s)	Volume(ml)	Velocity(l/s)	Flow(l/m)	Flow(m^3/h)	Uncertainty(m^3/h)
1	20.3	720	0.0354	2.120	0.128	± 0.007
2	20.0	1116	0.0555	3.331	0.200	± 0.009
3	20.1	1344	0.0668	4.012	0.24	± 0.01
4	15.1	1201	0.0797	4.784	0.29	± 0.01
5	10.0	977	0.0977	5.862	0.35	± 0.02
6	9.9	989	0.1001	6.006	0.36	± 0.02
7	10.2	1145	0.1123	6.735	0.40	± 0.03

Appendix B

Program code

B.1 Simulation of heat transfer

Here is a printout of the python code used in the simulations.

```
#!/usr/bin/env python
# load system and math module:
import sys, math, numpy, datetime
import Gnuplot

## User input:
# Discretized length
dL=float(sys.argv[1])
# Run time. Input hours -> seconds
sec = int(float(sys.argv[2])*3600)
# Calculate each parsec seconds
parsec = int(sys.argv[3])
# Initial temperature upper chamber
Tu = int(sys.argv[4])
# Initial temperature of active volume
Td = int(sys.argv[5])
# Height of separation plate
h = float(sys.argv[6])#m

## Constants:
# Specific heat capacity water
c = 4181.3 #J/kg*K
# Heat conduction water
k = 0.609 #W/m*K = J/s*m*K
# Modified heat conduction water-steel
k = 0.760 #W/m*K = J/s*m*K
# Area of cross section of tank
A = 0.3969#m^2 (0.63m x 0.63m)
# Height of tank
H = 1.26#m
# Width and depth of tank
B = 0.63#m
# Mass of one discretized volume
m = A*dL*1000#kg

# Constant for heatflow
con = k/(dL**2*c*1000)
```

```
##### Making the array of layers #####
#
heat = []
heat_add = []
for i in range(int(h/dL)):
    heat.append([i*dL*1000,Td])
    heat_add.append(0)

for i in range(int(H/dL-h/dL)):
    heat.append([i*dL*1000+h*1000,Tu])
    heat_add.append(0)

#
#####
#
#Loop through each timestep
for t in range(int(sec/parsec)):
    #Loop through each volume
    for i in range(int(h/dL),len(heat)):
        if i < len(heat) - 1 and i > 0:
            heat_add[i] = parsec * con * ( heat[i+1][1] + heat[i-1][1] - 2 * heat[i][1] ←
            )

            #Add new heat to volume
            for x in range(len(heat)):
                heat[x][1] += heat_add[x]
            #Reset variable
            heat_add[x] = 0
#Visual check of the numbers
print heat
#
#####

# Plot
gp = Gnuplot.Gnuplot(persist = 1)
gp('set data style lines')
gp('set yrange[5:'+str(Tu+10)+'}')
gp('set title "Input parameters: ' + str(dL) + ', ' + str(sec/3600) + ', ' + str(parsec)←
    + ', ' + str(Tu) + ', ' + str(Td) + ', ' + str(h) + '"')
gp('set xrange[0:' + str(1260) + ']')
gp('set ylabel "Temperature(^oC)" 2,0')
gp('set xlabel "Height(mm)" 2,0')
gp.plot(heat)
gp('set terminal postscript enhanced solid "Computer Modern Roman" 16')

# Save to file. Different name each time to prevent overwriting
gp.hardcopy(filename=(str(datetime.date.today()) + '-' + str(datetime.datetime.today().←
    minute) + '-' + str(datetime.datetime.today().second) + '-' + str(sec) + '-' + str(dL←
    *1000)[0:2] + '.ps'),terminal="postscript")

# Resolution needed for cm accuracy = 0.01
```

B.2 Plotting of simulations together with measurements

```
#!/usr/bin/env python
# Filename = sammenligne.py
# author = Øystein Soteland
# version = 1.0 final
# load modules needed:
import sys, math, numpy, datetime, Gnuplot

# var3 holds the arrays of two simulations and
# the extracted measurements from each experiment
# val1 and val 2 holds the simulations with the input parameters:
# vali holds the initial values for the measurement
```

B.2 Plotting of simulations together with measurements

```
# val holds the final values for the measurement
# Import var3:
from var3 import *

runtime = [6.42,2.93,3.85]
dates = ['21.10.2008','27.10.2008','28.10.2008']
temperatures = [80,55,55]

# Input parameters from user
g = int(sys.argv[1])

# Find values and arrays for the plotting
T = str(temperatures[g])
d = dates[g]
r = str(runtime[g])

# Create plotlines
plot1 = Gnuplot.PlotItems.Data(val1[g], title="Measurement, i")
plot2 = Gnuplot.PlotItems.Data(val[g], title="Measurement, f")

plot3 = Gnuplot.PlotItems.Data(val1[g], title="Simulated, f a")
plot4 = Gnuplot.PlotItems.Data(val2[g], title="Simulated, f b")

# Plot
gp = Gnuplot.Gnuplot(persist = 1)
gp('set key rmargin')
gp('set data style linespoints')
gp('set yrange[10:'+T+')')
gp('set title "Date: '+d+'. Runtime: '+r+' h."')
gp('set xrange[0:1260]')
gp('set ylabel "Temperature(^oC)" 2,0')
gp('set xlabel "Height(mm)" 2,0')
gp('set size ratio +0.8')
gp.plot(plot1,plot2,plot3,plot4)
gp('set terminal postscript enhanced solid "Computer Modern Roman" 18')

# Save to file.
gp.hardcopy(filename=(str(g)+'.ps'),terminal="postscript")
```

B.2.1 Variables for plotting

```
# Filename = var3.py
val = []
val.append([[160, '17.095181'], [260, '17.867692'], [310, '19.960178'], [360, '38.154072'], [410, '50.654082'], [460, '54.812224'], [560, '57.524646'], [810, '67.228112'], [1060, '70.157529']])
val.append([[160, '18.168613'], [260, '19.807977'], [310, '22.054538'], [360, '37.452305'], [410, '44.131216'], [460, '45.627473'], [560, '46.690191'], [810, '49.726507'], [1060, '49.833665']])
val.append([[160, '16.845674'], [260, '18.068774'], [310, '22.071202'], [360, '38.696014'], [410, '41.014053'], [460, '41.606232'], [560, '42.475602'], [810, '49.116059'], [1060, '49.618801']])

val1 = []
val1.append([[160, '73.460345'], [260, '73.504373'], [310, '73.566994'], [360, '73.578128'], [410, '73.547900'], [460, '73.574112'], [560, '73.545483'], [810, '73.752933'], [1060, '73.747391']])
val1.append([[160, '50.205467'], [260, '50.211004'], [310, '50.150535'], [360, '50.200253'], [410, '50.217718'], [460, '50.213189'], [560, '50.208456'], [810, '50.269999'], [1060, '50.366670']])
val1.append([[160, '49.716046'], [260, '49.791343'], [310, '49.747196'], [360, '49.762607'], [410, '49.753031'], [460, '49.736133'], [560, '49.758158'], [810, '49.990219'], [1060, '50.568186']])

val1 = []
val1.append([[0.0, 20], [10.0, 20], [20.0, 20], [30.0, 20], [40.0, 20], [50.0, 20], [60.0, 20], [70.0, 20], [80.0, 20], [90.0, 20], [100.0, 20], [110.0, 20], [120.0, 20], [130.0, 20], [140.0, 20], [150.0, 20], [160.0, 20], [170.0, 20], [180.0, 20],
```

Chapter B: Program code

```
[190.0, 20], [200.0, 20], [210.0, 20], [220.0, 20], [230.0, 20], [240.0, 20], ←
[250.0, 20], [260.0, 20], [270.0, 20], [280.0, 20], [290.0, 20], [300.0, 20], ←
[310.0, 24.56531710487274], [320.0, 29.076475290969057], [330.0, ←
33.484193804324597], [340.0, 37.742717999574914], [350.0, 41.811226497348429], ←
[360.0, 45.654967563708169], [370.0, 49.246074385629392], [380.0, ←
52.564032534690995], [390.0, 55.595797212090631], [400.0, 58.335580700050095], ←
[410.0, 60.784349949483278], [420.0, 62.949089024297116], [430.0, 64.8418903900224], ←
[440.0, 66.47894257764122], [450.0, 67.879479935247431], [460.0, ←
69.064753822830994], [470.0, 70.057074846828129], [480.0, 70.878963863743735], ←
[490.0, 71.55243679834318], [500.0, 72.098435981980984], [510.0, ←
72.536409653610988], [520.0, 72.884032131712345], [530.0, 73.157050317061362], ←
[540.0, 73.369237708183533], [550.0, 73.532434861295513], [560.0, ←
73.656654897570419], [570.0, 73.750233846538066], [580.0, 73.820007871787155], ←
[590.0, 73.87150232402476], [600.0, 73.909120728308636], [610.0, ←
73.936324932247445], [620.0, 73.955800498825894], [630.0, 73.969603881563756], ←
[640.0, 73.979289903364617], [650.0, 73.986019564002035], [660.0, ←
73.990649257121802], [670.0, 73.993803144924641], [680.0, 73.995930789592407], ←
[690.0, 73.997352249960713], [700.0, 73.998292790044204], [710.0, ←
73.998909173502682], [720.0, 73.999309284119349], [730.0, 73.999566554044932], ←
[740.0, 73.999730425120703], [750.0, 73.999833830822936], [760.0, ←
73.999898476604542], [770.0, 73.999938518449426], [780.0, 73.999963093298391], ←
[790.0, 73.999978038275458], [800.0, 73.999987044691778], [810.0, ←
73.999992423498028], [820.0, 73.999995607121235], [830.0, 73.999997474722008], ←
[840.0, 73.999998560641814], [850.0, 73.999999186516703], [860.0, ←
73.999999544100618], [870.0, 73.999999746632653], [880.00000000000011, ←
73.999999860358571], [890.0, 73.999999923672561], [900.0, 73.999999958621842], ←
[910.0, 73.999999977751216], [920.0, 73.999999988133922], [930.0, ←
73.999999993722369], [940.0, 73.999999996705483], [950.0, 73.999999998284778], ←
[960.0, 73.999999999114081], [970.0, 73.999999999546006], [980.0, ←
73.999999999769159], [990.0, 73.999999999883528], [1000.0000000000001, ←
73.999999999941679], [1010.00000000000001, 73.999999999971024], [1020.0, ←
73.999999999985704], [1030.0, 73.99999999999298], [1040.0, 73.999999999996561], ←
[1050.0, 73.999999999998309], [1060.0, 73.999999999999147], [1070.0, ←
73.999999999999602], [1080.0, 73.999999999999858], [1090.0, 73.99999999999986], ←
[1100.0, 74.0], [1110.0, 74.0], [1120.0, 74.0], [1130.0, 74.0], [1140.0, 74.0], ←
[1150.0, 74.0], [1160.0, 74.0], [1170.0, 74.0], [1180.0, 74.0], [1190.0, 74.0], ←
[1200.0, 74.0], [1210.0, 74.0], [1220.0, 74.0], [1230.0, 74.0], [1240.0, 74.0], ←
[1250.0, 74]]
val1.append([[0.0, 20], [10.0, 20], [20.0, 20], [30.0, 20], [40.0, 20], [50.0, 20], ←
[60.0, 20], [70.0, 20], [80.0, 20], [90.0, 20], [100.0, 20], [110.0, 20], [120.0, ←
20], [130.0, 20], [140.0, 20], [150.0, 20], [160.0, 20], [170.0, 20], [180.0, 20], ←
[190.0, 20], [200.0, 20], [210.0, 20], [220.0, 20], [230.0, 20], [240.0, 20], ←
[250.0, 20], [260.0, 20], [270.0, 20], [280.0, 20], [290.0, 20], [300.0, 20], ←
[310.0, 23.750175228063391], [320.0, 27.403201711502561], [330.0, ←
30.874756167136155], [340.0, 34.093781047211408], [350.0, 37.006638541330616], ←
[360.0, 39.579283692064706], [370.0, 41.797393411935758], [380.0, ←
43.664678585884111], [390.0, 45.199824615960019], [400.0, 46.432621977764704], ←
[410.0, 47.399857972832393], [420.0, 48.141461271757876], [430.0, ←
48.697253602579828], [440.0, 49.104504054721822], [450.0, 49.396332754040614], ←
[460.0, 49.600894103865876], [470.0, 49.741195574960834], [480.0, ←
49.835375785287212], [490.0, 49.897267583622657], [500.0, 49.937096729198451], ←
[510.0, 49.962203026191695], [520.0, 49.9770896632268], [530.0, ←
49.987094688329172], [540.0, 49.992664133607164], [550.0, 49.995904926864306], ←
[560.0, 49.997754647043593], [570.0, 49.998790494494266], [580.0, ←
49.999359792601965], [590.0, 49.999666946608848], [600.0, 49.99982967470909], ←
[610.0, 49.999914353612503], [620.0, 49.999957645789401], [630.0, ←
49.99997939678444], [640.0, 49.999990139077177], [650.0, 49.999995355517243], ←
[660.0, 49.99999784678613], [670.0, 49.999999017213227], [680.0, ←
49.999999558281637], [690.0, 49.999999804459549], [700.0, 49.999999914724768], ←
[710.0, 49.999999963356771], [720.0, 49.999999984481938], [730.0, ←
49.999999993522003], [740.0, 49.999999997333816], [750.0, 49.999999998917893], ←
[760.0, 49.999999999566818], [770.0, 49.99999999982893], [780.0, ←
49.999999999933337], [790.0, 49.999999999974364], [800.0, 49.999999999990258], ←
[810.0, 49.999999999996341], [820.0, 49.99999999999865], [830.0, ←
49.999999999999503], [840.0, 49.999999999999815], [850.0, 49.999999999999936], ←
[860.0, 50.0], [870.0, 50.0], [880.00000000000011, 50.0], [890.0, 50.0], [900.0, ←
50.0], [910.0, 50.0], [920.0, 50.0], [930.0, 50.0], [940.0, 50.0], [950.0, 50.0], ←
[960.0, 50.0], [970.0, 50.0], [980.0, 50.0], [990.0, 50.0], [1000.0000000000001, ←
50.0], [1010.00000000000001, 50.0], [1020.0, 50.0], [1030.0, 50.0], [1040.0, 50.0], ←
[1050.0, 50.0], [1060.0, 50.0], [1070.0, 50.0], [1080.0, 50.0], [1090.0, 50.0], ←
[1100.0, 50.0], [1110.0, 50.0], [1120.0, 50.0], [1130.0, 50.0], [1140.0, 50.0], ←
[1150.0, 50.0], [1160.0, 50.0], [1170.0, 50.0], [1180.0, 50.0], [1190.0, 50.0], ←
[1200.0, 50.0], [1210.0, 50.0], [1220.0, 50.0], [1230.0, 50.0], [1240.0, 50.0], ←
[1250.0, 50]]
val1.append([[0.0, 20], [10.0, 20], [20.0, 20], [30.0, 20], [40.0, 20], [50.0, 20], ←
[60.0, 20], [70.0, 20], [80.0, 20], [90.0, 20], [100.0, 20], [110.0, 20], [120.0, ←
```


B.2 Plotting of simulations together with measurements

```
20], [130.0, 20], [140.0, 20], [150.0, 20], [160.0, 20], [170.0, 20], [180.0, 20], ←
[190.0, 20], [200.0, 20], [210.0, 20], [220.0, 20], [230.0, 20], [240.0, 20], ←
[250.0, 20], [260.0, 20], [270.0, 20], [280.0, 20], [290.0, 20], [300.0, 20], ←
[310.0, 23.271228658819695], [320.0, 26.477944493463198], [330.0, ←
29.562960930770661], [340.0, 32.475919088925593], [350.0, 35.17568297802903], ←
[360.0, 37.631916909748938], [370.0, 39.825763424067169], [380.0, ←
41.749643238514196], [390.0, 43.406289504776268], [400.0, 44.807195532377847], ←
[410.0, 45.970691709344798], [420.0, 46.919872775261958], [430.0, ←
47.680574956535473], [440.0, 48.27956127496747], [450.0, 48.743021691068883], ←
[460.0, 49.095441520743478], [470.0, 49.358844013905653], [480.0, ←
49.552375905198446], [490.0, 49.69218029590013], [500.0, 49.791489227395644], ←
[510.0, 49.860866889471197], [520.0, 49.908540757511297], [530.0, ←
49.94076901413834], [540.0, 49.962205615580523], [550.0, 49.976237155648057], ←
[560.0, 49.985276836845074], [570.0, 49.99100964924444], [580.0, ←
49.994589113008182], [590.0, 49.996789873793311], [600.0, 49.998122478922966], ←
[610.0, 49.998917306824865], [620.0, 49.99938434987039], [630.0, ←
49.999654759416615], [640.0, 49.999809049287329], [650.0, 49.999895819742804], ←
[660.0, 49.999943925153673], [670.0, 49.999970220069329], [680.0, ←
49.999984393444883], [690.0, 49.999991928144084], [700.0, 49.99999587923174], ←
[710.0, 49.999997923284319], [720.0, 49.999998966701831], [730.0, ←
49.999999492332037], [740.0, 49.999999753682658], [750.0, 49.999999881960633], ←
[760.0, 49.999999944123289], [770.0, 49.999999973868633], [780.0, ←
49.999999987925328], [790.0, 49.999999994486529], [800.0, 49.999999997511907], ←
[810.0, 49.999999998890168], [820.0, 49.999999999510621], [830.0, ←
49.999999999786652], [840.0, 49.999999999908027], [850.0, 49.999999999960792], ←
[860.0, 49.999999999983473], [870.0, 49.999999999993101], [880.000000000000011, ←
49.999999999997151], [890.0, 49.99999999999828], [900.0, 49.999999999999524], ←
[910.0, 49.999999999999815], [920.0, 49.999999999999936], [930.0, 50.0], [940.0, ←
50.0], [950.0, 50.0], [960.0, 50.0], [970.0, 50.0], [980.0, 50.0], [990.0, 50.0], ←
[1000.000000000000001, 50.0], [1010.000000000000001, 50.0], [1020.0, 50.0], [1030.0, ←
50.0], [1040.0, 50.0], [1050.0, 50.0], [1060.0, 50.0], [1070.0, 50.0], [1080.0, ←
50.0], [1090.0, 50.0], [1100.0, 50.0], [1110.0, 50.0], [1120.0, 50.0], [1130.0, ←
50.0], [1140.0, 50.0], [1150.0, 50.0], [1160.0, 50.0], [1170.0, 50.0], [1180.0, ←
50.0], [1190.0, 50.0], [1200.0, 50.0], [1210.0, 50.0], [1220.0, 50.0], [1230.0, ←
50.0], [1240.0, 50.0], [1250.0, 50]]))

val2 = []
val2.append([[0.0, 20], [10.0, 20], [20.0, 20], [30.0, 20], [40.0, 20], [50.0, 20], ←
[60.0, 20], [70.0, 20], [80.0, 20], [90.0, 20], [100.0, 20], [110.0, 20], [120.0, ←
20], [130.0, 20], [140.0, 20], [150.0, 20], [160.0, 20], [170.0, 20], [180.0, 20], ←
[190.0, 20], [200.0, 20], [210.0, 20], [220.0, 20], [230.0, 20], [240.0, 20], ←
[250.0, 20], [260.0, 20], [270.0, 20], [280.0, 20], [290.0, 20], [300.0, 20], ←
[310.0, 20], [320.0, 20], [330.0, 20], [340.0, 20], [350.000000000000006, 20], ←
[360.0, 24.56531710487274], [370.0, 29.076475290969057], [380.0, ←
33.484193804324597], [390.0, 37.742717999574914], [400.0, 41.811226497348429], ←
[410.0, 45.654967563708169], [420.0, 49.246074385629392], [430.0, ←
52.564032534690995], [440.0, 55.595797212090631], [450.0, 58.335580700050095], ←
[460.0, 60.784349949483278], [470.0, 62.949089024297116], [480.0, 64.8418903900224], ←
[490.0, 66.47894257764122], [500.0, 67.879479935247431], [510.0, ←
69.064753822830994], [520.0, 70.057074846828129], [530.0, 70.878963863743735], ←
[540.0, 71.55243679834318], [550.0, 72.098435981980984], [560.0, ←
72.536409653610988], [570.0, 72.884032131712345], [580.0, 73.157050317061362], ←
[590.0, 73.369237708183533], [600.0, 73.532434861295513], [610.0, ←
73.656654897570419], [620.0, 73.750233846538066], [630.0, 73.820007871787155], ←
[640.0, 73.87150232402476], [650.0, 73.909120728308636], [660.0, ←
73.936324932247445], [670.0, 73.955800498825894], [680.0, 73.969603881563756], ←
[690.0, 73.979289903364617], [700.0, 73.986019564002035], [710.0, ←
73.990649257121802], [720.0, 73.993803144924641], [730.0, 73.995930789592407], ←
[740.0, 73.997352249960713], [750.0, 73.998292790044204], [760.0, ←
73.998909173502682], [770.0, 73.999309284119349], [780.0, 73.999566554044932], ←
[790.0, 73.999730425120703], [800.0, 73.999833830822936], [810.0, ←
73.999898476604542], [820.0, 73.999938518449426], [830.0, 73.999963093298391], ←
[840.0, 73.999978038275458], [850.0, 73.999987044691778], [860.0, ←
73.999992423498028], [870.0, 73.999995607121235], [880.0, 73.999997474722008], ←
[890.0, 73.999998560641814], [900.0, 73.999999186516703], [910.0, ←
73.999999544100618], [920.0, 73.999999746632653], [930.000000000000011, ←
73.999999860358571], [940.0, 73.999999923672561], [950.0, 73.999999958621842], ←
[960.0, 73.999999977751216], [970.0, 73.999999988133922], [980.0, ←
73.999999993722369], [990.0, 73.999999996705483], [1000.0, 73.999999998284778], ←
[1010.0, 73.999999999114081], [1020.0, 73.999999999546006], [1030.0, ←
73.999999999769159], [1040.0, 73.999999999883528], [1050.0, 73.999999999941679], ←
[1060.0, 73.99999999971024], [1070.0, 73.99999999985704], [1080.0, ←
73.9999999999298], [1090.0, 73.99999999996561], [1100.0, 73.99999999998309], ←
[1110.0, 73.99999999999147], [1120.0, 73.99999999999602], [1130.0, ←
73.99999999999858], [1140.0, 73.99999999999986], [1150.0, 74.0], [1160.0, 74.0], ←
[1170.0, 74.0], [1180.0, 74.0], [1190.0, 74.0], [1200.0, 74.0], [1210.0, 74.0], ←
```

Chapter B: Program code

```
[1220.0, 74.0], [1230.0, 74.0], [1240.0, 74.0], [1250.0, 74]])
val2.append([[0.0, 20], [10.0, 20], [20.0, 20], [30.0, 20], [40.0, 20], [50.0, 20], ←
[60.0, 20], [70.0, 20], [80.0, 20], [90.0, 20], [100.0, 20], [110.0, 20], [120.0, ←
20], [130.0, 20], [140.0, 20], [150.0, 20], [160.0, 20], [170.0, 20], [180.0, 20], ←
[190.0, 20], [200.0, 20], [210.0, 20], [220.0, 20], [230.0, 20], [240.0, 20], ←
[250.0, 20], [260.0, 20], [270.0, 20], [280.0, 20], [290.0, 20], [300.0, 20], ←
[310.0, 20], [320.0, 20], [330.0, 20], [340.0, 20], [350.00000000000006, 20], ←
[360.0, 23.750175228063391], [370.0, 27.403201711502561], [380.0, ←
30.874756167136155], [390.0, 34.093781047211408], [400.0, 37.006638541330616], ←
[410.0, 39.579283692064706], [420.0, 41.797393411935758], [430.0, ←
43.664678585884111], [440.0, 45.199824615960019], [450.0, 46.43262197764704], ←
[460.0, 47.399857972832393], [470.0, 48.141461271757876], [480.0, ←
48.697253602579828], [490.0, 49.104504054721822], [500.0, 49.396332754040614], ←
[510.0, 49.600894103865876], [520.0, 49.741195574960834], [530.0, ←
49.835375785287212], [540.0, 49.897267583622657], [550.0, 49.937096729198451], ←
[560.0, 49.962203026191695], [570.0, 49.9770896632268], [580.0, ←
49.987094688329172], [590.0, 49.992664133607164], [600.0, 49.995904926864306], ←
[610.0, 49.997754647043593], [620.0, 49.998790494494266], [630.0, ←
49.999359792601965], [640.0, 49.999666946608848], [650.0, 49.99982967470909], ←
[660.0, 49.999914353612503], [670.0, 49.999957645789401], [680.0, ←
49.99997939678444], [690.0, 49.999990139077177], [700.0, 49.999995355517243], ←
[710.0, 49.99999784678613], [720.0, 49.999999017213227], [730.0, ←
49.999999558281637], [740.0, 49.999999804459549], [750.0, 49.999999914724768], ←
[760.0, 49.99999963356771], [770.0, 49.99999984481938], [780.0, ←
49.99999993522003], [790.0, 49.99999997333816], [800.0, 49.99999998917893], ←
[810.0, 49.99999999566818], [820.0, 49.9999999982893], [830.0, ←
49.99999999933337], [840.0, 49.99999999974364], [850.0, 49.99999999990258], ←
[860.0, 49.99999999996341], [870.0, 49.9999999999865], [880.0, ←
49.99999999999503], [890.0, 49.99999999999815], [900.0, 49.99999999999936], ←
[910.0, 50.0], [920.0, 50.0], [930.00000000000011, 50.0], [940.0, 50.0], [950.0, ←
50.0], [960.0, 50.0], [970.0, 50.0], [980.0, 50.0], [990.0, 50.0], [1000.0, 50.0], ←
[1010.0, 50.0], [1020.0, 50.0], [1030.0, 50.0], [1040.0, 50.0], [1050.0, 50.0], ←
[1060.0, 50.0], [1070.0, 50.0], [1080.0, 50.0], [1090.0, 50.0], [1100.0, 50.0], ←
[1110.0, 50.0], [1120.0, 50.0], [1130.0, 50.0], [1140.0, 50.0], [1150.0, 50.0], ←
[1160.0, 50.0], [1170.0, 50.0], [1180.0, 50.0], [1190.0, 50.0], [1200.0, 50.0], ←
[1210.0, 50.0], [1220.0, 50.0], [1230.0, 50.0], [1240.0, 50.0], [1250.0, 50]])
val2.append([[0.0, 20], [10.0, 20], [20.0, 20], [30.0, 20], [40.0, 20], [50.0, 20], ←
[60.0, 20], [70.0, 20], [80.0, 20], [90.0, 20], [100.0, 20], [110.0, 20], [120.0, ←
20], [130.0, 20], [140.0, 20], [150.0, 20], [160.0, 20], [170.0, 20], [180.0, 20], ←
[190.0, 20], [200.0, 20], [210.0, 20], [220.0, 20], [230.0, 20], [240.0, 20], ←
[250.0, 20], [260.0, 20], [270.0, 20], [280.0, 20], [290.0, 20], [300.0, 20], ←
[310.0, 20], [320.0, 20], [330.0, 20], [340.0, 20], [350.00000000000006, 20], ←
[360.0, 23.271228658819695], [370.0, 26.477944493463198], [380.0, ←
29.562960930770661], [390.0, 32.475919088925593], [400.0, 35.17568297802903], ←
[410.0, 37.631916909748938], [420.0, 39.825763424067169], [430.0, ←
41.749643238514196], [440.0, 43.406289504776268], [450.0, 44.807195532377847], ←
[460.0, 45.970691709344798], [470.0, 46.919872775261958], [480.0, ←
47.680574956535473], [490.0, 48.27956127496747], [500.0, 48.743021691068883], ←
[510.0, 49.095441520743478], [520.0, 49.358844013905653], [530.0, ←
49.552375905198446], [540.0, 49.69218029590013], [550.0, 49.791489227395644], ←
[560.0, 49.860866889471197], [570.0, 49.908540757511297], [580.0, ←
49.94076901413834], [590.0, 49.962205615580523], [600.0, 49.976237155648057], ←
[610.0, 49.985276836845074], [620.0, 49.99100964924444], [630.0, ←
49.994589113008182], [640.0, 49.996789873793311], [650.0, 49.998122478922966], ←
[660.0, 49.998917306824865], [670.0, 49.99938434987039], [680.0, ←
49.999654759416615], [690.0, 49.999809049287329], [700.0, 49.999895819742804], ←
[710.0, 49.999943925153673], [720.0, 49.999970220069329], [730.0, ←
49.999984393444883], [740.0, 49.999991928144084], [750.0, 49.99999587923174], ←
[760.0, 49.999997923284319], [770.0, 49.999998966701831], [780.0, ←
49.999999492332037], [790.0, 49.99999753682658], [800.0, 49.99999881960633], ←
[810.0, 49.99999944123289], [820.0, 49.99999973868633], [830.0, ←
49.99999987925328], [840.0, 49.99999994486529], [850.0, 49.99999997511907], ←
[860.0, 49.99999998890168], [870.0, 49.99999999510621], [880.0, ←
49.99999999786652], [890.0, 49.99999999908027], [900.0, 49.99999999960792], ←
[910.0, 49.99999999983473], [920.0, 49.99999999993101], [930.00000000000011, ←
49.99999999997151], [940.0, 49.99999999998828], [950.0, 49.99999999999524], ←
[960.0, 49.99999999999815], [970.0, 49.99999999999936], [980.0, 50.0], [990.0, ←
50.0], [1000.0, 50.0], [1010.0, 50.0], [1020.0, 50.0], [1030.0, 50.0], [1040.0, ←
50.0], [1050.0, 50.0], [1060.0, 50.0], [1070.0, 50.0], [1080.0, 50.0], [1090.0, ←
50.0], [1100.0, 50.0], [1110.0, 50.0], [1120.0, 50.0], [1130.0, 50.0], [1140.0, ←
50.0], [1150.0, 50.0], [1160.0, 50.0], [1170.0, 50.0], [1180.0, 50.0], [1190.0, ←
50.0], [1200.0, 50.0], [1210.0, 50.0], [1220.0, 50.0], [1230.0, 50.0], [1240.0, ←
50.0], [1250.0, 50]])
```

Appendix C

Labview

The program, Virtual Instrument (VI), made in LabVIEW is shown here. The user interface is shown in Figure C.1. The underlying "code", the block diagram, is shown in Figure C.2.

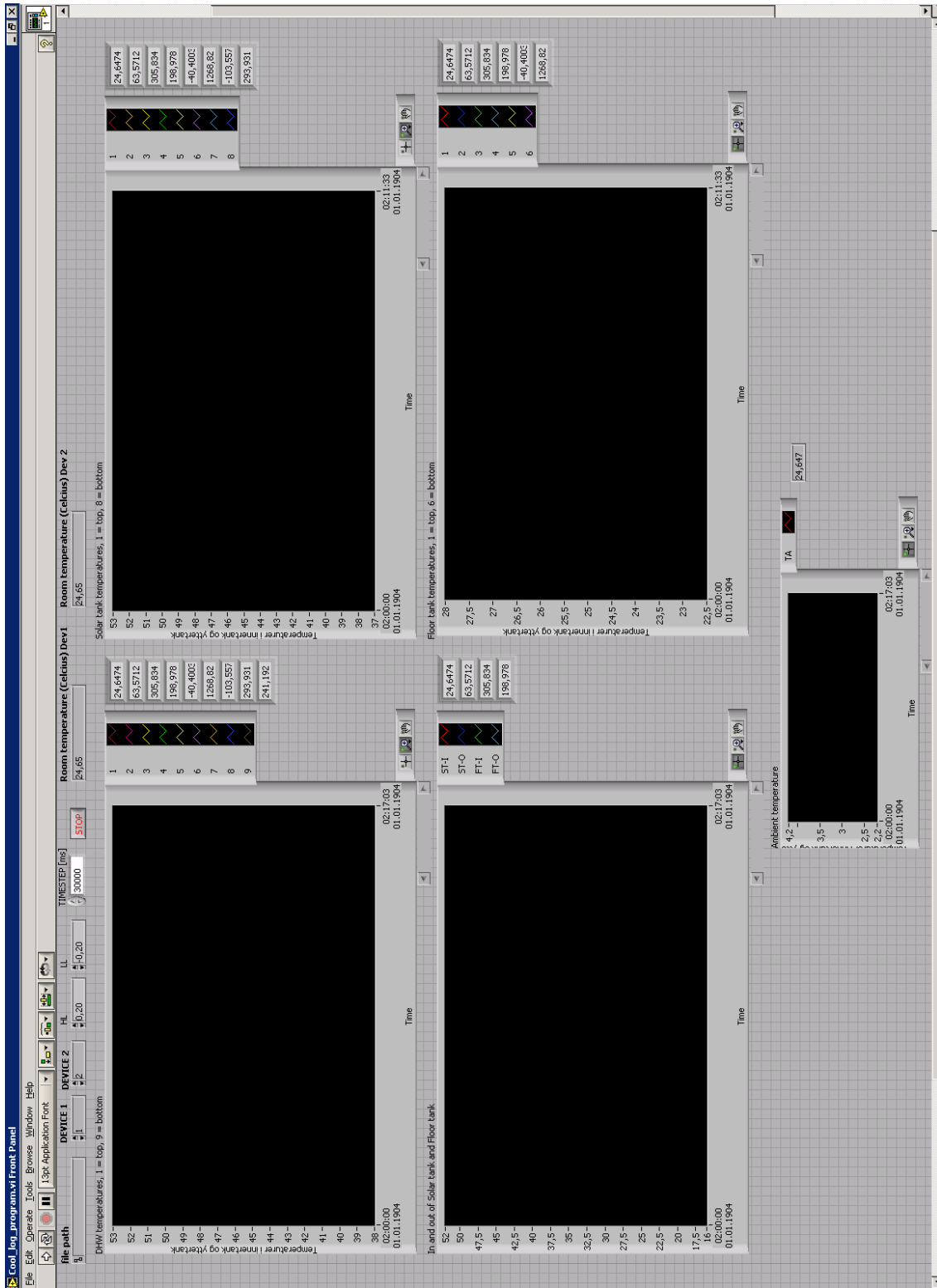


Figure C.1: The interface of the LabView program.

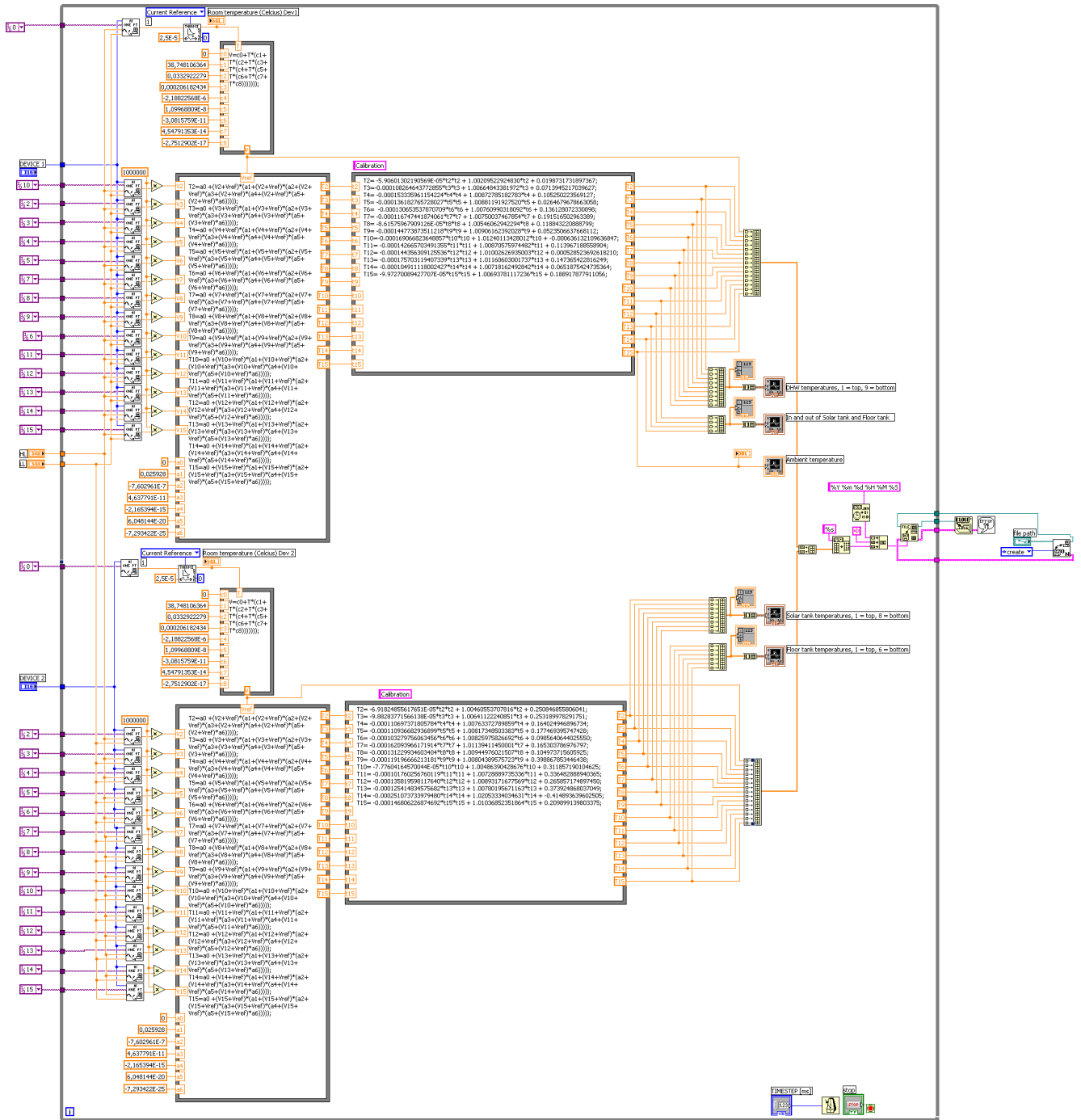


Figure C.2: The block diagram of the Labview program.

Appendix D

Supplementary technical drawings

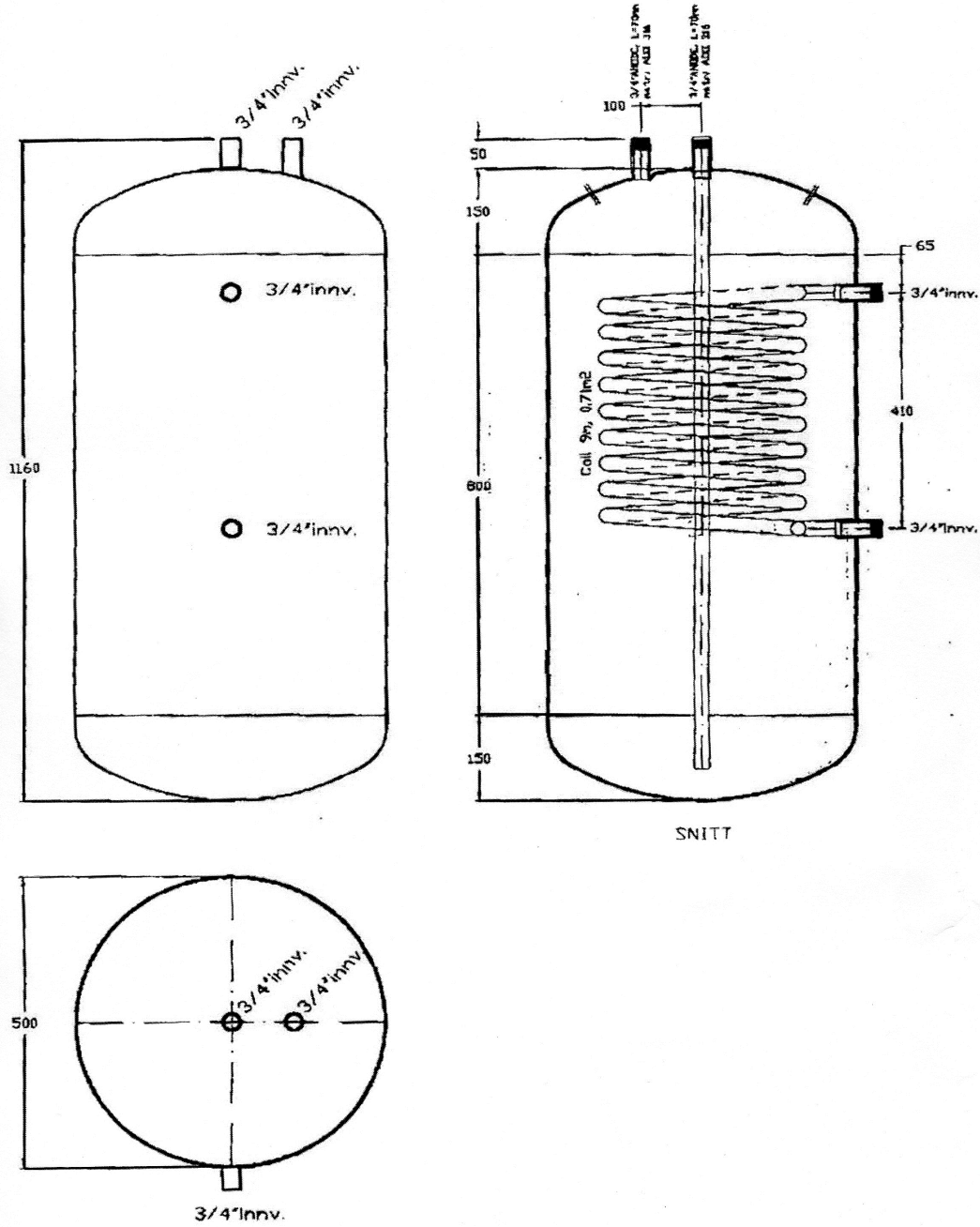


Figure D.1: The measures of the internal DHW tank. The inner loop is there for historical reasons.

Appendix E

Supplementary values

This section contains material properties for the materials used in this thesis.

Chapter E: Supplementary values

Table E.1: Thermal conductivity, k , for different materials used. [27]

Material	Thermal conductivity (W/mK)	Occurring temperature ($^{\circ}C$)
Copper (pure)	398	27.0
	401	0.000
Stainless steel 316L	16.2	100
	21.4	500
Water	0.609	27

Table E.2: Specific heat capacity under constant pressure, c_p , for different materials used. [27]

Material	Specific heat capacity (kJ/kgK)	Occurring temperature ($^{\circ}C$)
Copper (pure)	0.385	27.0
Stainless steel 316L	0.500	0.000 - 100
Water	4.1819	20
	4.216	100